

EUROPEAN ORGANISATION FOR NUCLEAR RESEARCH (CERN)



JHEP 01 (2024) 004
DOI: [10.1007/JHEP01\(2024\)004](https://doi.org/10.1007/JHEP01(2024)004)



CERN-EP-2023-152
29th August 2024

Differential cross-section measurements of the production of four charged leptons in association with two jets using the ATLAS detector

The ATLAS Collaboration

Differential cross-sections are measured for the production of four charged leptons in association with two jets. These measurements are sensitive to final states in which the jets are produced via the strong interaction as well as to the purely-electroweak vector boson scattering process. The analysis is performed using proton–proton collision data collected by ATLAS at $\sqrt{s} = 13$ TeV and with an integrated luminosity of 140 fb^{-1} . The data are corrected for the effects of detector inefficiency and resolution and are compared to state-of-the-art Monte Carlo event generator predictions. The differential cross-sections are used to search for anomalous weak-boson self-interactions that are induced by dimension-six and dimension-eight operators in Standard Model effective field theory.

Contents

1	Introduction	2
2	ATLAS detector	4
3	Data and simulation	5
4	Event and object selection	7
5	Backgrounds	8
6	Correction for detector effects	10
7	Systematic uncertainties	12
8	Results	14
9	Effective field theory interpretation	18
10	Conclusion	20
	Appendix	22

1 Introduction

The pair production of Z bosons in association with two jets ($ZZjj$ production) in proton–proton collisions is sensitive to a diverse range of physical phenomena. Of particular interest is the purely electroweak (EW) $ZZjj$ process (referred to here as EW $ZZjj$) in which the jets arise through the t -channel exchange of electroweak bosons as shown in Figure 1 (left). This process is sensitive to the WWZ and $WWZZ$ weak-boson self-interactions, which arise due to the non-Abelian nature of the electroweak interaction. Also of interest is the production of $ZZjj$ with the jets arising from the strong interaction. This is referred to as strong $ZZjj$ production and is shown in Figure 1 (right). Theoretical predictions for the strong $ZZjj$ process are very sensitive to the accuracy of the perturbative QCD calculations, both in the overall production rate and in the kinematic properties of the final state. Measurements of $ZZjj$ production can therefore be used to improve our understanding of both the electroweak and strong interactions that underpin the Standard Model (SM) of particle physics.

Measurements of $ZZjj$ production in proton–proton collisions at the LHC have thus far focussed on extracting the electroweak contribution. The ATLAS Collaboration recently published the observation of EW $ZZjj$ production at a significance of greater than five standard deviations [1]. Before that, the CMS Collaboration announced evidence for the process at a significance greater than three standard deviations [2]. Both of these measurements used multivariate discriminants to separate the electroweak and strong $ZZjj$ components, and reported a fiducial EW $ZZjj$ cross-section within the phase space of the analysis. In the ATLAS analysis, a cross-section for inclusive $ZZjj$ production was also reported. The inclusive $ZZjj$ cross-section is the sum of the strong and electroweak contributions, and the ATLAS measurement provides

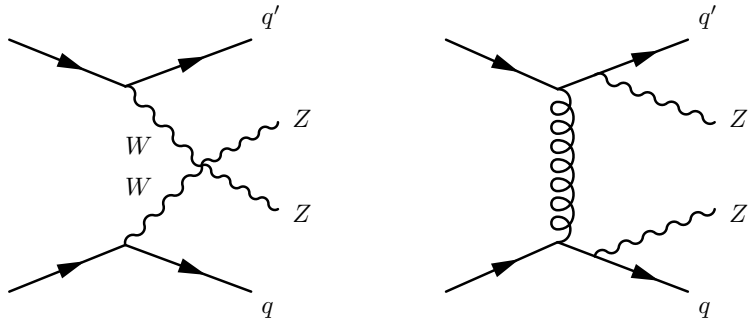


Figure 1: Example Feynman diagrams for EW $ZZjj$ production (left) and strong $ZZjj$ production (right). The scattered quarks (labelled q and q') produce the hadronic jets observed in the final state.

an important constraint on the overall rate of strong $ZZjj$ production. Measurements sensitive to inclusive ZZ production have also been performed by both experiments, in an inclusive phase space that is not enriched by EW production [3, 4].

In this paper, differential cross-section measurements for the production of four charged leptons in association with two jets are reported ($4\ell jj$ production, with $\ell = e, \mu$). For four-lepton invariant masses greater than twice the Z boson mass, this final state is dominated by the strong $ZZjj$ and EW $ZZjj$ processes, with the Z bosons decaying via $ZZ \rightarrow \ell^+\ell^-\ell^+\ell^-$. Contributions from γ^* and Z^* are increasingly important at four-lepton invariant masses that are lower than twice the Z boson mass. Differential cross-sections are particularly useful for probing the electroweak and strong production mechanisms. In the case of EW $4\ell jj$ production, differential cross-sections can be used to search for anomalous WWZ and $WWZZ$ interactions, which have different Lorentz structures to the corresponding interactions in the SM and can therefore distort the kinematic properties of the electroweak process. For strong $4\ell jj$ production, the differential cross-sections allow the perturbative QCD calculations to be confronted in extreme phase space regions such as high dijet invariant mass. The differential cross-sections are measured as a function of three types of observables:

- *Vector boson scattering (VBS) observables* are those that are used to characterise the vector-boson scattering process shown in Figure 1 (left). The measured observables are the four-lepton invariant mass, $m_{4\ell}$, the transverse momentum of the four-lepton system, $p_{T,4\ell}$, the dijet invariant mass, m_{jj} , the rapidity interval spanned by the dijet system, $|\Delta y_{jj}|$, and the transverse momentum of the dijet system, $p_{T,jj}$.¹
- *Polarisation, charge conjugation, and parity observables*: The polarisation of the Z boson can be probed using the cosine of the angle between the negatively-charged lepton and the Z boson as measured in the centre-of-mass frame of the Z boson. Two angles are measured, $\cos \theta_{12}^*$ and $\cos \theta_{34}^*$, which are sensitive to the polarisation of the leading and subleading Z boson candidates, respectively (the leading Z boson candidate is defined as part of the event selection in Section 4). The charge conjugation (C) and parity (P) structure of the WWZ and $WWZZ$ interactions can be probed using

¹ ATLAS uses a right-handed coordinate system with its origin at the nominal interaction point (IP) in the centre of the detector and the z -axis along the beam pipe. The x -axis points from the IP to the centre of the LHC ring, and the y -axis points upwards. Cylindrical coordinates (r, ϕ) are used in the transverse plane, ϕ being the azimuthal angle around the z -axis. The pseudorapidity is defined in terms of the polar angle θ as $\eta = -\ln \tan(\theta/2)$. Angular distance is measured in units of $\Delta R \equiv \sqrt{(\Delta\eta)^2 + (\Delta\phi)^2}$.

the signed azimuthal angle between the two jets, $\Delta\phi_{jj} = \phi_f - \phi_b$, where the jets in the dijet system are ordered such that $y_f > y_b$ [5].

- *QCD-sensitive observables* probe higher-order real emission of quarks and gluons from the $4\ell jj$ processes. The measured observables are the transverse momentum of the $4\ell jj$ system, $p_{\mathrm{T},4\ell jj}$, and the scalar sum of transverse momentum of the four leptons and the two jets, $S_{\mathrm{T},4\ell jj}$.

The observables are measured in VBS-enhanced and VBS-suppressed phase space regions. The selection cuts that define the fiducial region of the differential cross-section measurements is given in Section 6.

The differential cross-sections are sensitive to anomalous weak-boson self-interactions, which are predicted by effective field theory (EFT) extensions to the SM. Of particular interest are the operators in dimension-eight EFT, which induce anomalous quartic interactions (such as $WWZZ$) without any corresponding triple gauge coupling (such as WWZ) [6]. Such operators can only be tested using VBS and triboson processes. The differential cross-sections measured in this paper are used in Section 9 to constrain the contribution of these purely quartic weak-boson self-interactions.

2 ATLAS detector

The ATLAS detector [7] at the LHC covers nearly the entire solid angle around the collision point. It consists of an inner tracking detector surrounded by a thin superconducting solenoid, electromagnetic and hadron calorimeters, and a muon spectrometer incorporating three large superconducting air-core toroidal magnets.

The inner-detector system (ID) is immersed in a 2 T axial magnetic field and provides charged-particle tracking in the range $|\eta| < 2.5$. The high-granularity silicon pixel detector covers the vertex region and typically provides four measurements per track, the first hit normally being in the insertable B-layer (IBL) installed before Run 2 [8, 9]. It is followed by the silicon microstrip tracker (SCT), which usually provides eight measurements per track. These silicon detectors are complemented by the transition radiation tracker (TRT), which enables radially extended track reconstruction up to $|\eta| = 2.0$. The TRT also provides electron identification information based on the fraction of hits (typically 30 in total) above a higher energy-deposit threshold corresponding to transition radiation.

The calorimeter system covers the pseudorapidity range $|\eta| < 4.9$. Within the region $|\eta| < 3.2$, electromagnetic calorimetry is provided by barrel and endcap high-granularity lead/liquid-argon (LAr) calorimeters, with an additional thin LAr presampler covering $|\eta| < 1.8$ to correct for energy loss in material upstream of the calorimeters. Hadron calorimetry is provided by the steel/scintillator-tile calorimeter, segmented into three barrel structures within $|\eta| < 1.7$, and two copper/LAr hadron endcap calorimeters. The solid angle coverage is completed with forward copper/LAr and tungsten/LAr calorimeter modules optimised for electromagnetic and hadronic energy measurements respectively.

The muon spectrometer (MS) comprises separate trigger and high-precision tracking chambers measuring the deflection of muons in a magnetic field generated by the superconducting air-core toroidal magnets. The field integral of the toroids ranges between 2.0 and 6.0 T m across most of the detector. Three layers of precision chambers, each consisting of layers of monitored drift tubes, cover the region $|\eta| < 2.7$, complemented by cathode-strip chambers in the forward region, where the background is highest. The muon trigger system covers the range $|\eta| < 2.4$ with resistive-plate chambers in the barrel, and thin-gap chambers in the endcap regions.

Interesting events are selected by the first-level trigger system implemented in custom hardware, followed by selections made by algorithms implemented in software in the high-level trigger [10]. The first-level trigger accepts events from the 40 MHz bunch crossings at a rate below 100 kHz, which the high-level trigger further reduces in order to record events to disk at about 1 kHz.

An extensive software suite [11] is used in the reconstruction and analysis of real and simulated data, in detector operations, and in the trigger and data acquisition systems of the experiment.

3 Data and simulation

The data used in this measurement correspond to an integrated luminosity of 140 fb^{-1} and were recorded using single-lepton and multi-lepton triggers. The minimum trigger thresholds on transverse momentum depends on the lepton flavour, lepton multiplicity and data-taking periods, and vary between $20 - 26 \text{ GeV}$ and $8 - 24 \text{ GeV}$ for the single-lepton and multi-lepton triggers, respectively. The leptons that fire the trigger are required to be part of the four-lepton system that defines the signal region of the analysis (discussed in Section 4). The trigger efficiency for inclusive $4\ell jj$ events is close to unity.

The signal and background processes were modelled using Monte Carlo (MC) event generator simulations. Strong $4\ell jj$ production was modelled using **SHERPA** 2.2.2 [12]. The fully leptonic final state was simulated using matrix elements at next-to-leading-order (NLO) accuracy in perturbative QCD for up to one additional parton and at leading-order (LO) accuracy for up to three additional parton emissions. Samples for the loop-induced process $gg \rightarrow ZZ$ were simulated using matrix elements accurate a leading order (LO) in QCD for up to one additional parton emission, normalised using an $m_{4\ell}$ -dependent k -factor at NLO accuracy in QCD [13, 14], and including an additional, constant correction of about 1.2 to reproduce next-to-next-to-leading-order (NNLO) calculations for the Higgs-mediated process [15, 16]. Despite of the approximation of NNLO effects, the normalisation uncertainty for the $gg \rightarrow ZZ$ process is still conservatively considered from the NLO calculation. The matrix element calculations were matched and merged with the **SHERPA** parton shower based on Catani–Seymour dipole factorisation [17, 18] using the MEPS@NLO prescription [19–22]. The virtual QCD corrections were provided by the **OPENLOOPS** library [23–25]. The NNPDF3.0NNLO set of parton distribution functions (PDF) were used [26], along with the dedicated set of tuned parton-shower parameters developed by the **SHERPA** authors. This prediction is referred to as **SHERPA** strong $4\ell jj$.

An alternative prediction for strong $4\ell jj$ production is obtained using **MADGRAPH5_aMC@NLO** [27]. The sample was simulated using matrix elements at NLO accuracy in QCD for up to one parton in the final state, and with the PDF4LHC15 NLO set of PDFs [28]. The **MADGRAPH5_aMC@NLO** generator was interfaced to **PYTHIA8** to provide parton showering, hadronisation, and underlying-event activity, using the A14 set of tuned parameters [29]. To remove overlap between the matrix element and the parton shower, the different jet multiplicities were merged using the FxFx prescription [30]. **EVTGEN** was used for the properties of the bottom and charm hadron decays. The $gg \rightarrow ZZ$ contribution is again estimated by using **SHERPA**. This prediction is referred to as **MG5_NLO+Py8** strong $4\ell jj$.

Electroweak $4\ell jj$ production is modelled using **MADGRAPH5** [27]. The Feynman diagrams used in the calculation include the t -channel exchange of an electroweak boson and the s -channel processes that contribute at the same order in α_{EW} , i.e ZZV production (with $V \rightarrow jj$). The calculation is accurate to LO in perturbative QCD and uses the NNPDF3.0NLO PDF set. The events were passed through **PYTHIA8**

to provide parton showering, hadronisation, and underlying-event activity using the A14 set of tuned parameters. This prediction is referred to as MG5+Py8 EW $4\ell jj$.

An alternative prediction for EW $4\ell jj$ production is obtained using the Powheg-Box v2 event generator [31–35]. The Feynman diagrams are restricted to the t -channel exchange of an electroweak boson and the matrix elements calculated at NLO in perturbative QCD, using the NNPDF3.0NLO parton distribution functions. The events are passed through Pythia8 to produce the fully hadronic final state, using the A14 set of tuned parameters. The s -channel contributions from ZZV production are estimated with the Sherpa 2.2.2 generator, at NLO accuracy for the inclusive process and to LO accuracy for up to two additional parton emissions using the NNPDF3.0NNLO PDF set and the dedicated set of tuned parton-shower parameters developed by the Sherpa authors. The triboson events are added to those from Powheg+Pythia8 to produce the alternative EW $4\ell jj$ prediction. The triboson contribution is about 7% in the fiducial region used in this measurement. This prediction is referred to as Powheg+Pythia8 EW $4\ell jj$.

Background processes with four prompt leptons arise from $t\bar{t}Z$ production as well as WWZ and WZZ production. The production of $t\bar{t}Z$ events was modelled using the Sherpa 2.2.0 generator at LO accuracy, using the MEPS@LO set-up [21, 22] with up to one additional parton. The default Sherpa parton shower was used along with the NNPDF3.0NNLO [26] PDF set. The sample is scaled such that it reproduces the ATLAS measurement of $t\bar{t}Z$ production [36]. The production of WWZ and WZZ events were simulated with the Sherpa 2.2.2 generator. The predictions are accurate to NLO in QCD for the inclusive process and to LO for up to two additional parton emissions. The NNPDF3.0NNLO PDF set was used along with the dedicated set of tuned parton-shower parameters developed by the Sherpa authors. The sample is scaled such that it reproduces the ATLAS measurement of triboson production [37].

Background processes that do not contain four prompt leptons are estimated by using a data-driven technique as outlined in Section 5. The method is cross-checked using simulations of the relevant processes. Production of $WZjj$ with the subsequent leptonic decays of vector bosons was modelled with Sherpa 2.2.2, using the same approach as in strong $4\ell jj$ production. Non-prompt backgrounds arising from $Z + \text{jets}$ were simulated using Sherpa 2.2.1 [12] at NLO accuracy in perturbative QCD for up to two partons and LO accuracy for up to four partons. The matrix elements were calculated with the Comix [17] and OPENLOOPS libraries and matched with the Sherpa parton shower using the MEPS@NLO prescription. The sample was produced with the NNPDF3.0NNLO PDF set, the dedicated set of tuned parton-shower parameters developed by the Sherpa authors, and was normalised to a prediction accurate to NNLO in QCD [38]. The production of $t\bar{t}$ events was modelled using the Powheg-Box v2 [31–34] generator at NLO with the NNPDF3.0NLO PDF set and the h_{damp} parameter set to 1.5 times the top mass [39]. The events were interfaced to Pythia8 to model the parton shower, hadronisation, and underlying event, with parameters set according to the A14 tune.

All samples were passed through a detailed simulation of the ATLAS detector [40] based on GEANT4 [41]. Simulated inelastic pp collisions were overlaid to model additional pp collisions in the same and neighbouring bunch crossings (pile-up). The simulated events were then reweighted to match the pile-up conditions in the data. All simulated events were processed using the same reconstruction algorithms as used in data. Furthermore, the lepton and jet momentum scale and resolution, and the lepton reconstruction, identification, isolation and trigger efficiencies in the simulation were corrected to match those measured in data.

4 Event and object selection

Events are selected for analysis if they were recorded during stable beam conditions and if they satisfy stringent data-quality requirements [42]. Proton–proton interaction vertices are reconstructed using ID tracking information [43] and each reconstructed vertex is required to have at least two associated tracks. Events are required to have at least one reconstructed vertex, with the primary vertex defined as the one with the largest sum of squared track transverse momenta.

Muons are reconstructed from information in the MS and the ID. *Baseline* muons are required to satisfy the ‘Loose’ identification criteria [44] and are required to be associated with the primary hard-scatter vertex by requiring $|z_0 \sin\theta| < 0.5$ mm, where z_0 is the longitudinal difference between the primary vertex and the point at which the muon transverse impact parameter is measured. Baseline muons are required to have $p_T > 5$ GeV and $|\eta| < 2.7$. *Signal* muons are required to satisfy the baseline muon criteria and the ‘Loose’ particle-flow-based isolation working point [44]. They are also required to satisfy $d_0/\sigma_{d_0} < 3$, where d_0 is the transverse impact parameter calculated relative to the measured beam-line position and σ_{d_0} is its uncertainty.

Electrons are reconstructed from topological clusters of energy deposited in the electromagnetic calorimeter that are matched to an ID track. *Baseline* electrons are required to satisfy the ‘VeryLoose’ identification criteria [45] and to be associated with the primary hard-scatter vertex, by requiring $|z_0 \sin\theta| < 0.5$ mm. Baseline electrons are required to have $p_T > 7$ GeV and $|\eta| < 2.47$. *Signal* electrons are required to satisfy the baseline electron criteria and the ‘LooseAndBLayer’ identification [45] and ‘Loose’ isolation [46] working points. They are also required to satisfy $d_0/\sigma_{d_0} < 5$.

Jets are reconstructed using the anti- k_t algorithm [47, 48] with a radius parameter of $R = 0.4$. The inputs to the algorithm are objects constructed using the particle-flow algorithm [49], based on noise-suppressed positive-energy topological clusters in the calorimeter. Energy deposited in the calorimeter by charged particles is subtracted and replaced by the momenta of ID tracks which are matched to those topological clusters. The jets are initially calibrated using simulations and corrected using in situ measurements of the jet energy scale that is determined from dijet, $\gamma + \text{jet}$ and $Z + \text{jet}$ events [50]. Jets are required to have $p_T > 30$ GeV and $|\eta| < 4.5$. To reduce the impact of jets that originate from pile-up interactions, jets with $|\eta| < 2.4$ and $p_T < 60$ GeV, or with $2.4 < |\eta| < 4.5$ and $p_T < 50$ GeV, are required to satisfy the ‘Tight’ working points of the jet vertex tagging algorithms [51, 52]. To remove leptons reconstructed as jets, any jets within the range $\Delta R < 0.2$ of an electron are rejected. A similar requirement is applied to jets that overlap with muons, if there are less than three ghost-associated [53] ID tracks within the jet.

Events are required to have at least four (baseline) leptons. The two leptons with the largest transverse momentum are required to satisfy $p_T > 20$ GeV. All possible combinations of same-flavour opposite-charge (SFOC) lepton pairs are formed and each pair is required to satisfy $m_{\ell\ell} > 5$ GeV and $\Delta R(\ell, \ell) > 0.05$, which reduces backgrounds from the leptonic decays of hadrons. The SFOC pairs are then ordered by $|m_{\ell\ell} - m_Z|$. The two Z -boson candidates are defined as the two SFOC pairs that have the smallest value of $|m_{\ell\ell} - m_Z|$ and are formed from different leptons. The leading Z -boson candidate is defined as the one that has the largest value of $|y_{\ell\ell}|$. The invariant mass of the four leptons is required to satisfy $m_{4\ell} > 130$ GeV and each lepton in the quadruplet is required to satisfy the signal lepton definition discussed earlier. Events are also required to contain at least two jets, with the highest transverse momentum jet satisfying $p_T > 40$ GeV. The dijet system is then defined as the two leading (highest transverse momentum) jets in the event that have $\eta_{j_1} \times \eta_{j_2} < 0$. The dijet system is required to satisfy $|\Delta y_{jj}| > 2.0$ and $m_{jj} > 300$ GeV.

Process	Event yield \pm stat. \pm syst.	
	VBS-enhanced	VBS-suppressed
strong $4\ell jj$ (SHERPA)	$98.9 \pm 0.5 \pm 25.2$	$45.5 \pm 0.3 \pm 12.9$
EW $4\ell jj$ (MG5+Py8)	$24.1 \pm 0.1 \pm 1.8$	$2.12 \pm 0.02 \pm 0.14$
Prompt background	$18.8 \pm 0.2 \pm 2.2$	$5.5 \pm 0.1 \pm 0.4$
Non-prompt background	$3.0 \pm 0.6 \pm 3.2$	$1.1 \pm 0.5 \pm 1.2$
Total prediction	$144 \pm 1 \pm 26$	$54 \pm 1 \pm 13$
Data	169	53

Table 1: Measured and predicted event yields in the VBS-enhanced and VBS-suppressed regions. The background arising from non-prompt leptons is calculated using a data-driven technique as outlined in Section 5. The systematic uncertainties in the predictions are estimated by using the procedure outlined in Section 7.

The events that satisfy the selections listed above are then divided into *VBS-enhanced* and *VBS-suppressed* regions using the centrality of the four-lepton system,

$$\zeta = \left| \frac{[y_{4\ell} - 0.5(y_{j_1} + y_{j_2})]}{\Delta y_{jj}} \right|, \quad (1)$$

where $y_{4\ell}$ is the rapidity of the four lepton system and y_{j_1} (y_{j_2}) is the rapidity of the leading (subleading) jet in the dijet system. The VBS-enhanced (VBS-suppressed) region is defined as $\zeta < 0.4$ ($\zeta > 0.4$).

The measured and predicted event yields in the VBS-enhanced and VBS-suppressed regions are shown in Table 1. The event yields as a function of m_{jj} and $m_{4\ell}$ are shown in Figure 2, for both the VBS-enhanced and VBS-suppressed regions. In total, 169 events are reconstructed in the VBS-enhanced region and 53 events in the VBS-suppressed region. In both of the regions, the backgrounds are small and the event yields are dominated by $4\ell jj$ production. In the VBS-enhanced region, the electroweak process is predicted to be about 17% of the event yield, but this rises to about 40% of the event yield at high- m_{jj} . There is a modest contribution from background processes that is typically at the 5%–10% level, but reaching 20% at the lowest values of $m_{4\ell}$. The background arising from non-prompt leptons is calculated using a data-driven technique as outlined in Section 5. Overall, the data are in good agreement with the signal simulations and predicted backgrounds.

5 Backgrounds

Processes with leptons that do not originate from the decay of a Z boson are considered as backgrounds in this analysis. Background processes with at least four prompt leptons, such as $t\bar{t}Z$ production and the fully leptonic decays of WWZ and WZZ production, are estimated by using the MC simulations presented in Section 3.

Backgrounds that contain one or more non-prompt leptons arise from $WZjj$ production (where an additional jet produces a non-prompt lepton) and $t\bar{t}$ production (where the b -hadrons produced in the top/anti-top decay are the main sources of the non-prompt leptons). These backgrounds are typically poorly modelled in simulation and are estimated using a data-driven method, whereby their event yield is

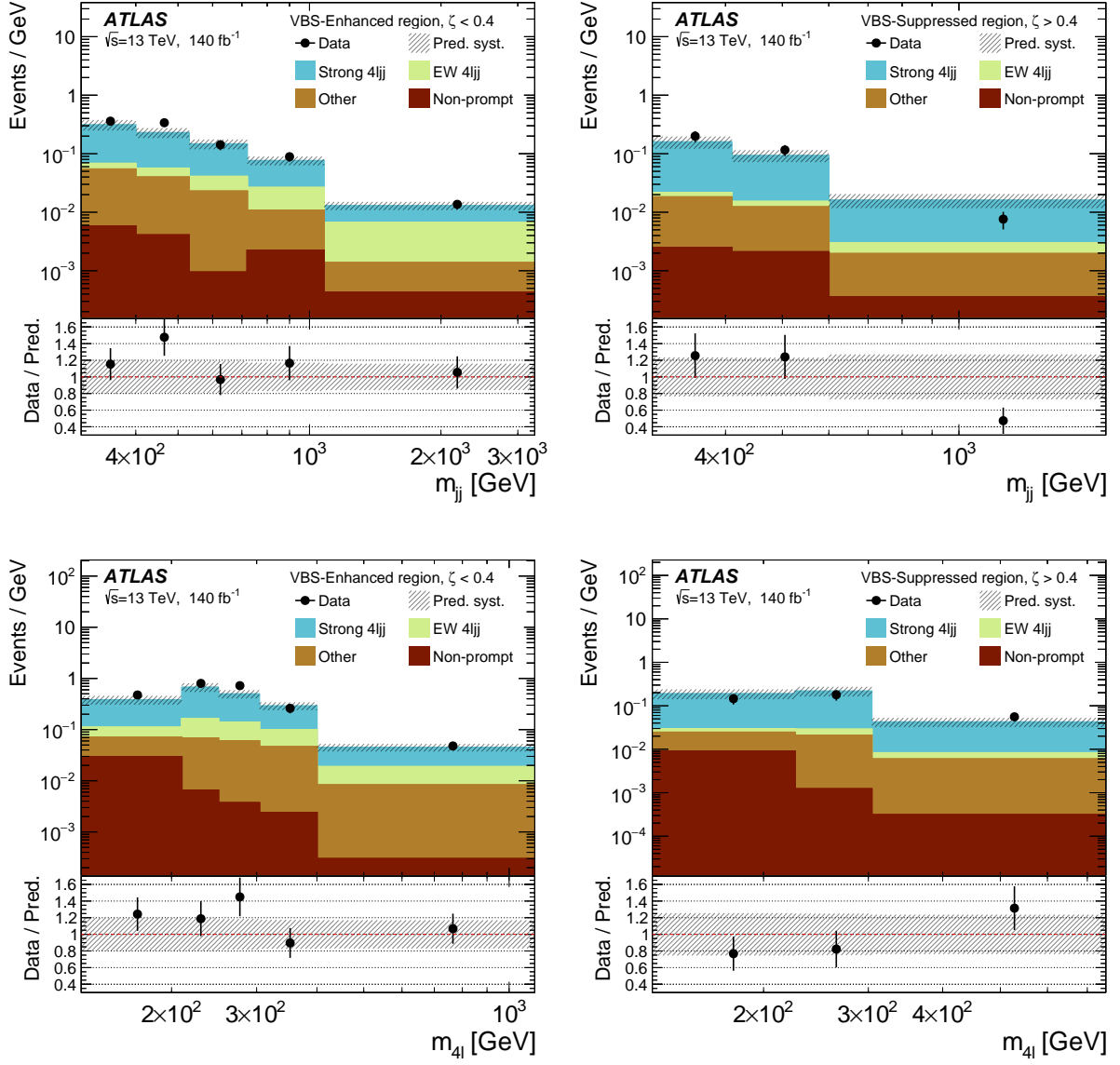


Figure 2: Predicted and observed yields as a function of m_{jj} (top) and m_{4l} (bottom), measured in the VBS-enhanced (left) and VBS-suppressed (right) regions. The data are represented as black points and the associated error bars represent the statistical uncertainty. The background arising from non-prompt leptons is estimated using a data-driven technique as outlined in Section 5. Background processes with four prompt leptons, such as $t\bar{t}Z$ production and the fully leptonic decays of WWZ and WZZ production, are estimated by using simulations and labelled as ‘Other.’ The total uncertainty on the combined signal and background prediction is shown as a grey band (the calculation of these uncertainties is outlined in Section 7).

measured in a control region enriched in non-prompt leptons and extrapolated to the signal region using a scaling factor based on the non-prompt lepton efficiency.

The control region is defined using the same event selection as outlined in Sec. 4, but with one (or more) of the four leptons that define the Z boson candidates failing to meet the *signal* lepton definition. The event yields per bin of a measured distribution are then extrapolated to the signal region by applying a weight of $f/(1 - f)$ for each non-*signal* lepton in each event, where f is the non-prompt lepton efficiency and defined as the fraction of *baseline* non-prompt leptons that satisfy the *signal*-lepton definition. The contribution to the event yields in the control region from processes with at least four prompt leptons are subtracted before the extrapolation. That contribution is typically at the 5%–10% level, though rises to 20% at the largest $m_{4\ell}$.

The non-prompt lepton efficiency is calculated in data using $Z + \text{jet}$ events and $t\bar{t}$ events. Candidate $Z + \text{jet}$ events are required to have a SFOC lepton pair with an invariant mass within 10 GeV of the Z boson mass, whereas the $t\bar{t}$ candidate events are required to have an opposite-flavour opposite-charge lepton pair. The events are then required to have one additional baseline lepton. The non-prompt lepton efficiency is calculated using this additional lepton, after correcting the event yields for contributions from processes that produce at least three prompt leptons, as a function of the lepton p_T , the lepton η and the number of jets in the event. The non-prompt leptons in $Z + \text{jet}$ events arise mainly from light-flavour decays, whereas they arise mainly from heavy-flavour decays in $t\bar{t}$ events. The two non-prompt lepton efficiency measurements are therefore combined to reflect the expected flavour composition of non-prompt leptons in the signal region of this analysis, as estimated by using the simulations presented in Section 3.

6 Correction for detector effects

Particle-level differential cross-sections for $4\ell jj$ production in the VBS-enhanced and VBS-suppressed regions are obtained by correcting the background-subtracted event yields for the effects of detector inefficiency and resolution.

The particle-level fiducial phase space is defined using stable final-state particles with a lifetime of $c\tau > 10$ mm. Dressed leptons are used to define the Z boson candidates. Electrons and muons are required to be prompt (i.e., to not originate from the decay of a hadron) and the dressed lepton is defined as the four-vector sum of the electron (or muon) and all prompt photons within a range of $\Delta R < 0.1$. Dressed electrons are required to have $p_T > 7$ GeV and $|\eta| < 2.47$. Dressed muons are required to have $p_T > 5$ GeV and $|\eta| < 2.7$. Jets are defined using the anti- k_t algorithm with radius parameter set to 0.4. All stable particles except dressed leptons are used as input to the jet-finding algorithm. Jets are required to have $p_T > 30$ GeV and $|\eta| < 4.5$.

To minimise model-dependence in the final result, the kinematic criteria used to define the particle-level fiducial regions are similar to the criteria applied to the reconstructed data in Sec 4. At least four dressed leptons are required and the two leptons with the largest transverse momenta are required to have $p_T > 20$ GeV. All possible SFOC lepton pairs are formed and later ordered by $|m_{\ell\ell} - m_Z|$. The two Z boson candidates are defined as the two SFOC pairs with the smallest value of $|m_{\ell\ell} - m_Z|$ that are constructed from different leptons. The leading Z boson candidate is defined as the one with the largest value of $|y_{\ell\ell}|$. The invariant mass of the four leptons is required to satisfy $m_{4\ell} > 130$ GeV. Events are required to contain at least two jets. The dijet system is then defined as the two leading (highest transverse momentum) jets in the event that have $\eta_{j_1} \times \eta_{j_2} < 0$. The highest transverse momentum jet is

required to have $p_T > 40$ GeV and the dijet system is required to satisfy $|\Delta y_{jj}| > 2.0$ and $m_{jj} > 300$ GeV. Measurements are carried out in two fiducial regions, with the VBF-enhanced and VBF-suppressed regions defined by $\zeta < 0.4$ and $\zeta > 0.4$, respectively, where ζ is the centrality of the diboson system defined in Equation 1.

The event yields are binned to ensure a minimum of 20 (15) events in each bin in the VBF-enhanced (VBS-suppressed) regions at detector level. The bins are also required to be larger than twice the detector resolution, which is determined using the simulated $4\ell jj$ events. For non-angular observables (e.g. m_{jj} , $m_{4\ell}$), the last bin is chosen such that less than one $4\ell jj$ event is predicted to lie above the upper bin edge. However, the ‘overflow’ events that lie above that bin edge are included in the last bin. The background-subtracted event yields are then corrected to particle level using an iterative Bayesian unfolding method [54, 55]. The measurements are unfolded using two iterations, except for the $p_{T,4\ell jj}$ distribution in the VBF-enhanced region for which three iterations are used.² The unfolding method uses simulations to (i) correct for events selected at detector level that do not satisfy the particle-level selection, (ii) correct for migrations between bins of the measured spectrum with a response matrix, and (iii) correct for events selected at particle level but not at detector level.

The default simulations used in the unfolding are the EW $4\ell jj$ sample produced using MG5+Py8 and the strong $4\ell jj$ samples produced using SHERPA. The fraction of detector-level events that are also reconstructed at particle level, referred as the fiducial fraction, is typically between 60% and 80%. About half of the non-fiducial events have at least one pile-up jet reconstructed in the dijet system, and the remaining non-fiducial events arise from low- p_T jets migrating into the fiducial volume due to jet resolution effects. The fraction of particle-level events that are also reconstructed at detector level, referred to as the efficiency, is typically between 40% and 60%. The low overall efficiency is due to inefficiencies in the trigger and the lepton reconstruction plus identification and isolation criteria. The migration among bins is typically small due to the binning methodology, and ranges from 10% to 30%.

Statistical uncertainties in the data are propagated through the unfolding using a bootstrap method [56], with 10 000 pseudo-experiments. For each pseudo-experiment, each event is randomly assigned a weight based on a Poisson distribution with a mean of one. The unfolding is then repeated using the modified distributions created from the event weights. The final statistical uncertainties in the measurement are taken to be the standard deviation of the unfolded values obtained from the ensemble of pseudo-experiments. The statistical uncertainties in the $4\ell jj$ simulations are propagated through the unfolding procedure in a similar fashion, whereby each pseudo-experiment modifies the simulations used in the unfolding procedure.

To ensure that the unfolding procedure is unaffected by the presence of beyond-the-SM physics in the data, a signal injection test has been performed using the effective field theory (EFT) predictions presented in Section 9. Pseudo-data from the EFT simulations are unfolded with the response matrices constructed from the nominal SM simulation, and the result is compared with the particle-level EFT simulation. The unfolding procedure is shown to introduce very little bias, with differences between the unfolded and particle-level distributions being much smaller than the experimental uncertainties in the measurement.

² The number of iterations is optimised so the quadrature sum of the statistical uncertainty and the unfolding bias uncertainty (discussed in Sec. 7) is minimised, whilst also requiring that the per-bin statistical uncertainty after unfolding is not smaller than that observed at detector level.

7 Systematic uncertainties

Experimental systematic uncertainties arise from differences between data and simulation in the trigger efficiency, the lepton reconstruction, the jet reconstruction, the luminosity determination, and the average number of proton–proton interactions per beam bunch crossing. These uncertainties affect the normalisation of the background processes estimated by using simulations and the simulations of the signal processes used in the unfolding procedure. For each source of uncertainty, the simulations are varied by ± 1 standard deviations and the analysis repeated. The systematic uncertainty is defined as the change in the differential cross-section relative to the nominal analysis with the default simulations.

The luminosity of the data sample is known to an accuracy of 0.83% using a combination of van der Meer beam separation scans in dedicated running periods and luminosity-sensitive detectors in standard data-taking periods [57].

The average number of proton–proton interactions per bunch crossing varies during the different data-taking periods, and the simulations are corrected to reproduce the distribution observed in the data. This procedure is impacted by an uncertainty in the ratio of the predicted and measured inelastic cross-sections within the ATLAS fiducial volume [58]. A systematic uncertainty is introduced to account for this, by scaling the average number of proton–proton interactions per bunch crossing in the simulation.

The lepton reconstruction, identification, isolation and trigger efficiencies in simulation are corrected, using scale factors, such that they match those observed in the data, as outlined in Section 3. Systematic uncertainties in this procedure are estimated by modifying the scale factors by their associated uncertainties [44, 46]. Uncertainties in the lepton momentum scale and resolution are estimated by scaling and smearing the lepton transverse momentum by the known differences between data and simulation [46, 59].

Jets are calibrated using a combination of MC-based and data-driven corrections, as discussed in Section 4. The jet energy scale and jet energy resolution uncertainties are estimated by scaling and smearing the jet four-momentum in the simulation by the associated uncertainties in the calibration procedure [50]. Furthermore, the JVT algorithm introduces an inefficiency in the jet reconstruction. The uncertainty that arises from imperfect modelling of the JVT in simulation is estimated by varying the JVT requirement [51, 52].

Backgrounds containing at least four prompt leptons are normalised to ATLAS measurements, as outlined in Section 3. The uncertainty that arises from subtracting these backgrounds is estimated by varying the normalisation of the simulated samples by an amount commensurate with the experimental precision of the ATLAS measurements. Backgrounds containing non-prompt leptons are estimated by using the data-driven method outlined in Section 5. The non-prompt background estimate contains statistical uncertainties from the finite event yields in the control regions and systematic uncertainties from the subtraction of prompt-lepton processes from those event yields. The uncertainty associated with subtracting the non-prompt backgrounds is estimated by varying the background estimates by an amount commensurate with the statistical and systematic uncertainty. Uncertainties associated with the expected flavour composition of non-prompt leptons in the signal region have been checked and found negligible.

Theoretical systematic uncertainties in the simulation of $4\ell jj$ production impact the measurement via the unfolding procedure. Three sources of uncertainty are investigated, arising from (i) the renormalisation and factorisation scale dependence in the $4\ell jj$ calculations, (ii) the parton distribution functions, and (iii) the choice of event generator.

Source	Uncertainty (%)	
	VBS-enhanced region	VBS-suppressed region
Luminosity	0.8 – 2.1	0.8 – 2.0
Leptons	0.8 – 1.6	1.0 – 1.5
Jets	2.7 – 18	3.4 – 13
Pile-up	0.0 – 2.5	0.0 – 0.7
Backgrounds	0.9 – 9.0	1.2 – 7.0
Theory modelling	0.6 – 7.5	1.2 – 8.8
Unfolding method	0.9 – 12	1.2 – 12
Total systematic	6 – 22	5 – 17

Table 2: Systematic uncertainties in the differential cross-section measurements. The range given for each uncertainty reflects the fact that the uncertainties depend on the underlying kinematics of the process and are therefore larger in some bins of certain distributions.

The default simulations used in the unfolding procedure are MG5+Py8 (EW $4\ell jj$) and SHERPA (strong $4\ell jj$). These predictions are produced with a default choice for factorisation scale, μ_F , and renormalisation scale, μ_R , but also have additional weights that allow the impact of renormalisation and scale variations to be assessed. There are six variations in total, corresponding to $\{\mu_R, \mu_F\}$ being scaled by $\{0.5, 0.5\}$, $\{0.5, 1.0\}$, $\{1.0, 0.5\}$, $\{1.0, 2.0\}$, $\{2.0, 1.0\}$, or $\{2.0, 2.0\}$. The systematic uncertainty due to scale choice for each generator prediction is then taken to be the envelope of the six scale variations. However, for the loop-induced $gg \rightarrow 4\ell$ contribution to the strong $4\ell jj$ process, the normalisation uncertainty is taken from the higher-order calculations to which the MC sample is normalised, and the scale variations are only used to assess the additional uncertainty in the shape of each distribution.

Uncertainties associated with PDFs are evaluated using the PDF4LHC recommendation [28]. First, the nominal prediction for each generator is reweighted by the 100 variations of the NNPDF PDF set (including the associated α_s variations). The standard deviation of the 100 predictions that are obtained is taken as the uncertainty in the NNPDF prediction. The nominal prediction is then reweighted to reproduce the nominal MMHT and CT14 NNLO PDF sets. The total PDF uncertainty for a given process is then taken as the envelope of the NNPDF uncertainty and the MMHT / CT14 predictions.

The dependence on the choice of event generator is evaluated by unfolding the Asimov data sample constructed from the MG5+Py8 strong $4\ell jj$ simulation with the nominal response matrix. The MG5+Py8 sample is first reweighted on an event-by-event basis to reproduce the SHERPA prediction at particle level, which avoids double counting uncertainties associated with the sample normalisation that is obtained from the factorisation and renormalisation scale variations. The difference between the unfolded event yield and the reweighted MG5_NLO+Py8 particle-level prediction is taken as a symmetric systematic uncertainty in the differential cross-section measurement.

The effect of interference between the EW $4\ell jj$ and strong $4\ell jj$ processes is estimated at leading-order in perturbative QCD using MADGRAPH5_AMC@NLO 2.6.1. The contribution is found to be far smaller than the theoretical uncertainties in the EW $4\ell jj$ and strong $4\ell jj$ calculations and no additional uncertainty is added.

Systematic uncertainties in the unfolding method are evaluated in two ways, using bias tests implemented in simulation. In the first approach, 10 000 pseudo-experiments are created by independently fluctuating

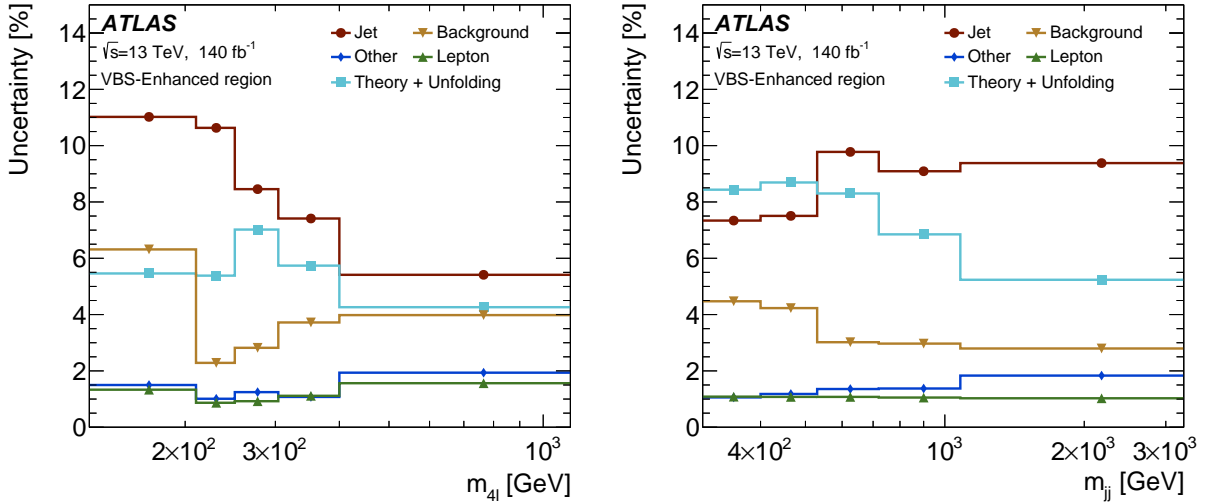


Figure 3: Systematic uncertainties in the differential cross section for $4\ell jj$ production in the VBS-enhanced region as a function of $m_{4\ell}$ (left) and m_{jj} (right).

each bin of the expected particle-level event yield for each observable. Each pseudo-experiment is then folded using the nominal response matrix and the nominal yield of ‘non-fiducial’ events is added (non fiducial events are those that satisfy the detector-level selection but not the particle-level selection). Each pseudo-experiment is then unfolded using the nominal response matrix and the bias for that pseudo-experiment is taken to be the difference between the unfolded yield and the particle-level yield for that pseudo-experiment. The bias in the unfolding method is taken to be the bias estimated when the particle-level yield has varied by ± 1 standard deviation. In the second approach, the particle-level events are reweighted such that the simulation better matches the data at detector level. The reweighted detector-level distribution is then unfolded using the nominal response matrix. The bias in the unfolding is taken to be the difference between the unfolded spectrum and the reweighted particle-level prediction. The two approaches for assessing bias in the unfolding method give similar results, and the uncertainty in the unfolding method is defined using the first approach.

A summary of the experimental and theoretical uncertainties in the differential cross-section measurements is shown in Table 2. The kinematic dependence of these uncertainties as a function of $m_{4\ell}$ and m_{jj} are shown in Figure 3. The dominant systematic uncertainties are those associated with the jet reconstruction, the theoretical modelling, and the unfolding method.

8 Results

The differential cross-sections for inclusive $4\ell jj$ production in the VBS-enhanced region as a function of $m_{4\ell}$, m_{jj} , $\Delta\phi_{jj}$, $\cos\theta_{12}^*$, $p_{T,4\ell jj}$, and $S_{T,4\ell jj}$ are shown in Figures 4, 5, and 6. The differential cross-sections as a function of $m_{4\ell}$ and m_{jj} are examples of observables that are typically used to study vector-boson scattering processes. The differential cross-sections as a function of $\cos\theta_{12}^*$ are sensitive to the polarisation of the leading Z boson candidate, whereas the differential cross-section as a function of $\Delta\phi_{jj}$ is sensitive to the charge-conjugation and parity structure of the WWZ and $WWZZ$ interactions. The differential cross-sections as a function of $p_{T,4\ell jj}$ and $S_{T,4\ell jj}$ are sensitive to the higher-order real emission of quarks

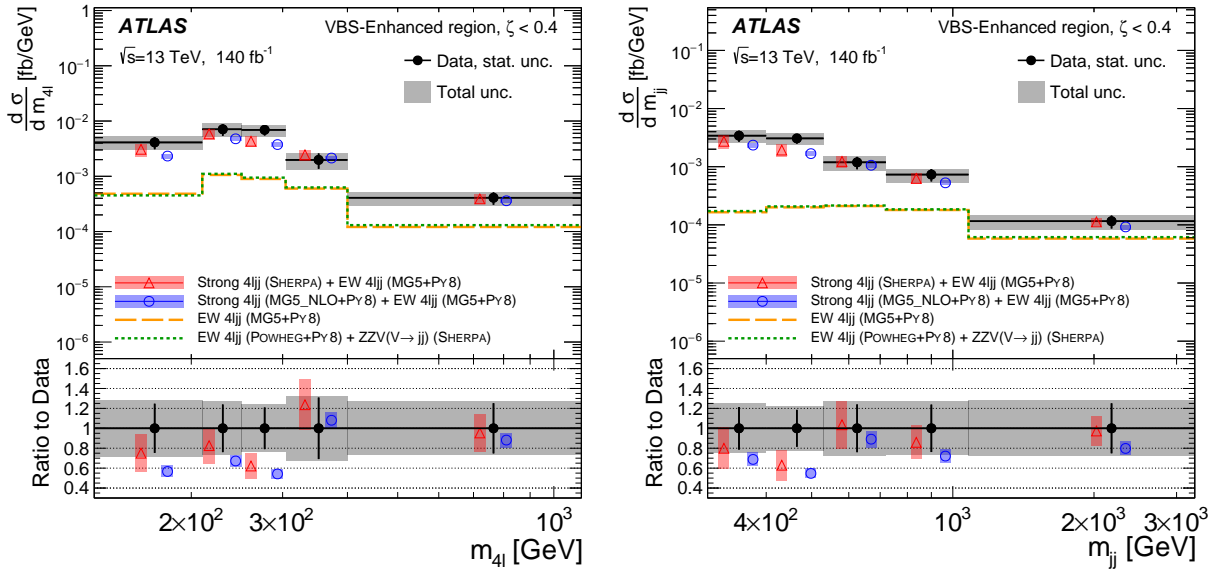


Figure 4: Differential cross-sections for inclusive $4\ell jj$ production in the VBS-enhanced region as a function of $m_{4\ell}$ (left) and m_{jj} (right). The data are represented as black points and the associated error bars represent the statistical uncertainty. The total uncertainty in the measurement is represented as a grey hatched band. The data are compared with two theoretical predictions, estimated by using SHERPA (triangles) and MADGRAPH5 (circles) for the strong $4\ell jj$ contribution and MG5+Py8 for the EW $4\ell jj$ contribution. The band on the theoretical predictions represents the theoretical uncertainty from renormalisation/factorisation scale choices and PDF choice. The dashed lines show the contribution of EW $4\ell jj$ production to the differential cross-section as predicted by MG5+Py8 and Powheg+Pythia8. The s -channel contributions from ZZV production are missing from the Powheg+Pythia8 prediction and are estimated with SHERPA. ‘Overflow’ events that lie above the upper bin edge of the last bin are included in that bin.

and gluons from the $4\ell jj$ processes. Differential cross-sections as a function of other kinematic variables (or in the VBS-suppressed region) are presented in the Appendix.

The data are compared with two theoretical predictions, constructed from MG5+Py8 for the EW $4\ell jj$ process and either SHERPA or MG5_NLO+Py8 for the strong $4\ell jj$ process. Scale uncertainties in each $4\ell jj$ prediction are estimated by varying the renormalisation and factorisation scales used in the matrix-element calculation independently by a factor of 0.5 or 2.0. Uncertainties in the $4\ell jj$ predictions due to PDFs are estimated for SHERPA by reweighting the nominal sample to reproduce the 100 variations of the NNPDF PDF sets (including the associated α_s variations) and taking the RMS of these variations, and for MG5+Py8 following the PDF4LHC recommendations. The impact of PDF-related uncertainties are found to be much smaller than the impact of scale uncertainties.

The prediction obtained using SHERPA for strong $4\ell jj$ production is found to be in satisfactory agreement with the data for all measured distributions in the VBS-enhanced region. However, the prediction obtained using MG5+Py8 for strong $4\ell jj$ production is found to underestimate the inclusive $4\ell jj$ cross-section in all distributions, but the disagreement is especially noticeable at low m_{jj} , low $m_{4\ell}$ and low $|\Delta\phi_{jj}|$. The central values of the SHERPA prediction are also below the data, but the agreement with data is improved for SHERPA due to the larger theoretical uncertainty in the prediction as estimated from scale variations. The formal accuracy of the calculations is similar, but not identical. Both the predictions are accurate at LO in QCD for the $4\ell jj$ final state. However, SHERPA simulates additional jet activity at LO in QCD whereas MG5+Py8 relies on the Pythia8 parton shower, which is only accurate to leading logarithm. This

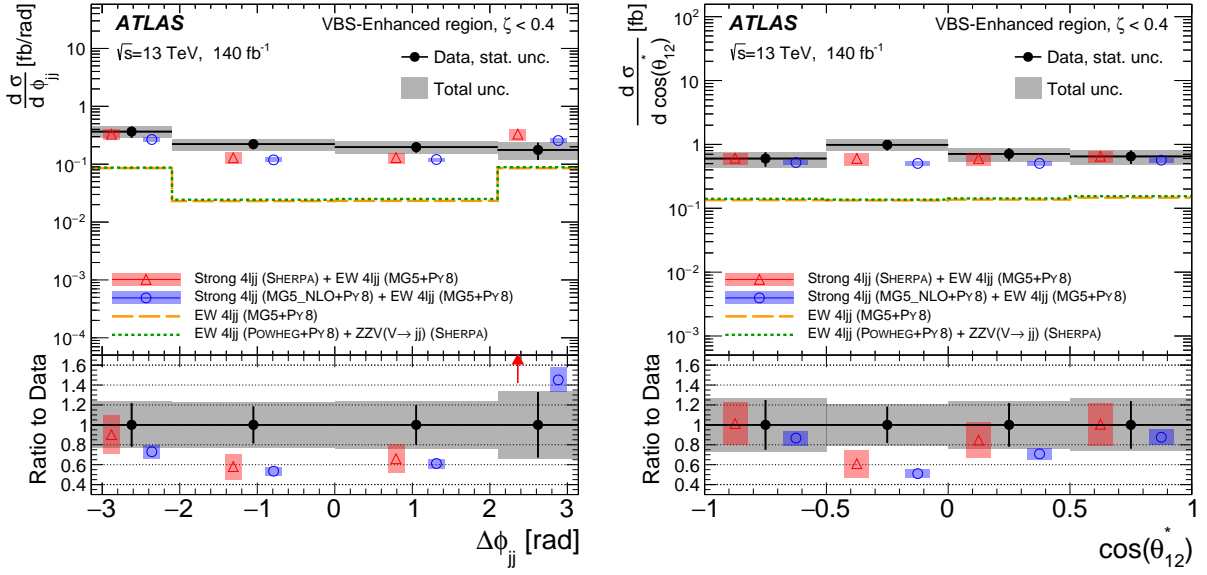


Figure 5: Differential cross-sections for inclusive $4\ell jj$ production in the VBS-enhanced region as a function of $\Delta\phi_{\ell j}$ (left) and $\cos \theta_{12}^*$ (right). The data are represented as black points and the associated error bars represent the statistical uncertainty. The total uncertainty in the measurement is represented as a grey hatched band. The theoretical predictions are constructed in the same way as in Figure 4.

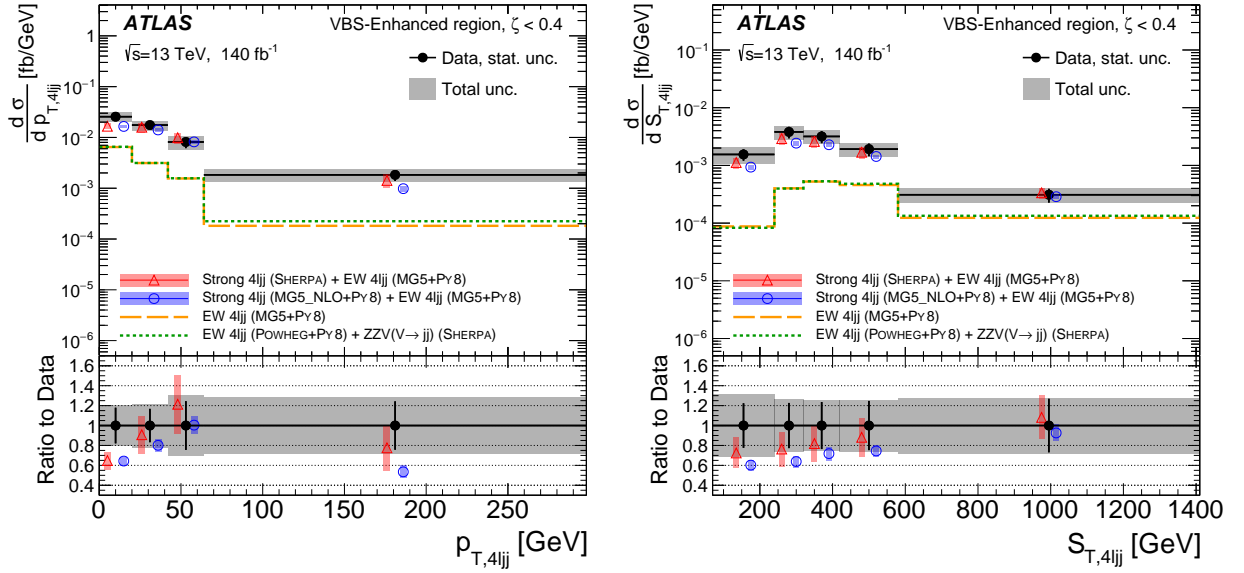


Figure 6: Differential cross-sections for inclusive $4\ell jj$ production in the VBS-enhanced region as a function of $p_{T,4\ell jj}$ (left) and $S_{T,4\ell jj}$ (right). The data are represented as black points and the associated error bars represent the statistical uncertainty. The total uncertainty in the measurement is represented as a grey hatched band. The theoretical predictions are constructed in the same way as in Figure 4. ‘Overflow’ events that lie above the upper bin edge of the last bin are included in that bin.

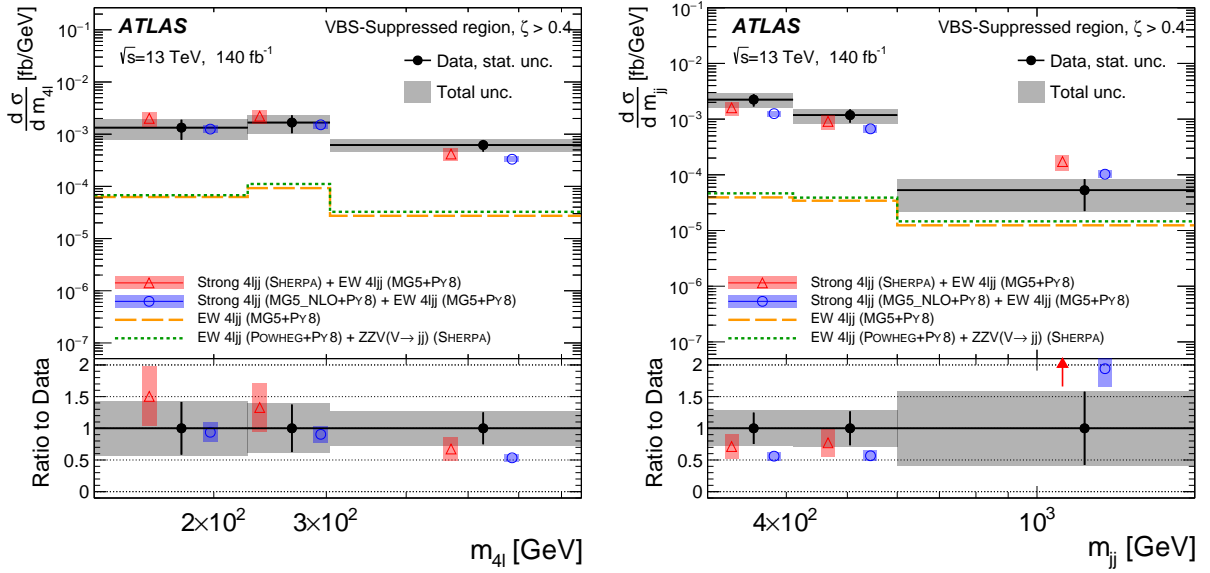


Figure 7: Differential cross-sections for inclusive $4\ell jj$ production in the VBS-suppressed region as a function of $m_{4\ell}$ (left) and m_{jj} (right). The data are represented as black points and the associated error bars represent the statistical uncertainty. The total uncertainty in the measurement is represented as a grey hatched band. The theoretical predictions are constructed in the same way as for Figure 4. ‘Overflow’ events that lie above the upper bin edge of the last bin are included in that bin.

may have an impact because the event selection identifies the two ‘tagging’ jets as the highest transverse momentum jets that satisfy $\eta_{j_1} \times \eta_{j_2} < 0$, which may select the third-highest transverse momentum jet in some instances.

The EW $4\ell jj$ contribution is also shown separately in Figures 4–6 to show the sensitivity of the measurements to the electroweak process. The electroweak contribution is about 20% of the measured $4\ell jj$ cross-section in the VBS-enhanced region. However, it is much larger at high m_{jj} , where it accounts for about 50% of the measured cross-section, and much lower at low m_{jj} , where it accounts for just 5%. Furthermore, the POWHEG+PYTHIA8 EW $4\ell jj$ prediction is in very good agreement with the MG5+Py8 EW $4\ell jj$ prediction for all measured distributions, demonstrating that the choice of EW $4\ell jj$ model has very little impact on the inclusive $4\ell jj$ prediction.

The differential cross-sections for inclusive $4\ell jj$ production in the VBS-suppressed region as a function of $m_{4\ell}$ and m_{jj} are shown in Figure 7. The data are again compared with the two theoretical predictions that are estimated by using MG5+Py8 for the EW $4\ell jj$ process and either SHERPA or MADGRAPH5 for the strong $4\ell jj$ process. The electroweak contribution is less than 5% of the measured $4\ell jj$ cross-section in this region, and remains below 15% even at the highest values of m_{jj} . The prediction obtained using SHERPA for strong $4\ell jj$ production is found to be in satisfactory agreement with the data for the measured distributions, except at the largest values of m_{jj} where the predicted cross section is too large. This feature has been observed in previous measurements sensitive to vector-boson fusion and vector-boson scattering [60]. The prediction obtained with MG5+Py8 is in good agreement with the data at low- $m_{4\ell}$, but underestimates the inclusive $4\ell jj$ cross-section at high- $m_{4\ell}$ and low- m_{jj} .

9 Effective field theory interpretation

The differential cross-sections can be used to search for signatures of physics beyond the SM. For measurements sensitive to vector-boson scattering, dimension-eight effective field theory (EFT) modeling can be a tool, whereby the SM Lagrangian is extended with new interactions encoded in dimension-eight operators, i.e.,

$$\mathcal{L} = \mathcal{L}_{\text{SM}} + \sum_i \frac{f_{\text{T},i}}{\Lambda^4} O_{\text{T},i}$$

where \mathcal{L}_{SM} is the SM Lagrangian, $O_{\text{T},i}$ are a set of the dimension-eight operators, and the $f_{\text{T},i}/\Lambda^4$ are Wilson coefficients that specify the strength of the anomalous interactions. The $O_{\text{T},i}$ operators are particularly interesting as they only induce anomalous quartic weak-boson self-interactions [6] and can only be tested using vector-boson scattering processes or triboson production. In focussing on the dimension-eight operators, it is implicitly assumed that the contribution from dimension-six operators is zero, i.e., that they are already constrained from measurements of diboson production [4, 61–64] and vector-boson fusion [60]. However, constraints on the Wilson coefficients of operators in a dimension-six effective field theory are presented in the Appendix for completeness.

The squared scattering amplitude for the effective field theory prediction can be written as

$$|\mathcal{M}|^2 = |\mathcal{M}_{\text{SM}}|^2 + 2 \text{Re}(\mathcal{M}_{\text{SM}}^* \mathcal{M}_{\text{d8}}) + |\mathcal{M}_{\text{d8}}|^2,$$

where \mathcal{M}_{SM} is the SM scattering amplitude and \mathcal{M}_{d8} is a non-SM scattering amplitude that contains anomalous interactions. The cross-section therefore contains three contributions: the SM contribution, the interference between the SM amplitude and the dimension-eight amplitude, and a pure dimension-8 contribution. The interference term and the pure dimension-eight term contribute at order $f_{\text{T},i}/\Lambda^4$ and $f_{\text{T},i}^2/\Lambda^8$, respectively. At large values of the Wilson coefficients, the contribution of the pure dimension-eight term can therefore be larger than the interference contribution, and the theoretical prediction is then sensitive to missing higher-orders in the EFT expansion that contribute at order $1/\Lambda^8$.

Theoretical predictions for the interference and pure dimension-eight contributions to EW $Z Z j j$ production are produced using **MADGRAPH5**. Simulated events are produced for each operator separately with the associated Wilson coefficient set to unity. The events are passed through **PYTHIA8** to produce the $Z Z \rightarrow \ell^+ \ell^- \ell^+ \ell^-$ decay channel and to simulate the fully hadronic final state using the A14 set of tuned parameters. For each operator, the effective field theory prediction is given by the sum of the interference contribution, the pure-dimension-8 contribution, the MG5+Py8 EW $4\ell jj$ prediction, and the **SHERPA** strong $4\ell jj$ prediction. The interference contribution has a linear dependence on the Wilson coefficient, whereas the pure-dimension-8 contribution has a quadratic dependence. This enables modelling of theoretical predictions for any value of a given Wilson coefficient.

The measured differential cross-section as a function of $m_{4\ell}$ and m_{jj} in the VBS-enhanced region and the associated EFT-dependent theoretical predictions are used to define a likelihood function, assuming Gaussian-distributed uncertainties. Statistical correlations between the bins of the differential cross-section measurements are estimated by using a bootstrap procedure (as outlined in Section 6) and included in the covariance matrix in the likelihood function. Each source of systematic uncertainty in the measurement is also included in the covariance matrix and is assumed to be fully correlated between the bins of $m_{4\ell}$ and m_{jj} . Scale and PDF uncertainties in the **SHERPA** strong $4\ell jj$ and MG5+Py8 EW $4\ell jj$ predictions are implemented as Gaussian-constrained nuisance parameters. The confidence level at each value of Wilson coefficient is calculated using the profile-likelihood test statistic [65], which is assumed to be distributed

Wilson coefficient	$ \mathcal{M}_{d8} ^2$	95% confidence interval [TeV $^{-4}$]	
	Included	Expected	Observed
$f_{T,0}/\Lambda^4$	yes	[-1.00, 0.97]	[-0.98, 0.93]
	no	[-19, 19]	[-23, 17]
$f_{T,1}/\Lambda^4$	yes	[-1.3, 1.3]	[-1.2, 1.2]
	no	[-140, 140]	[-160, 120]
$f_{T,2}/\Lambda^4$	yes	[-2.6, 2.5]	[-2.5, 2.4]
	no	[-63, 62]	[-74, 56]
$f_{T,5}/\Lambda^4$	yes	[-2.6, 2.5]	[-2.5, 2.4]
	no	[-68, 67]	[-79, 60]
$f_{T,6}/\Lambda^4$	yes	[-4.1, 4.1]	[-3.9, 3.9]
	no	[-550, 540]	[-640, 480]
$f_{T,7}/\Lambda^4$	yes	[-8.8, 8.4]	[-8.5, 8.1]
	no	[-220, 220]	[-260, 200]
$f_{T,8}/\Lambda^4$	yes	[-2.2, 2.2]	[-2.1, 2.1]
	no	[-3.9, 3.8]×10 ⁴	[-4.6, 3.1]×10 ⁴
$f_{T,9}/\Lambda^4$	yes	[-4.7, 4.7]	[-4.5, 4.5]
	no	[-6.4, 6.3]×10 ⁴	[-7.5, 5.5]×10 ⁴

Table 3: Expected and observed 95% confidence interval for the dimension-eight Wilson coefficients, using a two-dimensional fit to the $4\ell jj$ differential cross-sections measured as a function of $m_{4\ell}$ and m_{jj} . Results are presented when including or excluding the pure dimension-eight contributions to the EFT prediction.

according to a χ^2 distribution with one degree of freedom [66]. From this, 95% confidence intervals are constructed for each Wilson coefficient. The first bin of the $m_{4\ell}$ distribution is not used in the statistical test. This bin is insensitive to the dimension-eight operators, but removing the bin prevents a possible overconstraint on the Wilson coefficients, which arises due to one very small eigenvalue of the combined $m_{4\ell} - m_{jj}$ covariance matrix.

The 95% confidence intervals on the Wilson coefficients in the dimension-eight effective field theory are shown in Table 3. For each Wilson coefficient, confidence intervals are shown when including or excluding the pure dimension-eight contribution in the theoretical prediction. In all cases, the Wilson coefficients are consistent with zero. The Wilson coefficients associated with the $O_{T,0}$ and $O_{T,1}$ operators are the most tightly constrained. Furthermore, the constraints obtained with the pure dimension-eight contribution included in the theoretical prediction are more stringent than those obtained with only the interference contribution included in the theoretical calculation. This means that the limits are only valid if higher-order terms in the EFT expansion do not contribute significantly.

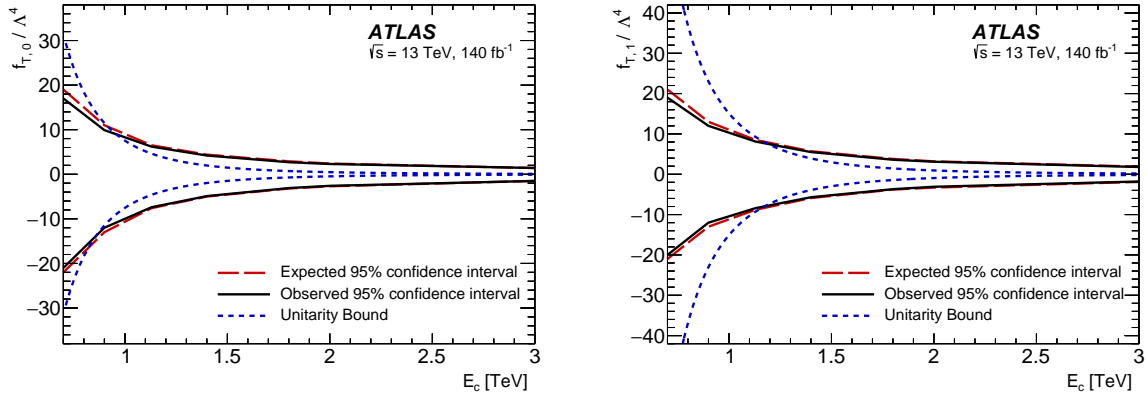


Figure 8: Expected and observed 95% confidence interval for the $f_{T,0}$ and $f_{T,1}$ Wilson coefficients as a function of a cut-off scale, E_c , which restricts the interference- and pure dimension-eight- contributions to have $m_{4\ell} < E_c$. The constraints are obtained using a two-dimensional fit to the $4\ell jj$ differential cross-sections measured as a function of $m_{4\ell}$ and m_{jj} .

Constraints are also placed on each Wilson coefficient after restricting the interference- and pure dimension-eight- contributions to have $m_{4\ell} < E_c$, where E_c is a cut-off that prevents unitarity being violated at large energy scales. The dependence of the 95% confidence intervals on the value of E_c is shown in Figure 8 for the $O_{T,0}$ and $O_{T,1}$ operators. The 95% confidence intervals degrade by a factor of 4–5 when the energy scale cut off is reduced from $E_c = \infty$ to $E_c = 1$ TeV. A similar trend is seen for the other operators and shown in the Appendix. Unitarity bounds are also shown in Figure 8, to indicate the consistency between the 95% confidence intervals and the partial-wave unitarity considerations for vector boson scattering processes [67].

10 Conclusion

Differential cross-sections are measured for the production of four charged leptons in association with two jets, using proton–proton collision data collected by the ATLAS experiment at a centre-of-mass energy of $\sqrt{s} = 13$ TeV and with an integrated luminosity of 140 fb^{-1} . This final state is sensitive to the strong $4\ell jj$ process, in which the jets arise from the strong interactions, and the electroweak $4\ell jj$ process, which is characterised by the t -channel exchange of an electroweak boson. The measurement of $4\ell jj$ production can therefore be used to improve the understanding of both the electroweak and strong interactions that underpin the Standard Model of particle physics. The differential cross-sections for $4\ell jj$ production are measured as a function of observables that collectively (i) characterise vector-boson scattering processes, (ii) probe the polarisation, parity and charge conjugation properties of the $4\ell jj$ process, and (iii) probe the real emission of quarks and gluons from the $4\ell jj$ process. The differential cross-sections are compared with various state-of-the-art Monte Carlo event generator predictions and the measurements are found to be sensitive to the event-generator modelling of strong $4\ell jj$ production and the EW $4\ell jj$ process at high dijet invariant mass and high values of $|\Delta\phi_{jj}|$. The differential cross-section measurements are consistent with Standard Model expectations and are used to set constraints on anomalous weak-boson self-interactions induced by dimension-six and dimension-eight operators in Standard Model effective field theory.

Acknowledgements

We thank CERN for the very successful operation of the LHC, as well as the support staff from our institutions without whom ATLAS could not be operated efficiently.

We acknowledge the support of ANPCyT, Argentina; YerPhI, Armenia; ARC, Australia; BMWFW and FWF, Austria; ANAS, Azerbaijan; CNPq and FAPESP, Brazil; NSERC, NRC and CFI, Canada; CERN; ANID, Chile; CAS, MOST and NSFC, China; Minciencias, Colombia; MEYS CR, Czech Republic; DNRF and DNSRC, Denmark; IN2P3-CNRS and CEA-DRF/IRFU, France; SRNSFG, Georgia; BMBF, HGF and MPG, Germany; GSRI, Greece; RGC and Hong Kong SAR, China; ISF and Benoziyo Center, Israel; INFN, Italy; MEXT and JSPS, Japan; CNRST, Morocco; NWO, Netherlands; RCN, Norway; MEiN, Poland; FCT, Portugal; MNE/IFA, Romania; MESTD, Serbia; MSSR, Slovakia; ARRS and MIZŠ, Slovenia; DSI/NRF, South Africa; MICINN, Spain; SRC and Wallenberg Foundation, Sweden; SERI, SNSF and Cantons of Bern and Geneva, Switzerland; MOST, Taiwan; TENMAK, Türkiye; STFC, United Kingdom; DOE and NSF, United States of America. In addition, individual groups and members have received support from BCKDF, CANARIE, Compute Canada and CRC, Canada; PRIMUS 21/SCI/017 and UNCE SCI/013, Czech Republic; COST, ERC, ERDF, Horizon 2020 and Marie Skłodowska-Curie Actions, European Union; Investissements d’Avenir Labex, Investissements d’Avenir Idex and ANR, France; DFG and AvH Foundation, Germany; Herakleitos, Thales and Aristeia programmes co-financed by EU-ESF and the Greek NSRF, Greece; BSF-NSF and MINERVA, Israel; Norwegian Financial Mechanism 2014-2021, Norway; NCN and NAWA, Poland; La Caixa Banking Foundation, CERCA Programme Generalitat de Catalunya and PROMETEO and GenT Programmes Generalitat Valenciana, Spain; Göran Gustafssons Stiftelse, Sweden; The Royal Society and Leverhulme Trust, United Kingdom.

The crucial computing support from all WLCG partners is acknowledged gratefully, in particular from CERN, the ATLAS Tier-1 facilities at TRIUMF (Canada), NDGF (Denmark, Norway, Sweden), CC-IN2P3 (France), KIT/GridKA (Germany), INFN-CNAF (Italy), NL-T1 (Netherlands), PIC (Spain), ASGC (Taiwan), RAL (UK) and BNL (USA), the Tier-2 facilities worldwide and large non-WLCG resource providers. Major contributors of computing resources are listed in Ref. [68].

Appendix

The differential cross-sections for inclusive $4\ell jj$ production in the VBS-enhanced region as a function of $p_{T,4\ell}$, $p_{T,jj}$, $|\Delta y_{jj}|$, and $\cos \theta_{34}^*$ are shown in Figure 9. The differential cross-sections for inclusive $4\ell jj$ production in the VBS-suppressed region as a function of $p_{T,4\ell}$, $p_{T,jj}$, $p_{T,4\ell jj}$, $S_{T,4\ell jj}$, $|\Delta y_{jj}|$, $\Delta\phi_{jj}$, $\cos \theta_{12}^*$ and $\cos \theta_{34}^*$ are shown in Figures 10 and 11. The data are compared with two theoretical predictions, constructed from MG5+Py8 for the EW $4\ell jj$ process and either SHERPA or MG5_NLO+Py8 for the strong $4\ell jj$ process. The EW $4\ell jj$ contribution is also shown separately to show the sensitivity of the measurements to the electroweak process.

The dependence of the 95% confidence intervals on the value of E_c is shown in Figure 12 for the $O_{T,2}$, $O_{T,5}$, $O_{T,6}$, $O_{T,7}$, $O_{T,8}$ and $O_{T,9}$ operators. The 95% confidence intervals degrade by a factor of 4–5 when the energy scale cut off is reduced from $E_c = \infty$ to $E_c = 1$ TeV.

Table 4 shows 95% confidence intervals on the Wilson coefficients of operators in a dimension-six effective field theory [69]. The method to constrain the Wilson coefficients is identical to that used for the dimension-eight operators in Section 9, with the interactions from the dimension-six operators provided by the SMEFTSim package [69]. In the case of CP-odd operators, the interference contribution is zero for parity-even observables such as m_{jj} and $m_{4\ell}$. However, the interference contribution produces large asymmetric effects in the parity-odd $\Delta\phi_{jj}$ observable. Constraints are therefore placed on the CP-odd Wilson coefficients using the measured differential cross-section as a function of $\Delta\phi_{jj}$ when the pure dimension-six contribution to the EFT is excluded. The constraints obtained on the dimension-six Wilson coefficients in this analysis are much weaker than those obtained measurements of diboson production [4, 61–64] and vector-boson fusion [60].

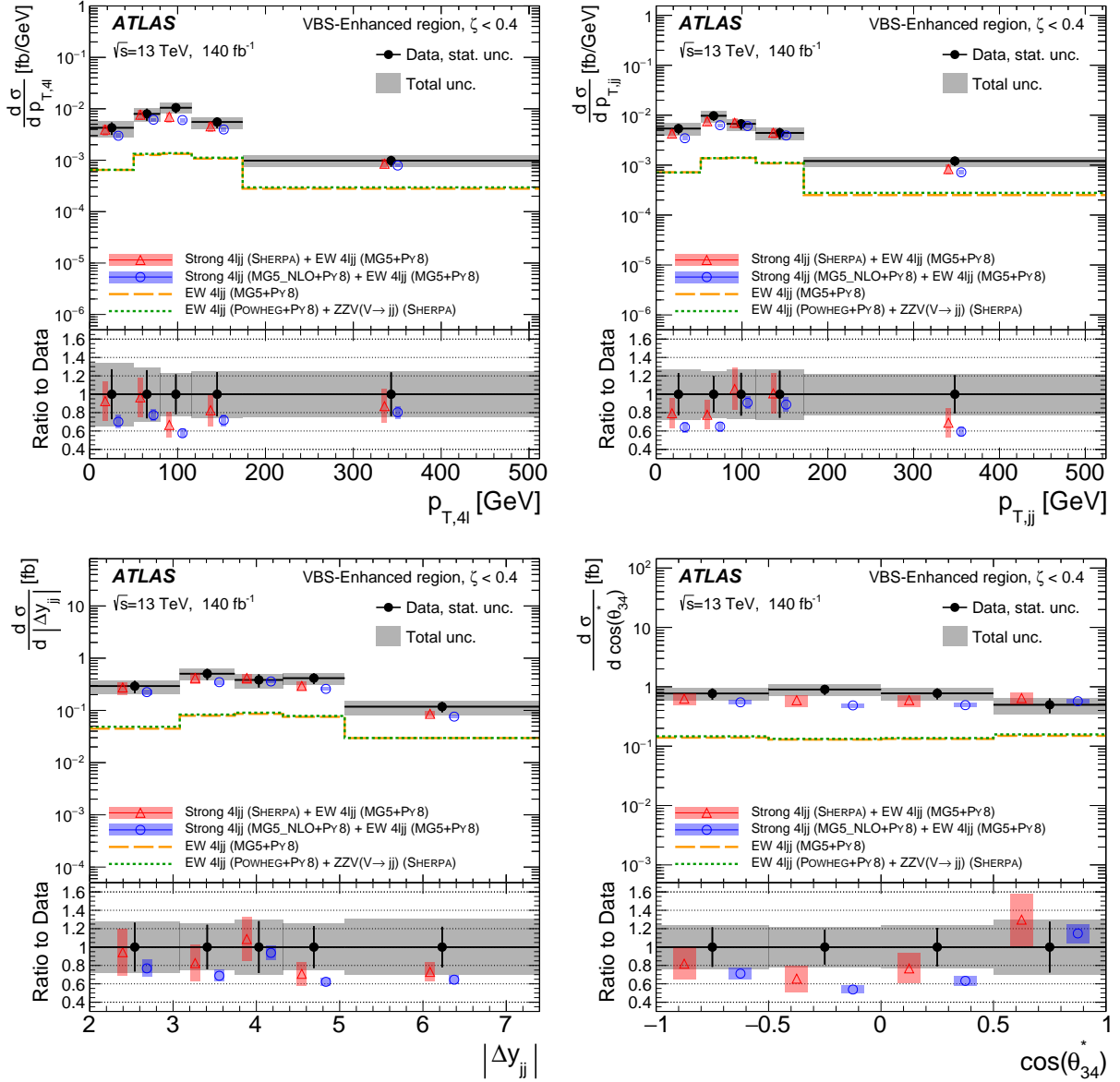


Figure 9: Differential cross-sections for inclusive $4\ell jj$ production in the VBS-enhanced region as a function of $p_{T,4\ell}$ (top left), $p_{T,jj}$ (top right), $|\Delta y_{jj}|$ (bottom left) and $\cos \theta_{34}^*$ for the second Z boson candidate (bottom right). The data are represented as black points and the associated error bars represent the statistical uncertainty. The total uncertainty in the measurement is represented as a grey hatched band. The data are compared to two theoretical predictions, estimated by using SHERPA (triangles) and MADGRAPH5 (circles) for the strong $4\ell jj$ contribution and MG5+Py8 for the EW $4\ell jj$ contribution. The band on the theoretical predictions represents the theoretical uncertainty from renormalisation/factorisation scale choices and PDF choice. The dashed lines show the contribution of EW $4\ell jj$ production to the differential cross-section as predicted by MG5+Py8 and Powheg+Pythia8. The s -channel contributions from ZZV production are missing from the Powheg+Pythia8 prediction and are estimated with SHERPA. For the $p_{T,4\ell}$, $p_{T,jj}$ and $|\Delta y_{jj}|$ measurements, any ‘overflow’ events that lie above the upper bin edge of the last bin are included in that bin.

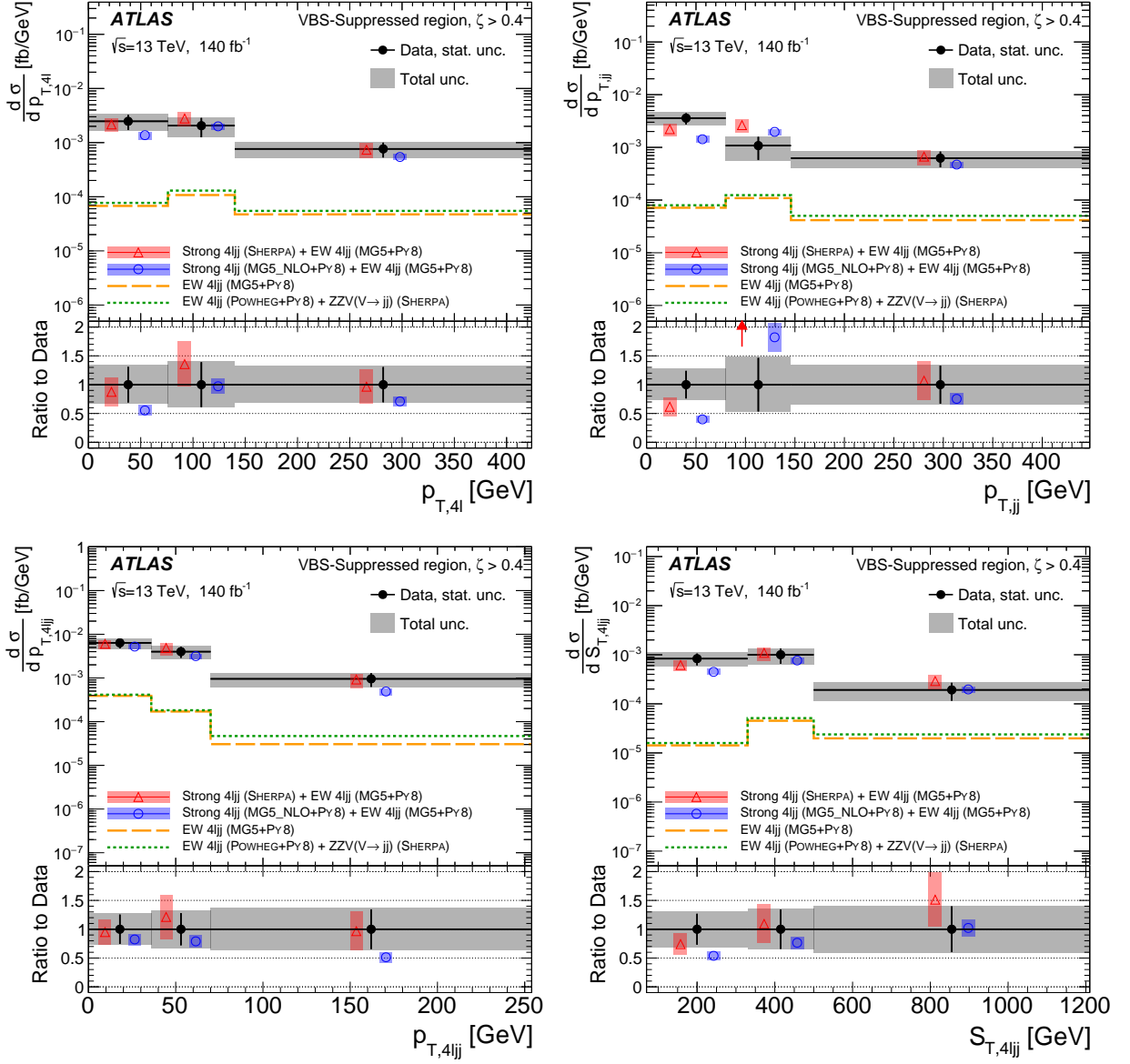


Figure 10: Differential cross-sections for inclusive $4\ell jj$ production in the VBS-suppressed region as a function of $p_{T,4\ell}$ (top left), $p_{T,jj}$ (top right), $p_{T,4\ell jj}$ (bottom left) and $S_{T,4\ell jj}$ (bottom right). The data are represented as black points and the associated error bars represent the statistical uncertainty. The total uncertainty in the measurement is represented as a grey hatched band. The data are compared to two theoretical predictions, estimated using SHERPA (triangles) and MADGRAPH5 (circles) for the strong $4\ell jj$ contribution and MG5+Py8 for the EW $4\ell jj$ contribution. The band on the theoretical predictions represents the theoretical uncertainty from renormalisation/factorisation scale choices and PDF choice. The dashed lines show the contribution of EW $4\ell jj$ production to the differential cross-section as predicted by MG5+Py8 and POWHEG+PYTHIA8. The s -channel contributions from ZZV production are missing from the POWHEG+PYTHIA8 prediction and are estimated with SHERPA. ‘Overflow’ events that lie above the upper bin edge of the last bin are included in that bin.

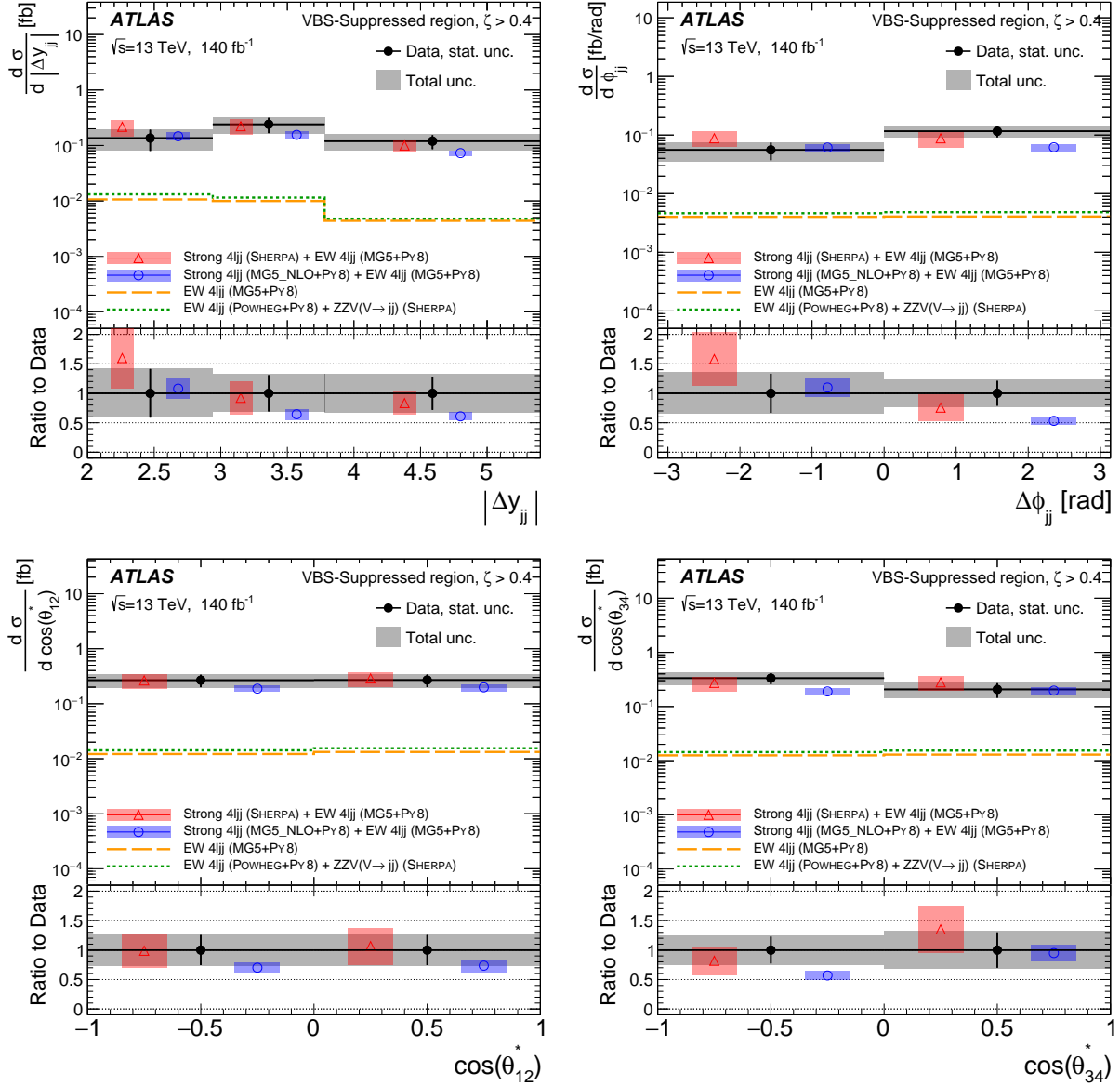


Figure 11: Differential cross-sections for inclusive $4\ell jj$ production in the VBS-suppressed region as a function of $|\Delta y_{\ell j}|$ (top left), $\Delta\phi_{\ell j}$ (top right), $\cos\theta_{12}^*$ (bottom left) and $\cos\theta_{34}^*$ (bottom right). The data are represented as black points and the associated error bars represent the statistical uncertainty. The total uncertainty in the measurement is represented as a grey hatched band. The data are compared to two theoretical predictions, estimated using SHERPA (triangles) and MADGRAPH5 (circles) for the strong $4\ell jj$ contribution and MG5+Py8 for the EW $4\ell jj$ contribution. The band on the theoretical predictions represent the theoretical uncertainty from renormalisation/factorisation scale choices and PDF choice. The dashed lines show the contribution of EW $4\ell jj$ production to the differential cross-section as predicted by MG5+Py8 and POWHEG+PYTHIA8. The s -channel contributions from ZZV production are missing from the POWHEG+PYTHIA8 prediction and are estimated with SHERPA. For the $|\Delta y_{\ell j}|$ measurement, any ‘overflow’ events that lie above the upper bin edge of the last bin are included in that bin.

Wilson coefficient	$ \mathcal{M}_{d6} ^2$	95% confidence interval [TeV^{-2}]	
	Included	Expected	Observed
c_W/Λ^2	yes	[-1.3, 1.3]	[-1.2, 1.2]
	no	[-32, 32]	[-37, 28]
$c_{\widetilde{W}}/\Lambda^2$	yes	[-1.3, 1.3]	[-1.2, 1.2]
	no	[-17, 17]*	[0, 30]*
c_{HWB}/Λ^2	yes	[-16, 7]	[-16, 6]
	no	[-12, 12]	[-15, 10]
$c_{H\widetilde{W}B}/\Lambda^2$	yes	[-1.3, 1.3]	[-1.2, 1.2]
	no	[-67, 67]*	[-25, 130]*
c_{HB}/Λ^2	yes	[-13, 13]	[-12, 12]
	no	[-38, 38]	[-38, 38]
$c_{H\widetilde{B}}/\Lambda^2$	yes	[-13, 13]	[-12, 12]
	no	[-420, 420]*	[-200, 790]*

Table 4: Expected and observed 95% confidence interval for the dimension-six Wilson coefficients. Results are presented when including or excluding the pure dimension-six contributions to the EFT prediction. The constraints are obtained using a two-dimensional fit to the $4\ell jj$ differential cross-sections measured as a function of $m_{4\ell}$ and m_{jj} , except for the constraints on CP-odd operators when the pure dimension-six contribution to the EFT is excluded. Those constraints, denoted by a (*), are obtained in a fit to the differential cross-section as a function of $\Delta\phi_{jj}$.

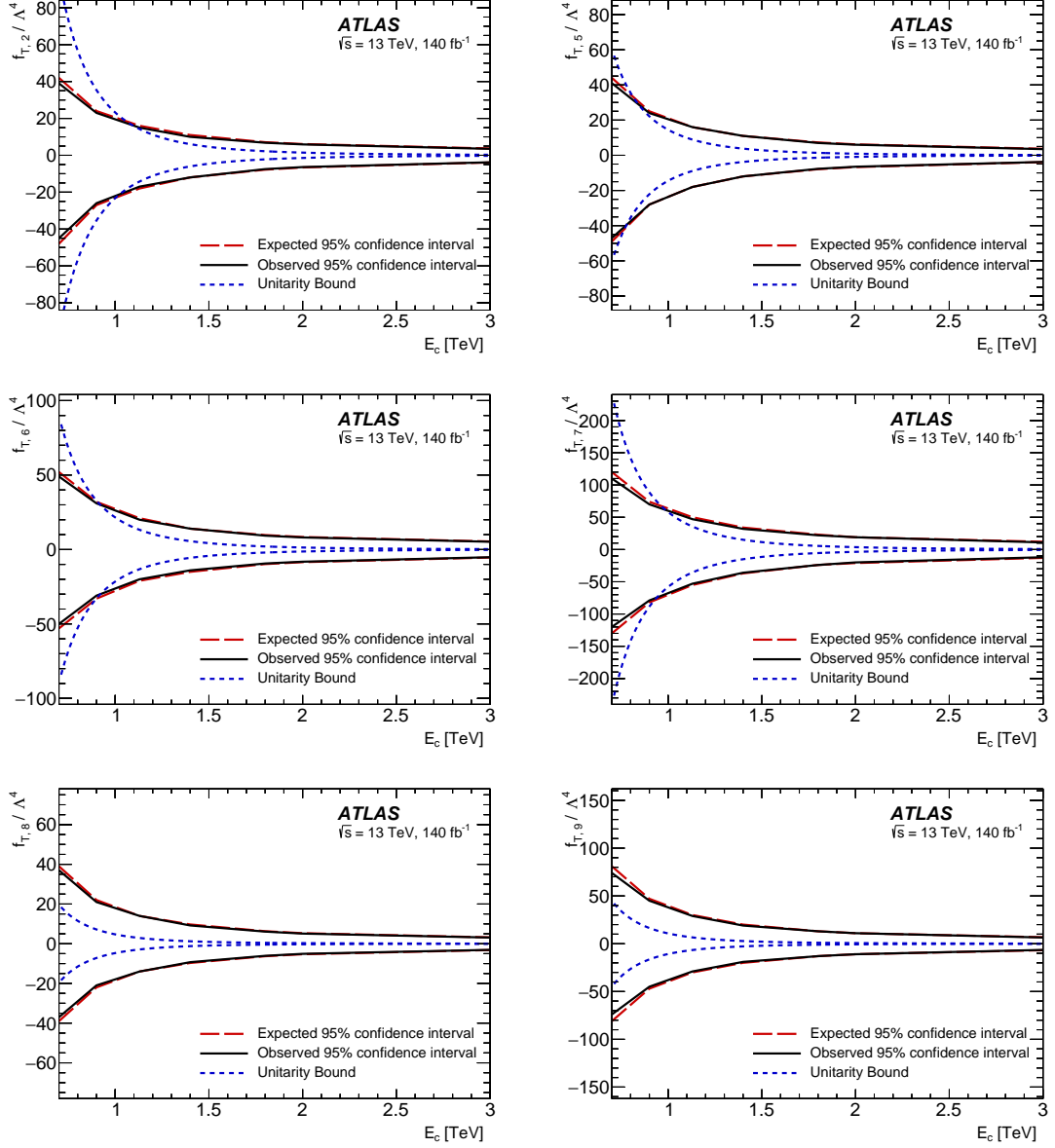


Figure 12: Expected and observed 95% confidence interval for the $f_{T,2}$, $f_{T,5}$, $f_{T,6}$, $f_{T,7}$, $f_{T,8}$ and $f_{T,9}$ Wilson coefficients as a function of a cut-off scale, E_c , which restricts the interference- and pure dimension-eight- contributions to have $m_{4\ell} < E_c$. The constraints are obtained using a two-dimensional fit to the $4\ell jj$ differential cross-sections measured as a function of $m_{4\ell}$ and m_{jj} .

References

- [1] ATLAS Collaboration, *Observation of electroweak production of two jets and a Z-boson pair*, *Nature Phys.* **19** (2023) 237, arXiv: [2004.10612 \[hep-ex\]](#).
- [2] CMS Collaboration, *Evidence for electroweak production of four charged leptons and two jets in proton-proton collisions at $\sqrt{s} = 13$ TeV*, *Phys. Lett. B* **812** (2021) 135992, arXiv: [2008.07013 \[hep-ex\]](#).
- [3] CMS Collaboration, *Measurements of $pp \rightarrow ZZ$ production cross sections and constraints on anomalous triple gauge couplings at $\sqrt{s} = 13$ TeV*, *Eur. Phys. J. C* **81** (2021) 200, arXiv: [2009.01186 \[hep-ex\]](#).
- [4] ATLAS Collaboration, *Measurements of differential cross-sections in four-lepton events in 13 TeV proton-proton collisions with the ATLAS detector*, *JHEP* **07** (2021) 005, arXiv: [2103.01918 \[hep-ex\]](#).
- [5] V. Hankele, G. Klamke, D. Zeppenfeld and T. Figy, *Anomalous Higgs boson couplings in vector boson fusion at the CERN LHC*, *Phys. Rev. D* **74** (2006) 095001, arXiv: [hep-ph/0609075 \[hep-ph\]](#).
- [6] O. J. P. Éboli and M. C. Gonzalez-Garcia, *Classifying the bosonic quartic couplings*, *Phys. Rev. D* **93** (2016) 093013, arXiv: [1604.03555 \[hep-ph\]](#).
- [7] ATLAS Collaboration, *The ATLAS Experiment at the CERN Large Hadron Collider*, *JINST* **3** (2008) S08003.
- [8] ATLAS Collaboration, *ATLAS Insertable B-Layer: Technical Design Report*, ATLAS-TDR-19; CERN-LHCC-2010-013, 2010, URL: <https://cds.cern.ch/record/1291633>, Addendum: ATLAS-TDR-19-ADD-1; CERN-LHCC-2012-009, 2012, URL: <https://cds.cern.ch/record/1451888>.
- [9] B. Abbott et al., *Production and integration of the ATLAS Insertable B-Layer*, *JINST* **13** (2018) T05008, arXiv: [1803.00844 \[physics.ins-det\]](#).
- [10] ATLAS Collaboration, *Performance of the ATLAS trigger system in 2015*, *Eur. Phys. J. C* **77** (2017) 317, arXiv: [1611.09661 \[hep-ex\]](#).
- [11] ATLAS Collaboration, *The ATLAS Collaboration Software and Firmware*, ATL-SOFT-PUB-2021-001, 2021, URL: <https://cds.cern.ch/record/2767187>.
- [12] E. Bothmann et al., *Event generation with Sherpa 2.2*, *SciPost Phys.* **7** (2019) 034, arXiv: [1905.09127 \[hep-ph\]](#).
- [13] F. Caola, K. Melnikov, R. Röntsch and L. Tancredi, *QCD corrections to ZZ production in gluon fusion at the LHC*, *Phys. Rev. D* **92** (2015) 094028, arXiv: [1509.06734 \[hep-ph\]](#).
- [14] F. Caola, M. Dowling, K. Melnikov, R. Röntsch and L. Tancredi, *QCD corrections to vector boson pair production in gluon fusion including interference effects with off-shell Higgs at the LHC*, *JHEP* **07** (2016) 087, arXiv: [1605.04610 \[hep-ph\]](#).
- [15] G. Passarino, *Higgs CAT*, *Eur. Phys. J. C* **74** (2014) 2866, arXiv: [1312.2397 \[hep-ph\]](#).
- [16] D. de Florian et al., *Handbook of LHC Higgs Cross Sections: 4. Deciphering the Nature of the Higgs Sector*, **2/2017** (2016), arXiv: [1610.07922 \[hep-ph\]](#).

- [17] T. Gleisberg and S. Höche, *Comix, a new matrix element generator*, JHEP **12** (2008) 039, arXiv: [0808.3674 \[hep-ph\]](#).
- [18] S. Schumann and F. Krauss,
A parton shower algorithm based on Catani–Seymour dipole factorisation, JHEP **03** (2008) 038, arXiv: [0709.1027 \[hep-ph\]](#).
- [19] S. Höche, F. Krauss, M. Schönher and F. Siegert,
A critical appraisal of NLO+PS matching methods, JHEP **09** (2012) 049, arXiv: [1111.1220 \[hep-ph\]](#).
- [20] S. Höche, F. Krauss, M. Schönher and F. Siegert,
QCD matrix elements + parton showers. The NLO case, JHEP **04** (2013) 027, arXiv: [1207.5030 \[hep-ph\]](#).
- [21] S. Catani, F. Krauss, B. R. Webber and R. Kuhn, *QCD Matrix Elements + Parton Showers*, JHEP **11** (2001) 063, arXiv: [hep-ph/0109231](#).
- [22] S. Höche, F. Krauss, S. Schumann and F. Siegert, *QCD matrix elements and truncated showers*, JHEP **05** (2009) 053, arXiv: [0903.1219 \[hep-ph\]](#).
- [23] F. Buccioni et al., *OpenLoops 2*, Eur. Phys. J. C **79** (2019) 866, arXiv: [1907.13071 \[hep-ph\]](#).
- [24] F. Cascioli, P. Maierhöfer and S. Pozzorini, *Scattering Amplitudes with Open Loops*, Phys. Rev. Lett. **108** (2012) 111601, arXiv: [1111.5206 \[hep-ph\]](#).
- [25] A. Denner, S. Dittmaier and L. Hofer,
COLLIER: A fortran-based complex one-loop library in extended regularizations, Comput. Phys. Commun. **212** (2017) 220, arXiv: [1604.06792 \[hep-ph\]](#).
- [26] The NNPDF Collaboration, R. D. Ball et al., *Parton distributions for the LHC run II*, JHEP **04** (2015) 040, arXiv: [1410.8849 \[hep-ph\]](#).
- [27] J. Alwall et al., *The automated computation of tree-level and next-to-leading order differential cross sections, and their matching to parton shower simulations*, JHEP **07** (2014) 079, arXiv: [1405.0301 \[hep-ph\]](#).
- [28] J. Butterworth et al., *PDF4LHC recommendations for LHC Run II*, J. Phys. G **43** (2016) 023001, arXiv: [1510.03865 \[hep-ph\]](#).
- [29] ATLAS Collaboration, *ATLAS Pythia 8 tunes to 7 TeV data*, ATL-PHYS-PUB-2014-021, 2014, URL: <https://cds.cern.ch/record/1966419>.
- [30] R. Frederix and S. Frixione, *Merging meets matching in MC@NLO*, JHEP **12** (2012) 061, arXiv: [1209.6215 \[hep-ph\]](#).
- [31] S. Frixione, G. Ridolfi and P. Nason,
A positive-weight next-to-leading-order Monte Carlo for heavy flavour hadroproduction, JHEP **09** (2007) 126, arXiv: [0707.3088 \[hep-ph\]](#).
- [32] P. Nason, *A new method for combining NLO QCD with shower Monte Carlo algorithms*, JHEP **11** (2004) 040, arXiv: [hep-ph/0409146](#).
- [33] S. Frixione, P. Nason and C. Oleari,
Matching NLO QCD computations with parton shower simulations: the POWHEG method, JHEP **11** (2007) 070, arXiv: [0709.2092 \[hep-ph\]](#).

- [34] S. Alioli, P. Nason, C. Oleari and E. Re, *A general framework for implementing NLO calculations in shower Monte Carlo programs: the POWHEG BOX*, JHEP **06** (2010) 043, arXiv: [1002.2581 \[hep-ph\]](#).
- [35] B. Jäger, A. Karlberg and G. Zanderighi, *Electroweak ZZjj production in the Standard Model and beyond in the POWHEG-BOX V2*, JHEP **03** (2014) 141, arXiv: [1312.3252 \[hep-ph\]](#).
- [36] ATLAS Collaboration, *Measurement of the $t\bar{t}Z$ and $t\bar{t}W$ cross sections in proton-proton collisions at $\sqrt{s} = 13$ TeV with the ATLAS detector*, Phys. Rev. D **99** (2019) 072009, arXiv: [1901.03584 \[hep-ex\]](#).
- [37] ATLAS Collaboration, *Evidence for the production of three massive vector bosons with the ATLAS detector*, Phys. Lett. B **798** (2019) 134913, arXiv: [1903.10415 \[hep-ex\]](#).
- [38] C. Anastasiou, L. Dixon, K. Melnikov and F. Petriello, *High-precision QCD at hadron colliders: Electroweak gauge boson rapidity distributions at next-to-next-to leading order*, Phys. Rev. D **69** (2004) 094008, arXiv: [hep-ph/0312266](#).
- [39] ATLAS Collaboration, *Studies on top-quark Monte Carlo modelling for Top2016*, ATL-PHYS-PUB-2016-020, 2016, URL: <https://cds.cern.ch/record/2216168>.
- [40] ATLAS Collaboration, *The ATLAS Simulation Infrastructure*, Eur. Phys. J. C **70** (2010) 823, arXiv: [1005.4568 \[physics.ins-det\]](#).
- [41] S. Agostinelli et al., *GEANT4 – a simulation toolkit*, Nucl. Instrum. Meth. A **506** (2003) 250.
- [42] ATLAS Collaboration, *ATLAS data quality operations and performance for 2015–2018 data-taking*, JINST **15** (2020) P04003, arXiv: [1911.04632 \[physics.ins-det\]](#).
- [43] ATLAS Collaboration, *Reconstruction of primary vertices at the ATLAS experiment in Run 1 proton–proton collisions at the LHC*, Eur. Phys. J. C **77** (2017) 332, arXiv: [1611.10235 \[hep-ex\]](#).
- [44] ATLAS Collaboration, *Muon reconstruction and identification efficiency in ATLAS using the full Run 2 pp collision data set at $\sqrt{s} = 13$ TeV*, Eur. Phys. J. C **81** (2021) 578, arXiv: [2012.00578 \[hep-ex\]](#).
- [45] ATLAS Collaboration, *Electron reconstruction and identification in the ATLAS experiment using the 2015 and 2016 LHC proton–proton collision data at $\sqrt{s} = 13$ TeV*, Eur. Phys. J. C **79** (2019) 639, arXiv: [1902.04655 \[hep-ex\]](#).
- [46] ATLAS Collaboration, *Electron and photon performance measurements with the ATLAS detector using the 2015–2017 LHC proton–proton collision data*, JINST **14** (2019) P12006, arXiv: [1908.00005 \[hep-ex\]](#).
- [47] M. Cacciari, G. P. Salam and G. Soyez, *The anti- k_t jet clustering algorithm*, JHEP **04** (2008) 063, arXiv: [0802.1189 \[hep-ph\]](#).
- [48] M. Cacciari, G. P. Salam and G. Soyez, *FastJet user manual*, Eur. Phys. J. C **72** (2012) 1896, arXiv: [1111.6097 \[hep-ph\]](#).
- [49] ATLAS Collaboration, *Jet reconstruction and performance using particle flow with the ATLAS Detector*, Eur. Phys. J. C **77** (2017) 466, arXiv: [1703.10485 \[hep-ex\]](#).

- [50] ATLAS Collaboration, *Jet energy scale and resolution measured in proton–proton collisions at $\sqrt{s} = 13\text{ TeV}$ with the ATLAS detector*, *Eur. Phys. J. C* **81** (2020) 689, arXiv: [2007.02645 \[hep-ex\]](#).
- [51] ATLAS Collaboration, *Performance of pile-up mitigation techniques for jets in pp collisions at $\sqrt{s} = 8\text{ TeV}$ using the ATLAS detector*, *Eur. Phys. J. C* **76** (2016) 581, arXiv: [1510.03823 \[hep-ex\]](#).
- [52] ATLAS Collaboration, *Identification and rejection of pile-up jets at high pseudorapidity with the ATLAS detector*, *Eur. Phys. J. C* **77** (2017) 580, arXiv: [1705.02211 \[hep-ex\]](#), Erratum: *Eur. Phys. J. C* **77** (2017) 712.
- [53] M. Cacciari, G. P. Salam and G. Soyez, *The Catchment Area of Jets*, *JHEP* **04** (2008) 005, arXiv: [0802.1188 \[hep-ph\]](#).
- [54] G. D Agostini, *A Multidimensional unfolding method based on Bayes theorem*, *Nucl. Instrum. Meth. A* **362** (1995) 487.
- [55] T. Adye, ‘Unfolding algorithms and tests using RooUnfold’, *PHYSTAT 2011*, Geneva: CERN, 2011 313, arXiv: [1105.1160 \[physics.data-an\]](#).
- [56] K. G. Hayes, M. L. Perl and B. Efron, *Application of the bootstrap statistical method to the tau-decay-mode problem*, *Phys. Rev. D* **39** (1 1989) 274.
- [57] ATLAS Collaboration, *Luminosity determination in pp collisions at $\sqrt{s} = 13\text{ TeV}$ using the ATLAS detector at the LHC*, (2022), arXiv: [2212.09379 \[hep-ex\]](#).
- [58] ATLAS Collaboration, *Measurement of the Inelastic Proton-Proton Cross Section at $\sqrt{s} = 13\text{ TeV}$ with the ATLAS Detector at the LHC*, *Phys. Rev. Lett.* **117** (2016) 182002, arXiv: [1606.02625 \[hep-ex\]](#).
- [59] ATLAS Collaboration, *Studies of the muon momentum calibration and performance of the ATLAS detector with pp collisions at $\sqrt{s}=13\text{ TeV}$* , (2022), arXiv: [2212.07338 \[hep-ex\]](#).
- [60] ATLAS Collaboration, *Differential cross-section measurements for the electroweak production of dijets in association with a Z boson in proton–proton collisions at ATLAS*, *Eur. Phys. J. C* **81** (2021) 163, arXiv: [2006.15458 \[hep-ex\]](#).
- [61] ATLAS Collaboration, *Measurement of fiducial and differential W^+W^- production cross-sections at $\sqrt{s} = 13\text{ TeV}$ with the ATLAS detector*, *Eur. Phys. J. C* **79** (2019) 884, arXiv: [1905.04242 \[hep-ex\]](#).
- [62] CMS Collaboration, *W^+W^- boson pair production in proton-proton collisions at $\sqrt{s} = 13\text{ TeV}$* , *Phys. Rev. D* **102** (2020) 092001, arXiv: [2009.00119 \[hep-ex\]](#).
- [63] CMS Collaboration, *Measurement of the inclusive and differential WZ production cross sections, polarization angles, and triple gauge couplings in pp collisions at $\sqrt{s} = 13\text{ TeV}$* , *JHEP* **07** (2022) 032, arXiv: [2110.11231 \[hep-ex\]](#).
- [64] CMS Collaboration, *Measurement of $W^\pm\gamma$ differential cross sections in proton-proton collisions at $\sqrt{s} = 13\text{ TeV}$ and effective field theory constraints*, *Phys. Rev. D* **105** (2022) 052003, arXiv: [2111.13948 \[hep-ex\]](#).

- [65] G. J. Feldman and R. D. Cousins,
Unified approach to the classical statistical analysis of small signals, Phys. Rev. D **57** (1998) 3873,
arXiv: [physics/9711021 \[physics.data-an\]](#).
- [66] S. S. Wilks,
The Large-Sample Distribution of the Likelihood Ratio for Testing Composite Hypotheses,
Ann. Math. Statist. **9** (1938) 60, URL: <https://doi.org/10.1214/aoms/1177732360>.
- [67] E. d. S. Almeida, O. J. P. Eboli and M. C. Gonzalez-Garcia,
Unitarity constraints on anomalous quartic couplings, Phys. Rev. D **101** (2020) 113003,
arXiv: [2004.05174 \[hep-ph\]](#).
- [68] ATLAS Collaboration, *ATLAS Computing Acknowledgements*, ATL-SOFT-PUB-2021-003, 2021,
URL: <https://cds.cern.ch/record/2776662>.
- [69] I. Brivio, Y. Jiang and M. Trott, *The SMEFTsim package, theory and tools*, JHEP **12** (2017) 070,
arXiv: [1709.06492 \[hep-ph\]](#).

The ATLAS Collaboration

G. Aad [ID¹⁰²](#), B. Abbott [ID¹²⁰](#), K. Abeling [ID⁵⁵](#), N.J. Abicht [ID⁴⁹](#), S.H. Abidi [ID²⁹](#), A. Aboulhorma [ID^{35e}](#), H. Abramowicz [ID¹⁵¹](#), H. Abreu [ID¹⁵⁰](#), Y. Abulaiti [ID¹¹⁷](#), A.C. Abusleme Hoffman [ID^{137a}](#), B.S. Acharya [ID^{69a,69b,n}](#), C. Adam Bourdarios [ID⁴](#), L. Adamczyk [ID^{86a}](#), L. Adamek [ID¹⁵⁵](#), S.V. Addepalli [ID²⁶](#), M.J. Addison [ID¹⁰¹](#), J. Adelman [ID¹¹⁵](#), A. Adiguzel [ID^{21c}](#), T. Adye [ID¹³⁴](#), A.A. Affolder [ID¹³⁶](#), Y. Afik [ID³⁶](#), M.N. Agaras [ID¹³](#), J. Agarwala [ID^{73a,73b}](#), A. Aggarwal [ID¹⁰⁰](#), C. Agheorghiesei [ID^{27c}](#), A. Ahmad [ID³⁶](#), F. Ahmadov [ID^{38,z}](#), W.S. Ahmed [ID¹⁰⁴](#), S. Ahuja [ID⁹⁵](#), X. Ai [ID^{62a}](#), G. Aielli [ID^{76a,76b}](#), A. Aikot [ID¹⁶³](#), M. Ait Tamlihat [ID^{35e}](#), B. Aitbenchikh [ID^{35a}](#), I. Aizenberg [ID¹⁶⁹](#), M. Akbiyik [ID¹⁰⁰](#), T.P.A. Åkesson [ID⁹⁸](#), A.V. Akimov [ID³⁷](#), D. Akiyama [ID¹⁶⁸](#), N.N. Akolkar [ID²⁴](#), K. Al Khoury [ID⁴¹](#), G.L. Alberghi [ID^{23b}](#), J. Albert [ID¹⁶⁵](#), P. Albicocco [ID⁵³](#), G.L. Albouy [ID⁶⁰](#), S. Alderweireldt [ID⁵²](#), M. Aleksić [ID³⁶](#), I.N. Aleksandrov [ID³⁸](#), C. Alexa [ID^{27b}](#), T. Alexopoulos [ID¹⁰](#), F. Alfonsi [ID^{23b}](#), M. Algren [ID⁵⁶](#), M. Alhroob [ID¹²⁰](#), B. Ali [ID¹³²](#), H.M.J. Ali [ID⁹¹](#), S. Ali [ID¹⁴⁸](#), S.W. Alibocus [ID⁹²](#), M. Aliev [ID¹⁴⁵](#), G. Alimonti [ID^{71a}](#), W. Alkakhi [ID⁵⁵](#), C. Allaire [ID⁶⁶](#), B.M.M. Allbrooke [ID¹⁴⁶](#), J.F. Allen [ID⁵²](#), C.A. Allendes Flores [ID^{137f}](#), P.P. Allport [ID²⁰](#), A. Aloisio [ID^{72a,72b}](#), F. Alonso [ID⁹⁰](#), C. Alpigiani [ID¹³⁸](#), M. Alvarez Estevez [ID⁹⁹](#), A. Alvarez Fernandez [ID¹⁰⁰](#), M. Alves Cardoso [ID⁵⁶](#), M.G. Alvaggi [ID^{72a,72b}](#), M. Aly [ID¹⁰¹](#), Y. Amaral Coutinho [ID^{83b}](#), A. Ambler [ID¹⁰⁴](#), C. Amelung [ID³⁶](#), M. Amerl [ID¹⁰¹](#), C.G. Ames [ID¹⁰⁹](#), D. Amidei [ID¹⁰⁶](#), S.P. Amor Dos Santos [ID^{130a}](#), K.R. Amos [ID¹⁶³](#), V. Ananiev [ID¹²⁵](#), C. Anastopoulos [ID¹³⁹](#), T. Andeen [ID¹¹](#), J.K. Anders [ID³⁶](#), S.Y. Andrean [ID^{47a,47b}](#), A. Andreazza [ID^{71a,71b}](#), S. Angelidakis [ID⁹](#), A. Angerami [ID^{41,ac}](#), A.V. Anisenkov [ID³⁷](#), A. Annovi [ID^{74a}](#), C. Antel [ID⁵⁶](#), M.T. Anthony [ID¹³⁹](#), E. Antipov [ID¹⁴⁵](#), M. Antonelli [ID⁵³](#), F. Anulli [ID^{75a}](#), M. Aoki [ID⁸⁴](#), T. Aoki [ID¹⁵³](#), J.A. Aparisi Pozo [ID¹⁶³](#), M.A. Aparo [ID¹⁴⁶](#), L. Aperio Bella [ID⁴⁸](#), C. Appelt [ID¹⁸](#), A. Apyan [ID²⁶](#), N. Aranzabal [ID³⁶](#), C. Arcangeletti [ID⁵³](#), A.T.H. Arce [ID⁵¹](#), E. Arena [ID⁹²](#), J-F. Arguin [ID¹⁰⁸](#), S. Argyropoulos [ID⁵⁴](#), J.-H. Arling [ID⁴⁸](#), O. Arnaez [ID⁴](#), H. Arnold [ID¹¹⁴](#), G. Artoni [ID^{75a,75b}](#), H. Asada [ID¹¹¹](#), K. Asai [ID¹¹⁸](#), S. Asai [ID¹⁵³](#), N.A. Asbah [ID⁶¹](#), J. Assahsah [ID^{35d}](#), K. Assamagan [ID²⁹](#), R. Astalos [ID^{28a}](#), S. Atashi [ID¹⁶⁰](#), R.J. Atkin [ID^{33a}](#), M. Atkinson [ID¹⁶²](#), H. Atmani [ID^{35f}](#), P.A. Atmasiddha [ID¹⁰⁶](#), K. Augsten [ID¹³²](#), S. Auricchio [ID^{72a,72b}](#), A.D. Auriol [ID²⁰](#), V.A. Astrup [ID¹⁰¹](#), G. Avolio [ID³⁶](#), K. Axiotis [ID⁵⁶](#), G. Azuelos [ID^{108,ah}](#), D. Babal [ID^{28b}](#), H. Bachacou [ID¹³⁵](#), K. Bachas [ID^{152,q}](#), A. Bachiu [ID³⁴](#), F. Backman [ID^{47a,47b}](#), A. Badea [ID⁶¹](#), P. Bagnaia [ID^{75a,75b}](#), M. Bahmani [ID¹⁸](#), A.J. Bailey [ID¹⁶³](#), V.R. Bailey [ID¹⁶²](#), J.T. Baines [ID¹³⁴](#), L. Baines [ID⁹⁴](#), C. Bakalis [ID¹⁰](#), O.K. Baker [ID¹⁷²](#), E. Bakos [ID¹⁵](#), D. Bakshi Gupta [ID⁸](#), V. Balakrishnan [ID¹²⁰](#), R. Balasubramanian [ID¹¹⁴](#),

E.M. Baldin [ID³⁷](#), P. Balek [ID^{86a}](#), E. Ballabene [ID^{23b,23a}](#), F. Balli [ID¹³⁵](#), L.M. Baltes [ID^{63a}](#), W.K. Balunas [ID³²](#), J. Balz [ID¹⁰⁰](#), E. Banas [ID⁸⁷](#), M. Bandieramonte [ID¹²⁹](#), A. Bandyopadhyay [ID²⁴](#), S. Bansal [ID²⁴](#), L. Barak [ID¹⁵¹](#), M. Barakat [ID⁴⁸](#), E.L. Barberio [ID¹⁰⁵](#), D. Barberis [ID^{57b,57a}](#), M. Barbero [ID¹⁰²](#), M.Z. Barel [ID¹¹⁴](#), K.N. Barends [ID^{33a}](#), T. Barillari [ID¹¹⁰](#), M-S. Barisits [ID³⁶](#), T. Barklow [ID¹⁴³](#), P. Baron [ID¹²²](#), D.A. Baron Moreno [ID¹⁰¹](#), A. Baroncelli [ID^{62a}](#), G. Barone [ID²⁹](#), A.J. Barr [ID¹²⁶](#), J.D. Barr [ID⁹⁶](#), L. Barranco Navarro [ID^{47a,47b}](#), F. Barreiro [ID⁹⁹](#), J. Barreiro Guimarães da Costa [ID^{14a}](#), U. Barron [ID¹⁵¹](#), M.G. Barros Teixeira [ID^{130a}](#), S. Barsov [ID³⁷](#), F. Bartels [ID^{63a}](#), R. Bartoldus [ID¹⁴³](#), A.E. Barton [ID⁹¹](#), P. Bartos [ID^{28a}](#), A. Basan [ID¹⁰⁰](#), M. Baselga [ID⁴⁹](#), A. Bassalat [ID^{66,b}](#), M.J. Basso [ID^{156a}](#), C.R. Basson [ID¹⁰¹](#), R.L. Bates [ID⁵⁹](#), S. Batlamous ^{35e}, J.R. Batley [ID³²](#), B. Batool [ID¹⁴¹](#), M. Battaglia [ID¹³⁶](#), D. Battulga [ID¹⁸](#), M. Bauce [ID^{75a,75b}](#), M. Bauer [ID³⁶](#), P. Bauer [ID²⁴](#), L.T. Bazzano Hurrell [ID³⁰](#), J.B. Beacham [ID⁵¹](#), T. Beau [ID¹²⁷](#), P.H. Beauchemin [ID¹⁵⁸](#), F. Becherer [ID⁵⁴](#), P. Bechtle [ID²⁴](#), H.P. Beck [ID^{19,p}](#), K. Becker [ID¹⁶⁷](#), A.J. Beddall [ID⁸²](#), V.A. Bednyakov [ID³⁸](#), C.P. Bee [ID¹⁴⁵](#), L.J. Beemster ¹⁵, T.A. Beermann [ID³⁶](#), M. Begalli [ID^{83d}](#), M. Begel [ID²⁹](#), A. Behera [ID¹⁴⁵](#), J.K. Behr [ID⁴⁸](#), J.F. Beirer [ID⁵⁵](#), F. Beisiegel [ID²⁴](#), M. Belfkir [ID¹⁵⁹](#), G. Bella [ID¹⁵¹](#), L. Bellagamba [ID^{23b}](#), A. Bellerive [ID³⁴](#), P. Bellos [ID²⁰](#), K. Beloborodov [ID³⁷](#), N.L. Belyaev [ID³⁷](#), D. Benchekroun [ID^{35a}](#), F. Bendebba [ID^{35a}](#), Y. Benhammou [ID¹⁵¹](#), M. Benoit [ID²⁹](#), J.R. Bensinger [ID²⁶](#), S. Bentvelsen [ID¹¹⁴](#), L. Beresford [ID⁴⁸](#), M. Beretta [ID⁵³](#), E. Bergeaas Kuutmann [ID¹⁶¹](#), N. Berger [ID⁴](#), B. Bergmann [ID¹³²](#), J. Beringer [ID^{17a}](#), G. Bernardi [ID⁵](#), C. Bernius [ID¹⁴³](#), F.U. Bernlochner [ID²⁴](#), F. Bernon [ID^{36,102}](#), T. Berry [ID⁹⁵](#), P. Berta [ID¹³³](#), A. Berthold [ID⁵⁰](#), I.A. Bertram [ID⁹¹](#), S. Bethke [ID¹¹⁰](#), A. Betti [ID^{75a,75b}](#), A.J. Bevan [ID⁹⁴](#), M. Bhamjee [ID^{33c}](#), S. Bhatta [ID¹⁴⁵](#), D.S. Bhattacharya [ID¹⁶⁶](#), P. Bhattacharai [ID¹⁴³](#), V.S. Bhopatkar [ID¹²¹](#), R. Bi^{29,aj}, R.M. Bianchi [ID¹²⁹](#), G. Bianco [ID^{23b,23a}](#), O. Biebel [ID¹⁰⁹](#), R. Bielski [ID¹²³](#), M. Biglietti [ID^{77a}](#), T.R.V. Billoud [ID¹³²](#), M. Bindi [ID⁵⁵](#), A. Bingul [ID^{21b}](#), C. Bini [ID^{75a,75b}](#), A. Biondini [ID⁹²](#), C.J. Birch-sykes [ID¹⁰¹](#), G.A. Bird [ID^{20,134}](#), M. Birman [ID¹⁶⁹](#), M. Biros [ID¹³³](#), S. Biryukov [ID¹⁴⁶](#), T. Bisanz [ID⁴⁹](#), E. Bisceglie [ID^{43b,43a}](#), J.P. Biswal [ID¹³⁴](#), D. Biswas [ID¹⁴¹](#), A. Bitadze [ID¹⁰¹](#), K. Bjørke [ID¹²⁵](#), I. Bloch [ID⁴⁸](#), C. Blocker [ID²⁶](#), A. Blue [ID⁵⁹](#), U. Blumenschein [ID⁹⁴](#), J. Blumenthal [ID¹⁰⁰](#), G.J. Bobbink [ID¹¹⁴](#), V.S. Bobrovnikov [ID³⁷](#), M. Boehler [ID⁵⁴](#), B. Boehm [ID¹⁶⁶](#), D. Bogavac [ID³⁶](#), A.G. Bogdanchikov [ID³⁷](#), C. Bohm [ID^{47a}](#), V. Boisvert [ID⁹⁵](#), P. Bokan [ID⁴⁸](#), T. Bold [ID^{86a}](#), M. Bomben [ID⁵](#), M. Bona [ID⁹⁴](#), M. Boonekamp [ID¹³⁵](#), C.D. Booth [ID⁹⁵](#), A.G. Borbély [ID⁵⁹](#), I.S. Bordulev [ID³⁷](#), H.M. Borecka-Bielska [ID¹⁰⁸](#), L.S. Borgna [ID⁹⁶](#), G. Borissov [ID⁹¹](#), D. Bortoletto [ID¹²⁶](#), D. Boscherini [ID^{23b}](#), M. Bosman [ID¹³](#), J.D. Bossio Sola [ID³⁶](#), K. Bouaouda [ID^{35a}](#), N. Bouchhar [ID¹⁶³](#), J. Boudreau [ID¹²⁹](#), E.V. Bouhova-Thacker [ID⁹¹](#), D. Boumediene [ID⁴⁰](#), R. Bouquet [ID⁵](#), A. Boveia [ID¹¹⁹](#), J. Boyd [ID³⁶](#), D. Boye [ID²⁹](#), I.R. Boyko [ID³⁸](#), J. Bracinik [ID²⁰](#), N. Brahimi [ID^{62d}](#), G. Brandt [ID¹⁷¹](#), O. Brandt [ID³²](#), F. Braren [ID⁴⁸](#), B. Brau [ID¹⁰³](#), J.E. Brau [ID¹²³](#), R. Brener [ID¹⁶⁹](#), L. Brenner [ID¹¹⁴](#), R. Brenner [ID¹⁶¹](#), S. Bressler [ID¹⁶⁹](#), D. Britton [ID⁵⁹](#), D. Britzger [ID¹¹⁰](#), I. Brock [ID²⁴](#), G. Brooijmans [ID⁴¹](#), W.K. Brooks [ID^{137f}](#), E. Brost [ID²⁹](#), L.M. Brown [ID¹⁶⁵](#), L.E. Bruce [ID⁶¹](#), T.L. Bruckler [ID¹²⁶](#), P.A. Bruckman de Renstrom [ID⁸⁷](#), B. Brüers [ID⁴⁸](#), A. Bruni [ID^{23b}](#), G. Bruni [ID^{23b}](#), M. Bruschi [ID^{23b}](#), N. Bruscino [ID^{75a,75b}](#), T. Buanes [ID¹⁶](#), Q. Buat [ID¹³⁸](#), D. Buchin [ID¹¹⁰](#), A.G. Buckley [ID⁵⁹](#), O. Bulekov [ID³⁷](#), B.A. Bullard [ID¹⁴³](#), S. Burdin [ID⁹²](#), C.D. Burgard [ID⁴⁹](#), A.M. Burger [ID⁴⁰](#), B. Burghgrave [ID⁸](#), O. Burlayenko [ID⁵⁴](#), J.T.P. Burr [ID³²](#), C.D. Burton [ID¹¹](#), J.C. Burzynski [ID¹⁴²](#), E.L. Busch [ID⁴¹](#), V. Büscher [ID¹⁰⁰](#), P.J. Bussey [ID⁵⁹](#), J.M. Butler [ID²⁵](#), C.M. Buttar [ID⁵⁹](#), J.M. Butterworth [ID⁹⁶](#), W. Buttinger [ID¹³⁴](#), C.J. Buxo Vazquez [ID¹⁰⁷](#), A.R. Buzykaev [ID³⁷](#), S. Cabrera Urbán [ID¹⁶³](#), L. Cadamuro [ID⁶⁶](#), D. Caforio [ID⁵⁸](#), H. Cai [ID¹²⁹](#), Y. Cai [ID^{14a,14e}](#), V.M.M. Cairo [ID³⁶](#), O. Cakir [ID^{3a}](#), N. Calace [ID³⁶](#), P. Calafiura [ID^{17a}](#), G. Calderini [ID¹²⁷](#), P. Calfayan [ID⁶⁸](#), G. Callea [ID⁵⁹](#), L.P. Caloba ^{83b}, D. Calvet [ID⁴⁰](#), S. Calvet [ID⁴⁰](#), T.P. Calvet [ID¹⁰²](#), M. Calvetti [ID^{74a,74b}](#), R. Camacho Toro [ID¹²⁷](#), S. Camarda [ID³⁶](#), D. Camarero Munoz [ID²⁶](#), P. Camarri [ID^{76a,76b}](#), M.T. Camerlingo [ID^{72a,72b}](#), D. Cameron [ID³⁶](#), C. Camincher [ID¹⁶⁵](#), M. Campanelli [ID⁹⁶](#), A. Camplani [ID⁴²](#), V. Canale [ID^{72a,72b}](#), A. Canesse [ID¹⁰⁴](#), J. Cantero [ID¹⁶³](#), Y. Cao [ID¹⁶²](#), F. Capocasa [ID²⁶](#), M. Capua [ID^{43b,43a}](#), A. Carbone [ID^{71a,71b}](#), R. Cardarelli [ID^{76a}](#), J.C.J. Cardenas [ID⁸](#), F. Cardillo [ID¹⁶³](#), T. Carli [ID³⁶](#), G. Carlino [ID^{72a}](#), J.I. Carlotto [ID¹³](#),

B.T. Carlson [ID^{129,r}](#), E.M. Carlson [ID^{165,156a}](#), L. Carminati [ID^{71a,71b}](#), A. Carnelli [ID¹³⁵](#),
 M. Carnesale [ID^{75a,75b}](#), S. Caron [ID¹¹³](#), E. Carquin [ID^{137f}](#), S. Carrá [ID^{71a,71b}](#), G. Carratta [ID^{23b,23a}](#),
 F. Carrio Argos [ID^{33g}](#), J.W.S. Carter [ID¹⁵⁵](#), T.M. Carter [ID⁵²](#), M.P. Casado [ID^{13,i}](#), M. Caspar [ID⁴⁸](#),
 E.G. Castiglia [ID¹⁷²](#), F.L. Castillo [ID⁴](#), L. Castillo Garcia [ID¹³](#), V. Castillo Gimenez [ID¹⁶³](#),
 N.F. Castro [ID^{130a,130e}](#), A. Catinaccio [ID³⁶](#), J.R. Catmore [ID¹²⁵](#), V. Cavalieri [ID²⁹](#), N. Cavalli [ID^{23b,23a}](#),
 V. Cavasinni [ID^{74a,74b}](#), Y.C. Cekmecelioglu [ID⁴⁸](#), E. Celebi [ID^{21a}](#), F. Celli [ID¹²⁶](#), M.S. Centonze [ID^{70a,70b}](#),
 V. Cepaitis [ID⁵⁶](#), K. Cerny [ID¹²²](#), A.S. Cerqueira [ID^{83a}](#), A. Cerri [ID¹⁴⁶](#), L. Cerrito [ID^{76a,76b}](#), F. Cerutti [ID^{17a}](#),
 B. Cervato [ID¹⁴¹](#), A. Cervelli [ID^{23b}](#), G. Cesarini [ID⁵³](#), S.A. Cetin [ID⁸²](#), Z. Chadi [ID^{35a}](#), D. Chakraborty [ID¹¹⁵](#),
 J. Chan [ID¹⁷⁰](#), W.Y. Chan [ID¹⁵³](#), J.D. Chapman [ID³²](#), E. Chapon [ID¹³⁵](#), B. Chargeishvili [ID^{149b}](#),
 D.G. Charlton [ID²⁰](#), T.P. Charman [ID⁹⁴](#), M. Chatterjee [ID¹⁹](#), C. Chauhan [ID¹³³](#), S. Chekanov [ID⁶](#),
 S.V. Chekulaev [ID^{156a}](#), G.A. Chelkov [ID^{38,a}](#), A. Chen [ID¹⁰⁶](#), B. Chen [ID¹⁵¹](#), B. Chen [ID¹⁶⁵](#), H. Chen [ID^{14c}](#),
 H. Chen [ID²⁹](#), J. Chen [ID^{62c}](#), J. Chen [ID¹⁴²](#), M. Chen [ID¹²⁶](#), S. Chen [ID¹⁵³](#), S.J. Chen [ID^{14c}](#), X. Chen [ID^{62c,135}](#),
 X. Chen [ID^{14b,ag}](#), Y. Chen [ID^{62a}](#), C.L. Cheng [ID¹⁷⁰](#), H.C. Cheng [ID^{64a}](#), S. Cheong [ID¹⁴³](#), A. Cheplakov [ID³⁸](#),
 E. Cheremushkina [ID⁴⁸](#), E. Cherepanova [ID¹¹⁴](#), R. Cherkaoui El Moursli [ID^{35e}](#), E. Cheu [ID⁷](#), K. Cheung [ID⁶⁵](#),
 L. Chevalier [ID¹³⁵](#), V. Chiarella [ID⁵³](#), G. Chiarelli [ID^{74a}](#), N. Chiedde [ID¹⁰²](#), G. Chiodini [ID^{70a}](#),
 A.S. Chisholm [ID²⁰](#), A. Chitan [ID^{27b}](#), M. Chitishvili [ID¹⁶³](#), M.V. Chizhov [ID³⁸](#), K. Choi [ID¹¹](#),
 A.R. Chomont [ID^{75a,75b}](#), Y. Chou [ID¹⁰³](#), E.Y.S. Chow [ID¹¹⁴](#), T. Chowdhury [ID^{33g}](#), K.L. Chu [ID¹⁶⁹](#),
 M.C. Chu [ID^{64a}](#), X. Chu [ID^{14a,14e}](#), J. Chudoba [ID¹³¹](#), J.J. Chwastowski [ID⁸⁷](#), D. Cieri [ID¹¹⁰](#), K.M. Ciesla [ID^{86a}](#),
 V. Cindro [ID⁹³](#), A. Ciocio [ID^{17a}](#), F. Cirotto [ID^{72a,72b}](#), Z.H. Citron [ID^{169,l}](#), M. Citterio [ID^{71a}](#), D.A. Ciubotaru [ID^{27b}](#),
 B.M. Ciungu [ID¹⁵⁵](#), A. Clark [ID⁵⁶](#), P.J. Clark [ID⁵²](#), J.M. Clavijo Columbie [ID⁴⁸](#), S.E. Clawson [ID⁴⁸](#),
 C. Clement [ID^{47a,47b}](#), J. Clercx [ID⁴⁸](#), L. Clissa [ID^{23b,23a}](#), Y. Coadou [ID¹⁰²](#), M. Cobal [ID^{69a,69c}](#),
 A. Coccaro [ID^{57b}](#), R.F. Coelho Barrue [ID^{130a}](#), R. Coelho Lopes De Sa [ID¹⁰³](#), S. Coelli [ID^{71a}](#), H. Cohen [ID¹⁵¹](#),
 A.E.C. Coimbra [ID^{71a,71b}](#), B. Cole [ID⁴¹](#), J. Collot [ID⁶⁰](#), P. Conde Muiño [ID^{130a,130g}](#), M.P. Connell [ID^{33c}](#),
 S.H. Connell [ID^{33c}](#), I.A. Connolly [ID⁵⁹](#), E.I. Conroy [ID¹²⁶](#), F. Conventi [ID^{72a,ai}](#), H.G. Cooke [ID²⁰](#),
 A.M. Cooper-Sarkar [ID¹²⁶](#), A. Cordeiro Oudot Choi [ID¹²⁷](#), F. Cormier [ID¹⁶⁴](#), L.D. Corpe [ID⁴⁰](#),
 M. Corradi [ID^{75a,75b}](#), F. Corriveau [ID^{104,x}](#), A. Cortes-Gonzalez [ID¹⁸](#), M.J. Costa [ID¹⁶³](#), F. Costanza [ID⁴](#),
 D. Costanzo [ID¹³⁹](#), B.M. Cote [ID¹¹⁹](#), G. Cowan [ID⁹⁵](#), K. Cranmer [ID¹⁷⁰](#), D. Cremonini [ID^{23b,23a}](#),
 S. Crépé-Renaudin [ID⁶⁰](#), F. Crescioli [ID¹²⁷](#), M. Cristinziani [ID¹⁴¹](#), M. Cristoforetti [ID^{78a,78b}](#), V. Croft [ID¹¹⁴](#),
 J.E. Crosby [ID¹²¹](#), G. Crosetti [ID^{43b,43a}](#), A. Cueto [ID⁹⁹](#), T. Cuhadar Donszelmann [ID¹⁶⁰](#), H. Cui [ID^{14a,14e}](#),
 Z. Cui [ID⁷](#), W.R. Cunningham [ID⁵⁹](#), F. Curcio [ID^{43b,43a}](#), P. Czodrowski [ID³⁶](#), M.M. Czurylo [ID^{63b}](#),
 M.J. Da Cunha Sargedas De Sousa [ID^{57b,57a}](#), J.V. Da Fonseca Pinto [ID^{83b}](#), C. Da Via [ID¹⁰¹](#),
 W. Dabrowski [ID^{86a}](#), T. Dado [ID⁴⁹](#), S. Dahbi [ID^{33g}](#), T. Dai [ID¹⁰⁶](#), D. Dal Santo [ID¹⁹](#), C. Dallapiccola [ID¹⁰³](#),
 M. Dam [ID⁴²](#), G. D'amen [ID²⁹](#), V. D'Amico [ID¹⁰⁹](#), J. Damp [ID¹⁰⁰](#), J.R. Dandoy [ID¹²⁸](#), M.F. Daneri [ID³⁰](#),
 M. Danninger [ID¹⁴²](#), V. Dao [ID³⁶](#), G. Darbo [ID^{57b}](#), S. Darmora [ID⁶](#), S.J. Das [ID^{29,aj}](#), S. D'Auria [ID^{71a,71b}](#),
 C. David [ID^{156b}](#), T. Davidek [ID¹³³](#), B. Davis-Purcell [ID³⁴](#), I. Dawson [ID⁹⁴](#), H.A. Day-hall [ID¹³²](#), K. De [ID⁸](#),
 R. De Asmundis [ID^{72a}](#), N. De Biase [ID⁴⁸](#), S. De Castro [ID^{23b,23a}](#), N. De Groot [ID¹¹³](#), P. de Jong [ID¹¹⁴](#),
 H. De la Torre [ID¹¹⁵](#), A. De Maria [ID^{14c}](#), A. De Salvo [ID^{75a}](#), U. De Sanctis [ID^{76a,76b}](#), A. De Santo [ID¹⁴⁶](#),
 J.B. De Vivie De Regie [ID⁶⁰](#), D.V. Dedovich [ID³⁸](#), J. Degens [ID¹¹⁴](#), A.M. Deiana [ID⁴⁴](#), F. Del Corso [ID^{23b,23a}](#),
 J. Del Peso [ID⁹⁹](#), F. Del Rio [ID^{63a}](#), F. Deliot [ID¹³⁵](#), C.M. Delitzsch [ID⁴⁹](#), M. Della Pietra [ID^{72a,72b}](#),
 D. Della Volpe [ID⁵⁶](#), A. Dell'Acqua [ID³⁶](#), L. Dell'Asta [ID^{71a,71b}](#), M. Delmastro [ID⁴](#), P.A. Delsart [ID⁶⁰](#),
 S. Demers [ID¹⁷²](#), M. Demichev [ID³⁸](#), S.P. Denisov [ID³⁷](#), L. D'Eramo [ID⁴⁰](#), D. Derendarz [ID⁸⁷](#), F. Derue [ID¹²⁷](#),
 P. Dervan [ID⁹²](#), K. Desch [ID²⁴](#), C. Deutsch [ID²⁴](#), F.A. Di Bello [ID^{57b,57a}](#), A. Di Ciaccio [ID^{76a,76b}](#),
 L. Di Ciaccio [ID⁴](#), A. Di Domenico [ID^{75a,75b}](#), C. Di Donato [ID^{72a,72b}](#), A. Di Girolamo [ID³⁶](#),
 G. Di Gregorio [ID⁵](#), A. Di Luca [ID^{78a,78b}](#), B. Di Micco [ID^{77a,77b}](#), R. Di Nardo [ID^{77a,77b}](#), C. Diaconu [ID¹⁰²](#),
 M. Diamantopoulou [ID³⁴](#), F.A. Dias [ID¹¹⁴](#), T. Dias Do Vale [ID¹⁴²](#), M.A. Diaz [ID^{137a,137b}](#),
 F.G. Diaz Capriles [ID²⁴](#), M. Didenko [ID¹⁶³](#), E.B. Diehl [ID¹⁰⁶](#), L. Diehl [ID⁵⁴](#), S. Díez Cornell [ID⁴⁸](#),
 C. Diez Pardos [ID¹⁴¹](#), C. Dimitriadi [ID^{161,24,161}](#), A. Dimitrieva [ID^{17a}](#), J. Dingfelder [ID²⁴](#), I-M. Dinu [ID^{27b}](#),

S.J. Dittmeier **ID**^{63b}, F. Dittus **ID**³⁶, F. Djama **ID**¹⁰², T. Djobava **ID**^{149b}, J.I. Djuvsland **ID**¹⁶,
 C. Doglioni **ID**^{101,98}, A. Dohnalova **ID**^{28a}, J. Dolejsi **ID**¹³³, Z. Dolezal **ID**¹³³, K.M. Dona **ID**³⁹,
 M. Donadelli **ID**^{83c}, B. Dong **ID**¹⁰⁷, J. Donini **ID**⁴⁰, A. D'Onofrio **ID**^{77a,77b}, M. D'Onofrio **ID**⁹²,
 J. Dopke **ID**¹³⁴, A. Doria **ID**^{72a}, N. Dos Santos Fernandes **ID**^{130a}, P. Dougan **ID**¹⁰¹, M.T. Dova **ID**⁹⁰,
 A.T. Doyle **ID**⁵⁹, M.A. Draguet **ID**¹²⁶, E. Dreyer **ID**¹⁶⁹, I. Drivas-koulouris **ID**¹⁰, A.S. Drobac **ID**¹⁵⁸,
 M. Drozdova **ID**⁵⁶, D. Du **ID**^{62a}, T.A. du Pree **ID**¹¹⁴, F. Dubinin **ID**³⁷, M. Dubovsky **ID**^{28a}, E. Duchovni **ID**¹⁶⁹,
 G. Duckeck **ID**¹⁰⁹, O.A. Ducu **ID**^{27b}, D. Duda **ID**⁵², A. Dudarev **ID**³⁶, E.R. Duden **ID**²⁶, M. D'uffizi **ID**¹⁰¹,
 L. Duflot **ID**⁶⁶, M. Dührssen **ID**³⁶, C. Dülzen **ID**¹⁷¹, A.E. Dumitriu **ID**^{27b}, M. Dunford **ID**^{63a}, S. Dungs **ID**⁴⁹,
 K. Dunne **ID**^{47a,47b}, A. Duperrin **ID**¹⁰², H. Duran Yildiz **ID**^{3a}, M. Düren **ID**⁵⁸, A. Durglishvili **ID**^{149b},
 B.L. Dwyer **ID**¹¹⁵, G.I. Dyckes **ID**^{17a}, M. Dyndal **ID**^{86a}, S. Dysch **ID**¹⁰¹, B.S. Dziedzic **ID**⁸⁷,
 Z.O. Earnshaw **ID**¹⁴⁶, G.H. Eberwein **ID**¹²⁶, B. Eckerova **ID**^{28a}, S. Eggebrecht **ID**⁵⁵,
 E. Egidio Purcino De Souza **ID**¹²⁷, L.F. Ehrke **ID**⁵⁶, G. Eigen **ID**¹⁶, K. Einsweiler **ID**^{17a}, T. Ekelof **ID**¹⁶¹,
 P.A. Ekman **ID**⁹⁸, S. El Farkh **ID**^{35b}, Y. El Ghazali **ID**^{35b}, H. El Jarrari **ID**^{35e,148}, A. El Moussaouy **ID**^{35a},
 V. Ellajosyula **ID**¹⁶¹, M. Ellert **ID**¹⁶¹, F. Ellinghaus **ID**¹⁷¹, A.A. Elliot **ID**⁹⁴, N. Ellis **ID**³⁶, J. Elmsheuser **ID**²⁹,
 M. Elsing **ID**³⁶, D. Emeliyanov **ID**¹³⁴, Y. Enari **ID**¹⁵³, I. Ene **ID**^{17a}, S. Epari **ID**¹³, J. Erdmann **ID**⁴⁹,
 P.A. Erland **ID**⁸⁷, M. Errenst **ID**¹⁷¹, M. Escalier **ID**⁶⁶, C. Escobar **ID**¹⁶³, E. Etzion **ID**¹⁵¹, G. Evans **ID**^{130a},
 H. Evans **ID**⁶⁸, L.S. Evans **ID**⁹⁵, M.O. Evans **ID**¹⁴⁶, A. Ezhilov **ID**³⁷, S. Ezzarqtouni **ID**^{35a}, F. Fabbri **ID**⁵⁹,
 L. Fabbri **ID**^{23b,23a}, G. Facini **ID**⁹⁶, V. Fadeev **ID**¹³⁶, R.M. Fakhrutdinov **ID**³⁷, S. Falciano **ID**^{75a},
 L.F. Falda Ulhoa Coelho **ID**³⁶, P.J. Falke **ID**²⁴, J. Faltova **ID**¹³³, C. Fan **ID**¹⁶², Y. Fan **ID**^{14a}, Y. Fang **ID**^{14a,14e},
 M. Fanti **ID**^{71a,71b}, M. Faraj **ID**^{69a,69b}, Z. Farazpay **ID**⁹⁷, A. Farbin **ID**⁸, A. Farilla **ID**^{77a}, T. Farooque **ID**¹⁰⁷,
 S.M. Farrington **ID**⁵², F. Fassi **ID**^{35e}, D. Fassouliotis **ID**⁹, M. Faucci Giannelli **ID**^{76a,76b}, W.J. Fawcett **ID**³²,
 L. Fayard **ID**⁶⁶, P. Federic **ID**¹³³, P. Federicova **ID**¹³¹, O.L. Fedin **ID**^{37,a}, G. Fedotov **ID**³⁷, M. Feickert **ID**¹⁷⁰,
 L. Feligioni **ID**¹⁰², D.E. Fellers **ID**¹²³, C. Feng **ID**^{62b}, M. Feng **ID**^{14b}, Z. Feng **ID**¹¹⁴, M.J. Fenton **ID**¹⁶⁰,
 A.B. Fenyuk **ID**³⁷, L. Ferencz **ID**⁴⁸, R.A.M. Ferguson **ID**⁹¹, S.I. Fernandez Luengo **ID**^{137f}, M.J.V. Fernoux **ID**¹⁰²,
 J. Ferrando **ID**⁴⁸, A. Ferrari **ID**¹⁶¹, P. Ferrari **ID**^{114,113}, R. Ferrari **ID**^{73a}, D. Ferrere **ID**⁵⁶, C. Ferretti **ID**¹⁰⁶,
 F. Fiedler **ID**¹⁰⁰, A. Filipčič **ID**⁹³, E.K. Filmer **ID**¹, F. Filthaut **ID**¹¹³, M.C.N. Fiolhais **ID**^{130a,130c,c},
 L. Fiorini **ID**¹⁶³, W.C. Fisher **ID**¹⁰⁷, T. Fitschen **ID**¹⁰¹, P.M. Fitzhugh **ID**¹³⁵, I. Fleck **ID**¹⁴¹, P. Fleischmann **ID**¹⁰⁶,
 T. Flick **ID**¹⁷¹, M. Flores **ID**^{33d,ad}, L.R. Flores Castillo **ID**^{64a}, L. Flores Sanz De Acedo **ID**³⁶,
 F.M. Follega **ID**^{78a,78b}, N. Fomin **ID**¹⁶, J.H. Foo **ID**¹⁵⁵, B.C. Forland **ID**⁶⁸, A. Formica **ID**¹³⁵, A.C. Forti **ID**¹⁰¹,
 E. Fortin **ID**³⁶, A.W. Fortman **ID**⁶¹, M.G. Foti **ID**^{17a}, L. Fountas **ID**^{9,j}, D. Fournier **ID**⁶⁶, H. Fox **ID**⁹¹,
 P. Francavilla **ID**^{74a,74b}, S. Francescato **ID**⁶¹, S. Franchellucci **ID**⁵⁶, M. Franchini **ID**^{23b,23a},
 S. Franchino **ID**^{63a}, D. Francis **ID**³⁶, L. Franco **ID**¹¹³, L. Franconi **ID**⁴⁸, M. Franklin **ID**⁶¹, G. Frattari **ID**²⁶,
 A.C. Freegard **ID**⁹⁴, W.S. Freund **ID**^{83b}, Y.Y. Frid **ID**¹⁵¹, J. Friend **ID**⁵⁹, N. Fritzsch **ID**⁵⁰, A. Froch **ID**⁵⁴,
 D. Froidevaux **ID**³⁶, J.A. Frost **ID**¹²⁶, Y. Fu **ID**^{62a}, M. Fujimoto **ID**^{118,ae}, E. Fullana Torregrosa **ID**^{163,*},
 K.Y. Fung **ID**^{64a}, E. Furtado De Simas Filho **ID**^{83b}, M. Furukawa **ID**¹⁵³, J. Fuster **ID**¹⁶³, A. Gabrielli **ID**^{23b,23a},
 A. Gabrielli **ID**¹⁵⁵, P. Gadow **ID**³⁶, G. Gagliardi **ID**^{57b,57a}, L.G. Gagnon **ID**^{17a}, E.J. Gallas **ID**¹²⁶,
 B.J. Gallop **ID**¹³⁴, K.K. Gan **ID**¹¹⁹, S. Ganguly **ID**¹⁵³, J. Gao **ID**^{62a}, Y. Gao **ID**⁵², F.M. Garay Walls **ID**^{137a,137b},
 B. Garcia **ID**^{29,aj}, C. García **ID**¹⁶³, A. Garcia Alonso **ID**¹¹⁴, A.G. Garcia Caffaro **ID**¹⁷²,
 J.E. García Navarro **ID**¹⁶³, M. Garcia-Sciveres **ID**^{17a}, G.L. Gardner **ID**¹²⁸, R.W. Gardner **ID**³⁹,
 N. Garelli **ID**¹⁵⁸, D. Garg **ID**⁸⁰, R.B. Garg **ID**^{143,o}, J.M. Gargan **ID**⁵², C.A. Garner **ID**¹⁵⁵, S.J. Gasiorowski **ID**¹³⁸,
 P. Gaspar **ID**^{83b}, G. Gaudio **ID**^{73a}, V. Gautam **ID**¹³, P. Gauzzi **ID**^{75a,75b}, I.L. Gavrilenko **ID**³⁷, A. Gavrilyuk **ID**³⁷,
 C. Gay **ID**¹⁶⁴, G. Gaycken **ID**⁴⁸, E.N. Gazis **ID**¹⁰, A.A. Geanta **ID**^{27b}, C.M. Gee **ID**¹³⁶, C. Gemme **ID**^{57b},
 M.H. Genest **ID**⁶⁰, S. Gentile **ID**^{75a,75b}, A.D. Gentry **ID**¹¹², S. George **ID**⁹⁵, W.F. George **ID**²⁰, T. Geralis **ID**⁴⁶,
 P. Gessinger-Befurt **ID**³⁶, M.E. Geyik **ID**¹⁷¹, M. Ghani **ID**¹⁶⁷, M. Ghneimat **ID**¹⁴¹, K. Ghorbanian **ID**⁹⁴,
 A. Ghosal **ID**¹⁴¹, A. Ghosh **ID**¹⁶⁰, A. Ghosh **ID**⁷, B. Giacobbe **ID**^{23b}, S. Giagu **ID**^{75a,75b}, T. Giani **ID**¹¹⁴,
 P. Giannetti **ID**^{74a}, A. Giannini **ID**^{62a}, S.M. Gibson **ID**⁹⁵, M. Gignac **ID**¹³⁶, D.T. Gil **ID**^{86b}, A.K. Gilbert **ID**^{86a},
 B.J. Gilbert **ID**⁴¹, D. Gillberg **ID**³⁴, G. Gilles **ID**¹¹⁴, N.E.K. Gillwald **ID**⁴⁸, L. Ginabat **ID**¹²⁷,

D.M. Gingrich [ID^{2,ah}](#), M.P. Giordani [ID^{69a,69c}](#), P.F. Giraud [ID¹³⁵](#), G. Giugliarelli [ID^{69a,69c}](#), D. Giugni [ID^{71a}](#), F. Giuli [ID³⁶](#), I. Gkialas [ID^{9,j}](#), L.K. Gladilin [ID³⁷](#), C. Glasman [ID⁹⁹](#), G.R. Gledhill [ID¹²³](#), G. Glemža [ID⁴⁸](#), M. Glisic [ID¹²³](#), I. Gnesi [ID^{43b,f}](#), Y. Go [ID^{29,aj}](#), M. Goblirsch-Kolb [ID³⁶](#), B. Gocke [ID⁴⁹](#), D. Godin [ID¹⁰⁸](#), B. Gokturk [ID^{21a}](#), S. Goldfarb [ID¹⁰⁵](#), T. Golling [ID⁵⁶](#), M.G.D. Gololo [ID^{33g}](#), D. Golubkov [ID³⁷](#), J.P. Gombas [ID¹⁰⁷](#), A. Gomes [ID^{130a,130b}](#), G. Gomes Da Silva [ID¹⁴¹](#), A.J. Gomez Delegido [ID¹⁶³](#), R. Gonçalo [ID^{130a,130c}](#), G. Gonella [ID¹²³](#), L. Gonella [ID²⁰](#), A. Gongadze [ID^{149c}](#), F. Gonnella [ID²⁰](#), J.L. Gonski [ID⁴¹](#), R.Y. González Andana [ID⁵²](#), S. González de la Hoz [ID¹⁶³](#), S. Gonzalez Fernandez [ID¹³](#), R. Gonzalez Lopez [ID⁹²](#), C. Gonzalez Renteria [ID^{17a}](#), M.V. Gonzalez Rodriguez [ID⁴⁸](#), R. Gonzalez Suarez [ID¹⁶¹](#), S. Gonzalez-Sevilla [ID⁵⁶](#), G.R. Gonzalvo Rodriguez [ID¹⁶³](#), L. Goossens [ID³⁶](#), B. Gorini [ID³⁶](#), E. Gorini [ID^{70a,70b}](#), A. Gorišek [ID⁹³](#), T.C. Gosart [ID¹²⁸](#), A.T. Goshaw [ID⁵¹](#), M.I. Gostkin [ID³⁸](#), S. Goswami [ID¹²¹](#), C.A. Gottardo [ID³⁶](#), S.A. Gotz [ID¹⁰⁹](#), M. Gouighri [ID^{35b}](#), V. Goumarre [ID⁴⁸](#), A.G. Goussiou [ID¹³⁸](#), N. Govender [ID^{33c}](#), I. Grabowska-Bold [ID^{86a}](#), K. Graham [ID³⁴](#), E. Gramstad [ID¹²⁵](#), S. Grancagnolo [ID^{70a,70b}](#), M. Grandi [ID¹⁴⁶](#), C.M. Grant [ID^{1,135}](#), P.M. Gravila [ID^{27f}](#), F.G. Gravili [ID^{70a,70b}](#), H.M. Gray [ID^{17a}](#), M. Greco [ID^{70a,70b}](#), C. Grefe [ID²⁴](#), I.M. Gregor [ID⁴⁸](#), P. Grenier [ID¹⁴³](#), C. Grieco [ID¹³](#), A.A. Grillo [ID¹³⁶](#), K. Grimm [ID³¹](#), S. Grinstein [ID^{13,t}](#), J.-F. Grivaz [ID⁶⁶](#), E. Gross [ID¹⁶⁹](#), J. Grosse-Knetter [ID⁵⁵](#), C. Grud [ID¹⁰⁶](#), J.C. Grundy [ID¹²⁶](#), L. Guan [ID¹⁰⁶](#), W. Guan [ID²⁹](#), C. Gubbels [ID¹⁶⁴](#), J.G.R. Guerrero Rojas [ID¹⁶³](#), G. Guerrrieri [ID^{69a,69c}](#), F. Guescini [ID¹¹⁰](#), R. Gugel [ID¹⁰⁰](#), J.A.M. Guhit [ID¹⁰⁶](#), A. Guida [ID¹⁸](#), T. Guillemin [ID⁴](#), E. Guilloton [ID^{167,134}](#), S. Guindon [ID³⁶](#), F. Guo [ID^{14a,14e}](#), J. Guo [ID^{62c}](#), L. Guo [ID⁴⁸](#), Y. Guo [ID¹⁰⁶](#), R. Gupta [ID⁴⁸](#), S. Gurbuz [ID²⁴](#), S.S. Gurdasani [ID⁵⁴](#), G. Gustavino [ID³⁶](#), M. Guth [ID⁵⁶](#), P. Gutierrez [ID¹²⁰](#), L.F. Gutierrez Zagazeta [ID¹²⁸](#), C. Gutschow [ID⁹⁶](#), C. Gwenlan [ID¹²⁶](#), C.B. Gwilliam [ID⁹²](#), E.S. Haaland [ID¹²⁵](#), A. Haas [ID¹¹⁷](#), M. Habedank [ID⁴⁸](#), C. Haber [ID^{17a}](#), H.K. Hadavand [ID⁸](#), A. Hadef [ID¹⁰⁰](#), S. Hadzic [ID¹¹⁰](#), J.J. Hahn [ID¹⁴¹](#), E.H. Haines [ID⁹⁶](#), M. Haleem [ID¹⁶⁶](#), J. Haley [ID¹²¹](#), J.J. Hall [ID¹³⁹](#), G.D. Hallewell [ID¹⁰²](#), L. Halser [ID¹⁹](#), K. Hamano [ID¹⁶⁵](#), M. Hamer [ID²⁴](#), G.N. Hamity [ID⁵²](#), E.J. Hampshire [ID⁹⁵](#), J. Han [ID^{62b}](#), K. Han [ID^{62a}](#), L. Han [ID^{14c}](#), L. Han [ID^{62a}](#), S. Han [ID^{17a}](#), Y.F. Han [ID¹⁵⁵](#), K. Hanagaki [ID⁸⁴](#), M. Hance [ID¹³⁶](#), D.A. Hangal [ID^{41,ac}](#), H. Hanif [ID¹⁴²](#), M.D. Hank [ID¹²⁸](#), R. Hankache [ID¹⁰¹](#), J.B. Hansen [ID⁴²](#), J.D. Hansen [ID⁴²](#), P.H. Hansen [ID⁴²](#), K. Hara [ID¹⁵⁷](#), D. Harada [ID⁵⁶](#), T. Harenberg [ID¹⁷¹](#), S. Harkusha [ID³⁷](#), M.L. Harris [ID¹⁰³](#), Y.T. Harris [ID¹²⁶](#), J. Harrison [ID¹³](#), N.M. Harrison [ID¹¹⁹](#), P.F. Harrison [ID¹⁶⁷](#), N.M. Hartman [ID¹¹⁰](#), N.M. Hartmann [ID¹⁰⁹](#), Y. Hasegawa [ID¹⁴⁰](#), A. Hasib [ID⁵²](#), S. Haug [ID¹⁹](#), R. Hauser [ID¹⁰⁷](#), C.M. Hawkes [ID²⁰](#), R.J. Hawkings [ID³⁶](#), Y. Hayashi [ID¹⁵³](#), S. Hayashida [ID¹¹¹](#), D. Hayden [ID¹⁰⁷](#), C. Hayes [ID¹⁰⁶](#), R.L. Hayes [ID¹¹⁴](#), C.P. Hays [ID¹²⁶](#), J.M. Hays [ID⁹⁴](#), H.S. Hayward [ID⁹²](#), F. He [ID^{62a}](#), M. He [ID^{14a,14e}](#), Y. He [ID¹⁵⁴](#), Y. He [ID⁴⁸](#), N.B. Heatley [ID⁹⁴](#), V. Hedberg [ID⁹⁸](#), A.L. Heggelund [ID¹²⁵](#), N.D. Hehir [ID⁹⁴](#), C. Heidegger [ID⁵⁴](#), K.K. Heidegger [ID⁵⁴](#), W.D. Heidorn [ID⁸¹](#), J. Heilman [ID³⁴](#), S. Heim [ID⁴⁸](#), T. Heim [ID^{17a}](#), J.G. Heinlein [ID¹²⁸](#), J.J. Heinrich [ID¹²³](#), L. Heinrich [ID^{110,af}](#), J. Hejbal [ID¹³¹](#), L. Helary [ID⁴⁸](#), A. Held [ID¹⁷⁰](#), S. Hellesund [ID¹⁶](#), C.M. Helling [ID¹⁶⁴](#), S. Hellman [ID^{47a,47b}](#), R.C.W. Henderson [ID⁹¹](#), L. Henkelmann [ID³²](#), A.M. Henriques Correia [ID³⁶](#), H. Herde [ID⁹⁸](#), Y. Hernández Jiménez [ID¹⁴⁵](#), L.M. Herrmann [ID²⁴](#), T. Herrmann [ID⁵⁰](#), G. Herten [ID⁵⁴](#), R. Hertenberger [ID¹⁰⁹](#), L. Hervas [ID³⁶](#), M.E. Hesping [ID¹⁰⁰](#), N.P. Hessey [ID^{156a}](#), H. Hibi [ID⁸⁵](#), S.J. Hillier [ID²⁰](#), J.R. Hinds [ID¹⁰⁷](#), F. Hinterkeuser [ID²⁴](#), M. Hirose [ID¹²⁴](#), S. Hirose [ID¹⁵⁷](#), D. Hirschbuehl [ID¹⁷¹](#), T.G. Hitchings [ID¹⁰¹](#), B. Hiti [ID⁹³](#), J. Hobbs [ID¹⁴⁵](#), R. Hobincu [ID^{27e}](#), N. Hod [ID¹⁶⁹](#), M.C. Hodgkinson [ID¹³⁹](#), B.H. Hodgkinson [ID³²](#), A. Hoecker [ID³⁶](#), J. Hofer [ID⁴⁸](#), T. Holm [ID²⁴](#), M. Holzbock [ID¹¹⁰](#), L.B.A.H. Hommels [ID³²](#), B.P. Honan [ID¹⁰¹](#), J. Hong [ID^{62c}](#), T.M. Hong [ID¹²⁹](#), B.H. Hooberman [ID¹⁶²](#), W.H. Hopkins [ID⁶](#), Y. Horii [ID¹¹¹](#), S. Hou [ID¹⁴⁸](#), A.S. Howard [ID⁹³](#), J. Howarth [ID⁵⁹](#), J. Hoya [ID⁶](#), M. Hrabovsky [ID¹²²](#), A. Hrynevich [ID⁴⁸](#), T. Hrynn'ova [ID⁴](#), P.J. Hsu [ID⁶⁵](#), S.-C. Hsu [ID¹³⁸](#), Q. Hu [ID^{62a}](#), Y.F. Hu [ID^{14a,14e}](#), S. Huang [ID^{64b}](#), X. Huang [ID^{14c}](#), Y. Huang [ID¹³⁹](#), Y. Huang [ID^{14a}](#), Z. Huang [ID¹⁰¹](#), Z. Hubacek [ID¹³²](#), M. Huebner [ID²⁴](#), F. Huegging [ID²⁴](#), T.B. Huffman [ID¹²⁶](#), C.A. Hugli [ID⁴⁸](#), M. Huhtinen [ID³⁶](#), S.K. Huiberts [ID¹⁶](#), R. Hulsken [ID¹⁰⁴](#), N. Huseynov [ID^{12,a}](#), J. Huston [ID¹⁰⁷](#), J. Huth [ID⁶¹](#), R. Hyneman [ID¹⁴³](#), G. Iacobucci [ID⁵⁶](#), G. Iakovidis [ID²⁹](#), I. Ibragimov [ID¹⁴¹](#), L. Iconomidou-Fayard [ID⁶⁶](#), P. Iengo [ID^{72a,72b}](#),

R. Iguchi [ID¹⁵³](#), T. Iizawa [ID¹²⁶](#), Y. Ikegami [ID⁸⁴](#), N. Ilic [ID¹⁵⁵](#), H. Imam [ID^{35a}](#), M. Ince Lezki [ID⁵⁶](#),
 T. Ingebretsen Carlson [ID^{47a,47b}](#), G. Introzzi [ID^{73a,73b}](#), M. Iodice [ID^{77a}](#), V. Ippolito [ID^{75a,75b}](#), R.K. Irwin [ID⁹²](#),
 M. Ishino [ID¹⁵³](#), W. Islam [ID¹⁷⁰](#), C. Issever [ID^{18,48}](#), S. Istin [ID^{21a,al}](#), H. Ito [ID¹⁶⁸](#), J.M. Iturbe Ponce [ID^{64a}](#),
 R. Iuppa [ID^{78a,78b}](#), A. Ivina [ID¹⁶⁹](#), J.M. Izen [ID⁴⁵](#), V. Izzo [ID^{72a}](#), P. Jacka [ID^{131,132}](#), P. Jackson [ID¹](#),
 R.M. Jacobs [ID⁴⁸](#), B.P. Jaeger [ID¹⁴²](#), C.S. Jagfeld [ID¹⁰⁹](#), G. Jain [ID^{156a}](#), P. Jain [ID⁵⁴](#), G. Jäkel [ID¹⁷¹](#),
 K. Jakobs [ID⁵⁴](#), T. Jakoubek [ID¹⁶⁹](#), J. Jamieson [ID⁵⁹](#), K.W. Janas [ID^{86a}](#), M. Javurkova [ID¹⁰³](#), F. Jeanneau [ID¹³⁵](#),
 L. Jeanty [ID¹²³](#), J. Jejelava [ID^{149a,aa}](#), P. Jenni [ID^{54,g}](#), C.E. Jessiman [ID³⁴](#), S. Jézéquel [ID⁴](#), C. Jia [ID^{62b}](#),
 J. Jia [ID¹⁴⁵](#), X. Jia [ID⁶¹](#), X. Jia [ID^{14a,14e}](#), Z. Jia [ID^{14c}](#), Y. Jiang [ID^{62a}](#), S. Jiggins [ID⁴⁸](#), J. Jimenez Pena [ID¹³](#),
 S. Jin [ID^{14c}](#), A. Jinaru [ID^{27b}](#), O. Jinnouchi [ID¹⁵⁴](#), P. Johansson [ID¹³⁹](#), K.A. Johns [ID⁷](#), J.W. Johnson [ID¹³⁶](#),
 D.M. Jones [ID³²](#), E. Jones [ID⁴⁸](#), P. Jones [ID³²](#), R.W.L. Jones [ID⁹¹](#), T.J. Jones [ID⁹²](#), H.L. Joos [ID^{55,36}](#),
 R. Joshi [ID¹¹⁹](#), J. Jovicevic [ID¹⁵](#), X. Ju [ID^{17a}](#), J.J. Junggeburth [ID¹⁰³](#), T. Junkermann [ID^{63a}](#),
 A. Juste Rozas [ID^{13,t}](#), M.K. Juzek [ID⁸⁷](#), S. Kabana [ID^{137e}](#), A. Kaczmarska [ID⁸⁷](#), M. Kado [ID¹¹⁰](#),
 H. Kagan [ID¹¹⁹](#), M. Kagan [ID¹⁴³](#), A. Kahn [ID⁴¹](#), A. Kahn [ID¹²⁸](#), C. Kahra [ID¹⁰⁰](#), T. Kaji [ID¹⁵³](#),
 E. Kajomovitz [ID¹⁵⁰](#), N. Kakati [ID¹⁶⁹](#), I. Kalaitzidou [ID⁵⁴](#), C.W. Kalderon [ID²⁹](#), A. Kamenshchikov [ID¹⁵⁵](#),
 N.J. Kang [ID¹³⁶](#), D. Kar [ID^{33g}](#), K. Karava [ID¹²⁶](#), M.J. Kareem [ID^{156b}](#), E. Karentzos [ID⁵⁴](#), I. Karkanias [ID¹⁵²](#),
 O. Karkout [ID¹¹⁴](#), S.N. Karpov [ID³⁸](#), Z.M. Karpova [ID³⁸](#), V. Kartvelishvili [ID⁹¹](#), A.N. Karyukhin [ID³⁷](#),
 E. Kasimi [ID¹⁵²](#), J. Katzy [ID⁴⁸](#), S. Kaur [ID³⁴](#), K. Kawade [ID¹⁴⁰](#), M.P. Kawale [ID¹²⁰](#), T. Kawamoto [ID¹³⁵](#),
 E.F. Kay [ID³⁶](#), F.I. Kaya [ID¹⁵⁸](#), S. Kazakos [ID¹⁰⁷](#), V.F. Kazanin [ID³⁷](#), Y. Ke [ID¹⁴⁵](#), J.M. Keaveney [ID^{33a}](#),
 R. Keeler [ID¹⁶⁵](#), G.V. Kehris [ID⁶¹](#), J.S. Keller [ID³⁴](#), A.S. Kelly [ID⁹⁶](#), J.J. Kempster [ID¹⁴⁶](#), K.E. Kennedy [ID⁴¹](#),
 P.D. Kennedy [ID¹⁰⁰](#), O. Kepka [ID¹³¹](#), B.P. Kerridge [ID¹⁶⁷](#), S. Kersten [ID¹⁷¹](#), B.P. Kerševan [ID⁹³](#),
 S. Keshri [ID⁶⁶](#), L. Keszeghova [ID^{28a}](#), S. Ketabchi Haghight [ID¹⁵⁵](#), M. Khandoga [ID¹²⁷](#), A. Khanov [ID¹²¹](#),
 A.G. Kharlamov [ID³⁷](#), T. Kharlamova [ID³⁷](#), E.E. Khoda [ID¹³⁸](#), T.J. Khoo [ID¹⁸](#), G. Khoriauli [ID¹⁶⁶](#),
 J. Khubua [ID^{149b}](#), Y.A.R. Khwaira [ID⁶⁶](#), A. Kilgallon [ID¹²³](#), D.W. Kim [ID^{47a,47b}](#), Y.K. Kim [ID³⁹](#),
 N. Kimura [ID⁹⁶](#), M.K. Kingston [ID⁵⁵](#), A. Kirchhoff [ID⁵⁵](#), C. Kirfel [ID²⁴](#), F. Kirfel [ID²⁴](#), J. Kirk [ID¹³⁴](#),
 A.E. Kiryunin [ID¹¹⁰](#), C. Kitsaki [ID¹⁰](#), O. Kivernyk [ID²⁴](#), M. Klassen [ID^{63a}](#), C. Klein [ID³⁴](#), L. Klein [ID¹⁶⁶](#),
 M.H. Klein [ID¹⁰⁶](#), M. Klein [ID⁹²](#), S.B. Klein [ID⁵⁶](#), U. Klein [ID⁹²](#), P. Klimek [ID³⁶](#), A. Klimentov [ID²⁹](#),
 T. Klioutchnikova [ID³⁶](#), P. Kluit [ID¹¹⁴](#), S. Kluth [ID¹¹⁰](#), E. Kneringer [ID⁷⁹](#), T.M. Knight [ID¹⁵⁵](#), A. Knue [ID⁴⁹](#),
 R. Kobayashi [ID⁸⁸](#), D. Kobylianskii [ID¹⁶⁹](#), S.F. Koch [ID¹²⁶](#), M. Kocian [ID¹⁴³](#), P. Kodyš [ID¹³³](#),
 D.M. Koeck [ID¹²³](#), P.T. Koenig [ID²⁴](#), T. Koffas [ID³⁴](#), M. Kolb [ID¹³⁵](#), I. Koletsou [ID⁴](#), T. Komarek [ID¹²²](#),
 K. Köneke [ID⁵⁴](#), A.X.Y. Kong [ID¹](#), T. Kono [ID¹¹⁸](#), N. Konstantinidis [ID⁹⁶](#), B. Konya [ID⁹⁸](#),
 R. Kopeliansky [ID⁶⁸](#), S. Koperny [ID^{86a}](#), K. Korcyl [ID⁸⁷](#), K. Kordas [ID^{152,e}](#), G. Koren [ID¹⁵¹](#), A. Korn [ID⁹⁶](#),
 S. Korn [ID⁵⁵](#), I. Korolkov [ID¹³](#), N. Korotkova [ID³⁷](#), B. Kortman [ID¹¹⁴](#), O. Kortner [ID¹¹⁰](#), S. Kortner [ID¹¹⁰](#),
 W.H. Kostecka [ID¹¹⁵](#), V.V. Kostyukhin [ID¹⁴¹](#), A. Kotsokechagia [ID¹³⁵](#), A. Kotwal [ID⁵¹](#), A. Koulouris [ID³⁶](#),
 A. Kourkoumeli-Charalampidi [ID^{73a,73b}](#), C. Kourkoumelis [ID⁹](#), E. Kourlitis [ID^{110,af}](#), O. Kovanda [ID¹⁴⁶](#),
 R. Kowalewski [ID¹⁶⁵](#), W. Kozanecki [ID¹³⁵](#), A.S. Kozhin [ID³⁷](#), V.A. Kramarenko [ID³⁷](#), G. Kramberger [ID⁹³](#),
 P. Kramer [ID¹⁰⁰](#), M.W. Krasny [ID¹²⁷](#), A. Krasznahorkay [ID³⁶](#), J.W. Kraus [ID¹⁷¹](#), J.A. Kremer [ID¹⁰⁰](#),
 T. Kresse [ID⁵⁰](#), J. Kretzschmar [ID⁹²](#), K. Kreul [ID¹⁸](#), P. Krieger [ID¹⁵⁵](#), S. Krishnamurthy [ID¹⁰³](#),
 M. Krivos [ID¹³³](#), K. Krizka [ID²⁰](#), K. Kroeninger [ID⁴⁹](#), H. Kroha [ID¹¹⁰](#), J. Kroll [ID¹³¹](#), J. Kroll [ID¹²⁸](#),
 K.S. Krowpman [ID¹⁰⁷](#), U. Kruchonak [ID³⁸](#), H. Krüger [ID²⁴](#), N. Krumnack ⁸¹, M.C. Kruse [ID⁵¹](#),
 J.A. Krzysiak [ID⁸⁷](#), O. Kuchinskai [ID³⁷](#), S. Kuday [ID^{3a}](#), S. Kuehn [ID³⁶](#), R. Kuesters [ID⁵⁴](#), T. Kuhl [ID⁴⁸](#),
 V. Kukhtin [ID³⁸](#), Y. Kulchitsky [ID^{37,a}](#), S. Kuleshov [ID^{137d,137b}](#), M. Kumar [ID^{33g}](#), N. Kumari [ID⁴⁸](#),
 A. Kupco [ID¹³¹](#), T. Kupfer ⁴⁹, A. Kupich [ID³⁷](#), O. Kuprash [ID⁵⁴](#), H. Kurashige [ID⁸⁵](#), L.L. Kurchaninov [ID^{156a}](#),
 O. Kurdysh [ID⁶⁶](#), Y.A. Kurochkin [ID³⁷](#), A. Kurova [ID³⁷](#), M. Kuze [ID¹⁵⁴](#), A.K. Kvam [ID¹⁰³](#), J. Kvita [ID¹²²](#),
 T. Kwan [ID¹⁰⁴](#), N.G. Kyriacou [ID¹⁰⁶](#), L.A.O. Laatu [ID¹⁰²](#), C. Lacasta [ID¹⁶³](#), F. Lacava [ID^{75a,75b}](#),
 H. Lacker [ID¹⁸](#), D. Lacour [ID¹²⁷](#), N.N. Lad [ID⁹⁶](#), E. Ladygin [ID³⁸](#), B. Laforge [ID¹²⁷](#), T. Lagouri [ID^{137e}](#),
 F.Z. Lahbab [ID^{35a}](#), S. Lai [ID⁵⁵](#), I.K. Lakomiec [ID^{86a}](#), N. Lalloue [ID⁶⁰](#), J.E. Lambert [ID¹⁶⁵](#), S. Lammers [ID⁶⁸](#),
 W. Lampl [ID⁷](#), C. Lampoudis [ID^{152,e}](#), A.N. Lancaster [ID¹¹⁵](#), E. Lançon [ID²⁹](#), U. Landgraf [ID⁵⁴](#),

M.P.J. Landon id^{94} , V.S. Lang id^{54} , R.J. Langenberg id^{103} , O.K.B. Langrekken id^{125} , A.J. Lankford id^{160} , F. Lanni id^{36} , K. Lantzsch id^{24} , A. Lanza id^{73a} , A. Lapertosa $\text{id}^{57b,57a}$, J.F. Laporte id^{135} , T. Lari id^{71a} , F. Lasagni Manghi id^{23b} , M. Lassnig id^{36} , V. Latonova id^{131} , A. Laudrain id^{100} , A. Laurier id^{150} , S.D. Lawlor id^{95} , Z. Lawrence id^{101} , M. Lazzaroni $\text{id}^{71a,71b}$, B. Le¹⁰¹, E.M. Le Boulicaut id^{51} , B. Leban id^{93} , A. Lebedev id^{81} , M. LeBlanc id^{101} , F. Ledroit-Guillon id^{60} , A.C.A. Lee⁹⁶, S.C. Lee id^{148} , S. Lee $\text{id}^{47a,47b}$, T.F. Lee id^{92} , L.L. Leeuw id^{33c} , H.P. Lefebvre id^{95} , M. Lefebvre id^{165} , C. Leggett id^{17a} , G. Lehmann Miotto id^{36} , M. Leigh id^{56} , W.A. Leight id^{103} , W. Leinonen id^{113} , A. Leisos $\text{id}^{152,s}$, M.A.L. Leite id^{83c} , C.E. Leitgeb id^{48} , R. Leitner id^{133} , K.J.C. Leney id^{44} , T. Lenz id^{24} , S. Leone id^{74a} , C. Leonidopoulos id^{52} , A. Leopold id^{144} , C. Leroy id^{108} , R. Les id^{107} , C.G. Lester id^{32} , M. Levchenko id^{37} , J. Levêque id^4 , D. Levin id^{106} , L.J. Levinson id^{169} , M.P. Lewicki id^{87} , D.J. Lewis id^4 , A. Li id^5 , B. Li id^{62b} , C. Li id^{62a} , C-Q. Li id^{62c} , H. Li id^{62a} , H. Li id^{62b} , H. Li id^{14c} , H. Li id^{14b} , H. Li id^{62b} , K. Li id^{138} , L. Li id^{62c} , M. Li $\text{id}^{14a,14e}$, Q.Y. Li id^{62a} , S. Li $\text{id}^{14a,14e}$, S. Li $\text{id}^{62d,62c,d}$, T. Li id^5 , X. Li id^{104} , Z. Li id^{126} , Z. Li id^{104} , Z. Li id^{92} , Z. Li $\text{id}^{14a,14e}$, S. Liang $\text{id}^{14a,14e}$, Z. Liang id^{14a} , M. Liberatore id^{135} , B. Liberti id^{76a} , K. Lie id^{64c} , J. Lieber Marin id^{83b} , H. Lien id^{68} , K. Lin id^{107} , R.E. Lindley id^7 , J.H. Lindon id^2 , E. Lipeles id^{128} , A. Lipniacka id^{16} , A. Lister id^{164} , J.D. Little id^4 , B. Liu id^{14a} , B.X. Liu id^{142} , D. Liu $\text{id}^{62d,62c}$, J.B. Liu id^{62a} , J.K.K. Liu id^{32} , K. Liu $\text{id}^{62d,62c}$, M. Liu id^{62a} , M.Y. Liu id^{62a} , P. Liu id^{14a} , Q. Liu $\text{id}^{62d,138,62c}$, X. Liu id^{62a} , Y. Liu $\text{id}^{14d,14e}$, Y.L. Liu id^{62b} , Y.W. Liu id^{62a} , J. Llorente Merino id^{142} , S.L. Lloyd id^{94} , E.M. Lobodzinska id^{48} , P. Loch id^7 , S. Loffredo $\text{id}^{76a,76b}$, T. Lohse id^{18} , K. Lohwasser id^{139} , E. Loiacono id^{48} , M. Lokajicek $\text{id}^{131,*}$, J.D. Lomas id^{20} , J.D. Long id^{162} , I. Longarini id^{160} , L. Longo $\text{id}^{70a,70b}$, R. Longo id^{162} , I. Lopez Paz id^{67} , A. Lopez Solis id^{48} , J. Lorenz id^{109} , N. Lorenzo Martinez id^4 , A.M. Lory id^{109} , G. Löschcke Centeno id^{146} , O. Loseva id^{37} , X. Lou $\text{id}^{47a,47b}$, X. Lou $\text{id}^{14a,14e}$, A. Lounis id^{66} , J. Love id^6 , P.A. Love id^{91} , G. Lu $\text{id}^{14a,14e}$, M. Lu id^{80} , S. Lu id^{128} , Y.J. Lu id^{65} , H.J. Lubatti id^{138} , C. Luci $\text{id}^{75a,75b}$, F.L. Lucio Alves id^{14c} , A. Lucotte id^{60} , F. Luehring id^{68} , I. Luise id^{145} , O. Lukianchuk id^{66} , O. Lundberg id^{144} , B. Lund-Jensen id^{144} , N.A. Luongo id^{123} , M.S. Lutz id^{151} , D. Lynn id^{29} , H. Lyons id^{92} , R. Lysak id^{131} , E. Lytken id^{98} , V. Lyubushkin id^{38} , T. Lyubushkina id^{38} , M.M. Lyukova id^{145} , H. Ma id^{29} , K. Ma^{62a}, L.L. Ma id^{62b} , Y. Ma id^{121} , D.M. Mac Donell id^{165} , G. Maccarrone id^{53} , J.C. MacDonald id^{100} , P.C. Machado De Abreu Farias id^{83b} , R. Madar id^{40} , W.F. Mader id^{50} , T. Madula id^{96} , J. Maeda id^{85} , T. Maeno id^{29} , M. Maerker id^{50} , H. Maguire id^{139} , V. Maiboroda id^{135} , A. Maio $\text{id}^{130a,130b,130d}$, K. Maj id^{86a} , O. Majersky id^{48} , S. Majewski id^{123} , N. Makovec id^{66} , V. Maksimovic id^{15} , B. Malaescu id^{127} , Pa. Malecki id^{87} , V.P. Maleev id^{37} , F. Malek id^{60} , M. Mali id^{93} , D. Malito id^{95} , U. Mallik id^{80} , S. Maltezos¹⁰, S. Malyukov³⁸, J. Mamuzic id^{13} , G. Mancini id^{53} , G. Manco $\text{id}^{73a,73b}$, J.P. Mandalia id^{94} , I. Mandić id^{93} , L. Manhaes de Andrade Filho id^{83a} , I.M. Maniatis id^{169} , J. Manjarres Ramos $\text{id}^{102,ab}$, D.C. Mankad id^{169} , A. Mann id^{109} , B. Mansoulie id^{135} , S. Manzoni id^{36} , A. Marantis $\text{id}^{152,s}$, G. Marchiori id^5 , M. Marcisovsky id^{131} , C. Marcon $\text{id}^{71a,71b}$, M. Marinescu id^{20} , M. Marjanovic id^{120} , E.J. Marshall id^{91} , Z. Marshall id^{17a} , S. Marti-Garcia id^{163} , T.A. Martin id^{167} , V.J. Martin id^{52} , B. Martin dit Latour id^{16} , L. Martinelli $\text{id}^{75a,75b}$, M. Martinez $\text{id}^{13,t}$, P. Martinez Agullo id^{163} , V.I. Martinez Outschoorn id^{103} , P. Martinez Suarez id^{13} , S. Martin-Haugh id^{134} , V.S. Martoiu id^{27b} , A.C. Martyniuk id^{96} , A. Marzin id^{36} , D. Mascione $\text{id}^{78a,78b}$, L. Masetti id^{100} , T. Mashimo id^{153} , J. Masik id^{101} , A.L. Maslennikov id^{37} , L. Massa id^{23b} , P. Massarotti $\text{id}^{72a,72b}$, P. Mastrandrea $\text{id}^{74a,74b}$, A. Mastroberardino $\text{id}^{43b,43a}$, T. Masubuchi id^{153} , T. Mathisen id^{161} , J. Matousek id^{133} , N. Matsuzawa¹⁵³, J. Maurer id^{27b} , B. Maček id^{93} , D.A. Maximov id^{37} , R. Mazini id^{148} , I. Maznas id^{152} , M. Mazza id^{107} , S.M. Mazza id^{136} , E. Mazzeo $\text{id}^{71a,71b}$, C. Mc Ginn id^{29} , J.P. Mc Gowan id^{104} , S.P. Mc Kee id^{106} , E.F. McDonald id^{105} , A.E. McDougall id^{114} , J.A. Mcfayden id^{146} , R.P. McGovern id^{128} , G. Mchedlidze id^{149b} , R.P. Mckenzie id^{33g} , T.C. Mclachlan id^{48} , D.J. McLaughlin id^{96} , K.D. McLean id^{165} , S.J. McMahon id^{134} , P.C. McNamara id^{105} , C.M. Mcpartland id^{92} , R.A. McPherson $\text{id}^{165,x}$, S. Mehlhase id^{109} , A. Mehta id^{92} , D. Melini id^{150} ,

B.R. Mellado Garcia [ID^{33g}](#), A.H. Melo [ID⁵⁵](#), F. Meloni [ID⁴⁸](#), A.M. Mendes Jacques Da Costa [ID¹⁰¹](#),
 H.Y. Meng [ID¹⁵⁵](#), L. Meng [ID⁹¹](#), S. Menke [ID¹¹⁰](#), M. Mentink [ID³⁶](#), E. Meoni [ID^{43b,43a}](#), C. Merlassino [ID¹²⁶](#),
 L. Merola [ID^{72a,72b}](#), C. Meroni [ID^{71a,71b}](#), G. Merz [ID¹⁰⁶](#), O. Meshkov [ID³⁷](#), J. Metcalfe [ID⁶](#), A.S. Mete [ID⁶](#),
 C. Meyer [ID⁶⁸](#), J.-P. Meyer [ID¹³⁵](#), R.P. Middleton [ID¹³⁴](#), L. Mijović [ID⁵²](#), G. Mikenberg [ID¹⁶⁹](#),
 M. Mikestikova [ID¹³¹](#), M. Mikuž [ID⁹³](#), H. Mildner [ID¹⁰⁰](#), A. Milic [ID³⁶](#), C.D. Milke [ID⁴⁴](#), D.W. Miller [ID³⁹](#),
 L.S. Miller [ID³⁴](#), A. Milov [ID¹⁶⁹](#), D.A. Milstead [ID^{47a,47b}](#), T. Min [ID^{14c}](#), A.A. Minaenko [ID³⁷](#),
 I.A. Minashvili [ID^{149b}](#), L. Mince [ID⁵⁹](#), A.I. Mincer [ID¹¹⁷](#), B. Mindur [ID^{86a}](#), M. Mineev [ID³⁸](#), Y. Mino [ID⁸⁸](#),
 L.M. Mir [ID¹³](#), M. Miralles Lopez [ID¹⁶³](#), M. Mironova [ID^{17a}](#), A. Mishima [ID¹⁵³](#), M.C. Missio [ID¹¹³](#),
 A. Mitra [ID¹⁶⁷](#), V.A. Mitsou [ID¹⁶³](#), Y. Mitsumori [ID¹¹¹](#), O. Miu [ID¹⁵⁵](#), P.S. Miyagawa [ID⁹⁴](#),
 T. Mkrtchyan [ID^{63a}](#), M. Mlinarevic [ID⁹⁶](#), T. Mlinarevic [ID⁹⁶](#), M. Mlynarikova [ID³⁶](#), S. Mobius [ID¹⁹](#),
 P. Moder [ID⁴⁸](#), P. Mogg [ID¹⁰⁹](#), A.F. Mohammed [ID^{14a,14e}](#), S. Mohapatra [ID⁴¹](#), G. Mokgatitswane [ID^{33g}](#),
 L. Moleri [ID¹⁶⁹](#), B. Mondal [ID¹⁴¹](#), S. Mondal [ID¹³²](#), K. Mönig [ID⁴⁸](#), E. Monnier [ID¹⁰²](#),
 L. Monsonis Romero [ID¹⁶³](#), J. Montejo Berlingen [ID¹³](#), M. Montella [ID¹¹⁹](#), F. Montereali [ID^{77a,77b}](#),
 F. Monticelli [ID⁹⁰](#), S. Monzani [ID^{69a,69c}](#), N. Morange [ID⁶⁶](#), A.L. Moreira De Carvalho [ID^{130a}](#),
 M. Moreno Llácer [ID¹⁶³](#), C. Moreno Martinez [ID⁵⁶](#), P. Morettini [ID^{57b}](#), S. Morgenstern [ID³⁶](#), M. Morii [ID⁶¹](#),
 M. Morinaga [ID¹⁵³](#), A.K. Morley [ID³⁶](#), F. Morodei [ID^{75a,75b}](#), L. Morvaj [ID³⁶](#), P. Moschovakos [ID³⁶](#),
 B. Moser [ID³⁶](#), M. Mosidze [ID^{149b}](#), T. Moskalets [ID⁵⁴](#), P. Moskvitina [ID¹¹³](#), J. Moss [ID^{31,m}](#), E.J.W. Moyse [ID¹⁰³](#),
 O. Mtintsilana [ID^{33g}](#), S. Muanza [ID¹⁰²](#), J. Mueller [ID¹²⁹](#), D. Muenstermann [ID⁹¹](#), R. Müller [ID¹⁹](#),
 G.A. Mullier [ID¹⁶¹](#), A.J. Mullin [ID³²](#), J.J. Mullin [ID¹²⁸](#), D.P. Mungo [ID¹⁵⁵](#), D. Munoz Perez [ID¹⁶³](#),
 F.J. Munoz Sanchez [ID¹⁰¹](#), M. Murin [ID¹⁰¹](#), W.J. Murray [ID^{167,134}](#), A. Murrone [ID^{71a,71b}](#), J.M. Muse [ID¹²⁰](#),
 M. Muškinja [ID^{17a}](#), C. Mwewa [ID²⁹](#), A.G. Myagkov [ID^{37,a}](#), A.J. Myers [ID⁸](#), A.A. Myers [ID¹²⁹](#), G. Myers [ID⁶⁸](#),
 M. Myska [ID¹³²](#), B.P. Nachman [ID^{17a}](#), O. Nackenhorst [ID⁴⁹](#), A. Nag [ID⁵⁰](#), K. Nagai [ID¹²⁶](#), K. Nagano [ID⁸⁴](#),
 J.L. Nagle [ID^{29,aj}](#), E. Nagy [ID¹⁰²](#), A.M. Nairz [ID³⁶](#), Y. Nakahama [ID⁸⁴](#), K. Nakamura [ID⁸⁴](#), K. Nakkalil [ID⁵](#),
 H. Nanjo [ID¹²⁴](#), R. Narayan [ID⁴⁴](#), E.A. Narayanan [ID¹¹²](#), I. Naryshkin [ID³⁷](#), M. Naseri [ID³⁴](#), S. Nasri [ID¹⁵⁹](#),
 C. Nass [ID²⁴](#), G. Navarro [ID^{22a}](#), J. Navarro-Gonzalez [ID¹⁶³](#), R. Nayak [ID¹⁵¹](#), A. Nayaz [ID¹⁸](#),
 P.Y. Nechaeva [ID³⁷](#), F. Nechansky [ID⁴⁸](#), L. Nedic [ID¹²⁶](#), T.J. Neep [ID²⁰](#), A. Negri [ID^{73a,73b}](#), M. Negrini [ID^{23b}](#),
 C. Nellist [ID¹¹⁴](#), C. Nelson [ID¹⁰⁴](#), K. Nelson [ID¹⁰⁶](#), S. Nemecek [ID¹³¹](#), M. Nessi [ID^{36,h}](#), M.S. Neubauer [ID¹⁶²](#),
 F. Neuhaus [ID¹⁰⁰](#), J. Neundorf [ID⁴⁸](#), R. Newhouse [ID¹⁶⁴](#), P.R. Newman [ID²⁰](#), C.W. Ng [ID¹²⁹](#), Y.W.Y. Ng [ID⁴⁸](#),
 B. Ngair [ID^{35e}](#), H.D.N. Nguyen [ID¹⁰⁸](#), R.B. Nickerson [ID¹²⁶](#), R. Nicolaïdou [ID¹³⁵](#), J. Nielsen [ID¹³⁶](#),
 M. Niemeyer [ID⁵⁵](#), J. Niermann [ID^{55,36}](#), N. Nikiforou [ID³⁶](#), V. Nikolaenko [ID^{37,a}](#), I. Nikolic-Audit [ID¹²⁷](#),
 K. Nikolopoulos [ID²⁰](#), P. Nilsson [ID²⁹](#), I. Ninca [ID⁴⁸](#), H.R. Nindhito [ID⁵⁶](#), G. Ninio [ID¹⁵¹](#), A. Nisati [ID^{75a}](#),
 N. Nishu [ID²](#), R. Nisius [ID¹¹⁰](#), J-E. Nitschke [ID⁵⁰](#), E.K. Nkadimeng [ID^{33g}](#), T. Nobe [ID¹⁵³](#), D.L. Noel [ID³²](#),
 T. Nommensen [ID¹⁴⁷](#), M.B. Norfolk [ID¹³⁹](#), R.R.B. Norisam [ID⁹⁶](#), B.J. Norman [ID³⁴](#), J. Novak [ID⁹³](#),
 T. Novak [ID⁴⁸](#), L. Novotny [ID¹³²](#), R. Novotny [ID¹¹²](#), L. Nozka [ID¹²²](#), K. Ntekas [ID¹⁶⁰](#),
 N.M.J. Nunes De Moura Junior [ID^{83b}](#), E. Nurse [ID⁹⁶](#), J. Ocariz [ID¹²⁷](#), A. Ochi [ID⁸⁵](#), I. Ochoa [ID^{130a}](#),
 S. Oerdek [ID⁴⁸](#), J.T. Offermann [ID³⁹](#), A. Ogrodnik [ID¹³³](#), A. Oh [ID¹⁰¹](#), C.C. Ohm [ID¹⁴⁴](#), H. Oide [ID⁸⁴](#),
 R. Oishi [ID¹⁵³](#), M.L. Ojeda [ID⁴⁸](#), M.W. O'Keefe [ID⁹²](#), Y. Okumura [ID¹⁵³](#), L.F. Oleiro Seabra [ID^{130a}](#),
 S.A. Olivares Pino [ID^{137d}](#), D. Oliveira Damazio [ID²⁹](#), D. Oliveira Goncalves [ID^{83a}](#), J.L. Oliver [ID¹⁶⁰](#),
 A. Olszewski [ID⁸⁷](#), Ö.O. Öncel [ID⁵⁴](#), A.P. O'Neill [ID¹⁹](#), A. Onofre [ID^{130a,130e}](#), P.U.E. Onyisi [ID¹¹](#),
 M.J. Oreglia [ID³⁹](#), G.E. Orellana [ID⁹⁰](#), D. Orestano [ID^{77a,77b}](#), N. Orlando [ID¹³](#), R.S. Orr [ID¹⁵⁵](#),
 V. O'Shea [ID⁵⁹](#), L.M. Osojnak [ID¹²⁸](#), R. Ospanov [ID^{62a}](#), G. Otero y Garzon [ID³⁰](#), H. Otono [ID⁸⁹](#),
 P.S. Ott [ID^{63a}](#), G.J. Ottino [ID^{17a}](#), M. Ouchrif [ID^{35d}](#), J. Ouellette [ID²⁹](#), F. Ould-Saada [ID¹²⁵](#), M. Owen [ID⁵⁹](#),
 R.E. Owen [ID¹³⁴](#), K.Y. Oyulmaz [ID^{21a}](#), V.E. Ozcan [ID^{21a}](#), N. Ozturk [ID⁸](#), S. Ozturk [ID⁸²](#), H.A. Pacey [ID¹²⁶](#),
 A. Pacheco Pages [ID¹³](#), C. Padilla Aranda [ID¹³](#), G. Padovano [ID^{75a,75b}](#), S. Pagan Griso [ID^{17a}](#),
 G. Palacino [ID⁶⁸](#), A. Palazzo [ID^{70a,70b}](#), S. Palestini [ID³⁶](#), J. Pan [ID¹⁷²](#), T. Pan [ID^{64a}](#), D.K. Panchal [ID¹¹](#),
 C.E. Pandini [ID¹¹⁴](#), J.G. Panduro Vazquez [ID⁹⁵](#), H.D. Pandya [ID¹](#), H. Pang [ID^{14b}](#), P. Pani [ID⁴⁸](#),
 G. Panizzo [ID^{69a,69c}](#), L. Paolozzi [ID⁵⁶](#), C. Papadatos [ID¹⁰⁸](#), S. Parajuli [ID⁴⁴](#), A. Paramonov [ID⁶](#),

C. Paraskevopoulos [ID¹⁰](#), D. Paredes Hernandez [ID^{64b}](#), T.H. Park [ID¹⁵⁵](#), M.A. Parker [ID³²](#), F. Parodi [ID^{57b,57a}](#), E.W. Parrish [ID¹¹⁵](#), V.A. Parrish [ID⁵²](#), J.A. Parsons [ID⁴¹](#), U. Parzefall [ID⁵⁴](#), B. Pascual Dias [ID¹⁰⁸](#), L. Pascual Dominguez [ID¹⁵¹](#), E. Pasqualucci [ID^{75a}](#), S. Passaggio [ID^{57b}](#), F. Pastore [ID⁹⁵](#), P. Pasuwan [ID^{47a,47b}](#), P. Patel [ID⁸⁷](#), U.M. Patel [ID⁵¹](#), J.R. Pater [ID¹⁰¹](#), T. Pauly [ID³⁶](#), J. Pearkes [ID¹⁴³](#), M. Pedersen [ID¹²⁵](#), R. Pedro [ID^{130a}](#), S.V. Peleganchuk [ID³⁷](#), O. Penc [ID³⁶](#), E.A. Pender [ID⁵²](#), H. Peng [ID^{62a}](#), K.E. Penski [ID¹⁰⁹](#), M. Penzin [ID³⁷](#), B.S. Peralva [ID^{83d}](#), A.P. Pereira Peixoto [ID⁶⁰](#), L. Pereira Sanchez [ID^{47a,47b}](#), D.V. Perepelitsa [ID^{29,aj}](#), E. Perez Codina [ID^{156a}](#), M. Perganti [ID¹⁰](#), L. Perini [ID^{71a,71b,*}](#), H. Pernegger [ID³⁶](#), O. Perrin [ID⁴⁰](#), K. Peters [ID⁴⁸](#), R.F.Y. Peters [ID¹⁰¹](#), B.A. Petersen [ID³⁶](#), T.C. Petersen [ID⁴²](#), E. Petit [ID¹⁰²](#), V. Petousis [ID¹³²](#), C. Petridou [ID^{152,e}](#), A. Petrukhin [ID¹⁴¹](#), M. Pettee [ID^{17a}](#), N.E. Pettersson [ID³⁶](#), A. Petukhov [ID³⁷](#), K. Petukhova [ID¹³³](#), R. Pezoa [ID^{137f}](#), L. Pezzotti [ID³⁶](#), G. Pezzullo [ID¹⁷²](#), T.M. Pham [ID¹⁷⁰](#), T. Pham [ID¹⁰⁵](#), P.W. Phillips [ID¹³⁴](#), G. Piacquadio [ID¹⁴⁵](#), E. Pianori [ID^{17a}](#), F. Piazza [ID^{71a,71b}](#), R. Piegaia [ID³⁰](#), D. Pietreanu [ID^{27b}](#), A.D. Pilkington [ID¹⁰¹](#), M. Pinamonti [ID^{69a,69c}](#), J.L. Pinfold [ID²](#), B.C. Pinheiro Pereira [ID^{130a}](#), A.E. Pinto Pinoargote [ID^{100,135}](#), L. Pintucci [ID^{69a,69c}](#), K.M. Piper [ID¹⁴⁶](#), A. Pirttikoski [ID⁵⁶](#), D.A. Pizzi [ID³⁴](#), L. Pizzimento [ID^{64b}](#), A. Pizzini [ID¹¹⁴](#), M.-A. Pleier [ID²⁹](#), V. Plesanovs [ID⁵⁴](#), V. Pleskot [ID¹³³](#), E. Plotnikova [ID³⁸](#), G. Poddar [ID⁴](#), R. Poettgen [ID⁹⁸](#), L. Poggioli [ID¹²⁷](#), I. Pokharel [ID⁵⁵](#), S. Polacek [ID¹³³](#), G. Polesello [ID^{73a}](#), A. Poley [ID^{142,156a}](#), R. Polifka [ID¹³²](#), A. Polini [ID^{23b}](#), C.S. Pollard [ID¹⁶⁷](#), Z.B. Pollock [ID¹¹⁹](#), V. Polychronakos [ID²⁹](#), E. Pompa Pacchi [ID^{75a,75b}](#), D. Ponomarenko [ID¹¹³](#), L. Pontecorvo [ID³⁶](#), S. Popa [ID^{27a}](#), G.A. Popeneciu [ID^{27d}](#), A. Poreba [ID³⁶](#), D.M. Portillo Quintero [ID^{156a}](#), S. Pospisil [ID¹³²](#), M.A. Postill [ID¹³⁹](#), P. Postolache [ID^{27c}](#), K. Potamianos [ID¹⁶⁷](#), P.A. Potepa [ID^{86a}](#), I.N. Potrap [ID³⁸](#), C.J. Potter [ID³²](#), H. Potti [ID¹](#), T. Poulsen [ID⁴⁸](#), J. Poveda [ID¹⁶³](#), M.E. Pozo Astigarraga [ID³⁶](#), A. Prades Ibanez [ID¹⁶³](#), J. Pretel [ID⁵⁴](#), D. Price [ID¹⁰¹](#), M. Primavera [ID^{70a}](#), M.A. Principe Martin [ID⁹⁹](#), R. Privara [ID¹²²](#), T. Procter [ID⁵⁹](#), M.L. Proffitt [ID¹³⁸](#), N. Proklova [ID¹²⁸](#), K. Prokofiev [ID^{64c}](#), G. Proto [ID¹¹⁰](#), S. Protopopescu [ID²⁹](#), J. Proudfoot [ID⁶](#), M. Przybycien [ID^{86a}](#), W.W. Przygoda [ID^{86b}](#), J.E. Puddefoot [ID¹³⁹](#), D. Pudzha [ID³⁷](#), D. Pyatiizbyantseva [ID³⁷](#), J. Qian [ID¹⁰⁶](#), D. Qichen [ID¹⁰¹](#), Y. Qin [ID¹⁰¹](#), T. Qiu [ID⁵²](#), A. Quadt [ID⁵⁵](#), M. Queitsch-Maitland [ID¹⁰¹](#), G. Quetant [ID⁵⁶](#), R.P. Quinn [ID¹⁶⁴](#), G. Rabanal Bolanos [ID⁶¹](#), D. Rafanoharana [ID⁵⁴](#), F. Ragusa [ID^{71a,71b}](#), J.L. Rainbolt [ID³⁹](#), J.A. Raine [ID⁵⁶](#), S. Rajagopalan [ID²⁹](#), E. Ramakoti [ID³⁷](#), K. Ran [ID^{48,14e}](#), N.P. Rapheeha [ID^{33g}](#), H. Rasheed [ID^{27b}](#), V. Raskina [ID¹²⁷](#), D.F. Rassloff [ID^{63a}](#), S. Rave [ID¹⁰⁰](#), B. Ravina [ID⁵⁵](#), I. Ravinovich [ID¹⁶⁹](#), M. Raymond [ID³⁶](#), A.L. Read [ID¹²⁵](#), N.P. Readioff [ID¹³⁹](#), D.M. Rebuzzi [ID^{73a,73b}](#), G. Redlinger [ID²⁹](#), A.S. Reed [ID¹¹⁰](#), K. Reeves [ID²⁶](#), J.A. Reidelsturz [ID¹⁷¹](#), D. Reikher [ID¹⁵¹](#), A. Rej [ID¹⁴¹](#), C. Rembser [ID³⁶](#), A. Renardi [ID⁴⁸](#), M. Renda [ID^{27b}](#), M.B. Rendel [ID¹¹⁰](#), F. Renner [ID⁴⁸](#), A.G. Rennie [ID¹⁶⁰](#), A.L. Rescia [ID⁴⁸](#), S. Resconi [ID^{71a}](#), M. Ressegotti [ID^{57b,57a}](#), S. Rettie [ID³⁶](#), J.G. Reyes Rivera [ID¹⁰⁷](#), E. Reynolds [ID^{17a}](#), O.L. Rezanova [ID³⁷](#), P. Reznicek [ID¹³³](#), N. Ribaric [ID⁹¹](#), E. Ricci [ID^{78a,78b}](#), R. Richter [ID¹¹⁰](#), S. Richter [ID^{47a,47b}](#), E. Richter-Was [ID^{86b}](#), M. Ridel [ID¹²⁷](#), S. Ridouani [ID^{35d}](#), P. Rieck [ID¹¹⁷](#), P. Riedler [ID³⁶](#), E.M. Riefel [ID^{47a,47b}](#), M. Rijssenbeek [ID¹⁴⁵](#), A. Rimoldi [ID^{73a,73b}](#), M. Rimoldi [ID⁴⁸](#), L. Rinaldi [ID^{23b,23a}](#), T.T. Rinn [ID²⁹](#), M.P. Rinnagel [ID¹⁰⁹](#), G. Ripellino [ID¹⁶¹](#), I. Riu [ID¹³](#), P. Rivadeneira [ID⁴⁸](#), J.C. Rivera Vergara [ID¹⁶⁵](#), F. Rizatdinova [ID¹²¹](#), E. Rizvi [ID⁹⁴](#), B.A. Roberts [ID¹⁶⁷](#), B.R. Roberts [ID^{17a}](#), S.H. Robertson [ID^{104,x}](#), D. Robinson [ID³²](#), C.M. Robles Gajardo [ID^{137f}](#), M. Robles Manzano [ID¹⁰⁰](#), A. Robson [ID⁵⁹](#), A. Rocchi [ID^{76a,76b}](#), C. Roda [ID^{74a,74b}](#), S. Rodriguez Bosca [ID^{63a}](#), Y. Rodriguez Garcia [ID^{22a}](#), A. Rodriguez Rodriguez [ID⁵⁴](#), A.M. Rodriguez Vera [ID^{156b}](#), S. Roe [ID³⁶](#), J.T. Roemer [ID¹⁶⁰](#), A.R. Roepe-Gier [ID¹³⁶](#), J. Roggel [ID¹⁷¹](#), O. Røhne [ID¹²⁵](#), R.A. Rojas [ID¹⁰³](#), C.P.A. Roland [ID⁶⁸](#), J. Roloff [ID²⁹](#), A. Romaniouk [ID³⁷](#), E. Romano [ID^{73a,73b}](#), M. Romano [ID^{23b}](#), A.C. Romero Hernandez [ID¹⁶²](#), N. Rompotis [ID⁹²](#), L. Roos [ID¹²⁷](#), S. Rosati [ID^{75a}](#), B.J. Rosser [ID³⁹](#), E. Rossi [ID¹²⁶](#), E. Rossi [ID^{72a,72b}](#), L.P. Rossi [ID^{57b}](#), L. Rossini [ID⁵⁴](#), R. Rosten [ID¹¹⁹](#), M. Rotaru [ID^{27b}](#), B. Rottler [ID⁵⁴](#), C. Rougier [ID^{102,ab}](#), D. Rousseau [ID⁶⁶](#), D. Roussel [ID³²](#), A. Roy [ID¹⁶²](#), S. Roy-Garand [ID¹⁵⁵](#), A. Rozanov [ID¹⁰²](#), Y. Rozen [ID¹⁵⁰](#), X. Ruan [ID^{33g}](#), A. Rubio Jimenez [ID¹⁶³](#), A.J. Ruby [ID⁹²](#), V.H. Ruelas Rivera [ID¹⁸](#), T.A. Ruggeri [ID¹](#), A. Ruggiero [ID¹²⁶](#), A. Ruiz-Martinez [ID¹⁶³](#), A. Rummler [ID³⁶](#), Z. Rurikova [ID⁵⁴](#), N.A. Rusakovich [ID³⁸](#), H.L. Russell [ID¹⁶⁵](#),

G. Russo [ID^{75a,75b}](#), J.P. Rutherford [ID⁷](#), S. Rutherford Colmenares [ID³²](#), K. Rybacki [ID⁹¹](#), M. Rybar [ID¹³³](#), E.B. Rye [ID¹²⁵](#), A. Ryzhov [ID⁴⁴](#), J.A. Sabater Iglesias [ID⁵⁶](#), P. Sabatini [ID¹⁶³](#), L. Sabetta [ID^{75a,75b}](#), H.F-W. Sadrozinski [ID¹³⁶](#), F. Safai Tehrani [ID^{75a}](#), B. Safarzadeh Samani [ID¹⁴⁶](#), M. Safdari [ID¹⁴³](#), S. Saha [ID¹⁶⁵](#), M. Sahinsoy [ID¹¹⁰](#), M. Saimpert [ID¹³⁵](#), M. Saito [ID¹⁵³](#), T. Saito [ID¹⁵³](#), D. Salamani [ID³⁶](#), A. Salnikov [ID¹⁴³](#), J. Salt [ID¹⁶³](#), A. Salvador Salas [ID¹³](#), D. Salvatore [ID^{43b,43a}](#), F. Salvatore [ID¹⁴⁶](#), A. Salzburger [ID³⁶](#), D. Sammel [ID⁵⁴](#), D. Sampsonidis [ID^{152,e}](#), D. Sampsonidou [ID¹²³](#), J. Sánchez [ID¹⁶³](#), A. Sanchez Pineda [ID⁴](#), V. Sanchez Sebastian [ID¹⁶³](#), H. Sandaker [ID¹²⁵](#), C.O. Sander [ID⁴⁸](#), J.A. Sandesara [ID¹⁰³](#), M. Sandhoff [ID¹⁷¹](#), C. Sandoval [ID^{22b}](#), D.P.C. Sankey [ID¹³⁴](#), T. Sano [ID⁸⁸](#), A. Sansoni [ID⁵³](#), L. Santi [ID^{75a,75b}](#), C. Santoni [ID⁴⁰](#), H. Santos [ID^{130a,130b}](#), S.N. Santpur [ID^{17a}](#), A. Santra [ID¹⁶⁹](#), K.A. Saoucha [ID^{116b}](#), J.G. Saraiva [ID^{130a,130d}](#), J. Sardain [ID⁷](#), O. Sasaki [ID⁸⁴](#), K. Sato [ID¹⁵⁷](#), C. Sauer [ID^{63b}](#), F. Sauerburger [ID⁵⁴](#), E. Sauvan [ID⁴](#), P. Savard [ID^{155,ah}](#), R. Sawada [ID¹⁵³](#), C. Sawyer [ID¹³⁴](#), L. Sawyer [ID⁹⁷](#), I. Sayago Galvan [ID¹⁶³](#), C. Sbarra [ID^{23b}](#), A. Sbrizzi [ID^{23b,23a}](#), T. Scanlon [ID⁹⁶](#), J. Schaarschmidt [ID¹³⁸](#), P. Schacht [ID¹¹⁰](#), D. Schaefer [ID³⁹](#), U. Schäfer [ID¹⁰⁰](#), A.C. Schaffer [ID^{66,44}](#), D. Schaile [ID¹⁰⁹](#), R.D. Schamberger [ID¹⁴⁵](#), C. Scharf [ID¹⁸](#), M.M. Schefer [ID¹⁹](#), V.A. Schegelsky [ID³⁷](#), D. Scheirich [ID¹³³](#), F. Schenck [ID¹⁸](#), M. Schernau [ID¹⁶⁰](#), C. Scheulen [ID⁵⁵](#), C. Schiavi [ID^{57b,57a}](#), E.J. Schioppa [ID^{70a,70b}](#), M. Schioppa [ID^{43b,43a}](#), B. Schlag [ID^{143,o}](#), K.E. Schleicher [ID⁵⁴](#), S. Schlenker [ID³⁶](#), J. Schmeing [ID¹⁷¹](#), M.A. Schmidt [ID¹⁷¹](#), K. Schmieden [ID¹⁰⁰](#), C. Schmitt [ID¹⁰⁰](#), S. Schmitt [ID⁴⁸](#), L. Schoeffel [ID¹³⁵](#), A. Schoening [ID^{63b}](#), P.G. Scholer [ID⁵⁴](#), E. Schopf [ID¹²⁶](#), M. Schott [ID¹⁰⁰](#), J. Schovancova [ID³⁶](#), S. Schramm [ID⁵⁶](#), F. Schroeder [ID¹⁷¹](#), T. Schroer [ID⁵⁶](#), H-C. Schultz-Coulon [ID^{63a}](#), M. Schumacher [ID⁵⁴](#), B.A. Schumm [ID¹³⁶](#), Ph. Schune [ID¹³⁵](#), A.J. Schuy [ID¹³⁸](#), H.R. Schwartz [ID¹³⁶](#), A. Schwartzman [ID¹⁴³](#), T.A. Schwarz [ID¹⁰⁶](#), Ph. Schwemling [ID¹³⁵](#), R. Schwienhorst [ID¹⁰⁷](#), A. Sciandra [ID¹³⁶](#), G. Sciolla [ID²⁶](#), F. Scuri [ID^{74a}](#), C.D. Sebastiani [ID⁹²](#), K. Sedlaczek [ID¹¹⁵](#), P. Seema [ID¹⁸](#), S.C. Seidel [ID¹¹²](#), A. Seiden [ID¹³⁶](#), B.D. Seidlitz [ID⁴¹](#), C. Seitz [ID⁴⁸](#), J.M. Seixas [ID^{83b}](#), G. Sekhniaidze [ID^{72a}](#), S.J. Sekula [ID⁴⁴](#), L. Selem [ID⁶⁰](#), N. Semprini-Cesari [ID^{23b,23a}](#), D. Sengupta [ID⁵⁶](#), V. Senthilkumar [ID¹⁶³](#), L. Serin [ID⁶⁶](#), L. Serkin [ID^{69a,69b}](#), M. Sessa [ID^{76a,76b}](#), H. Severini [ID¹²⁰](#), F. Sforza [ID^{57b,57a}](#), A. Sfyrla [ID⁵⁶](#), E. Shabalina [ID⁵⁵](#), R. Shaheen [ID¹⁴⁴](#), J.D. Shahinian [ID¹²⁸](#), D. Shaked Renous [ID¹⁶⁹](#), L.Y. Shan [ID^{14a}](#), M. Shapiro [ID^{17a}](#), A. Sharma [ID³⁶](#), A.S. Sharma [ID¹⁶⁴](#), P. Sharma [ID⁸⁰](#), S. Sharma [ID⁴⁸](#), P.B. Shatalov [ID³⁷](#), K. Shaw [ID¹⁴⁶](#), S.M. Shaw [ID¹⁰¹](#), A. Shcherbakova [ID³⁷](#), Q. Shen [ID^{62c,5}](#), P. Sherwood [ID⁹⁶](#), L. Shi [ID⁹⁶](#), X. Shi [ID^{14a}](#), C.O. Shimmin [ID¹⁷²](#), J.D. Shinner [ID⁹⁵](#), I.P.J. Shipsey [ID¹²⁶](#), S. Shirabe [ID^{56,h}](#), M. Shiyakova [ID^{38,v}](#), J. Shlomi [ID¹⁶⁹](#), M.J. Shochet [ID³⁹](#), J. Shojaii [ID¹⁰⁵](#), D.R. Shope [ID¹²⁵](#), B. Shrestha [ID¹²⁰](#), S. Shrestha [ID^{119,ak}](#), E.M. Shrif [ID^{33g}](#), M.J. Shroff [ID¹⁶⁵](#), P. Sicho [ID¹³¹](#), A.M. Sickles [ID¹⁶²](#), E. Sideras Haddad [ID^{33g}](#), A. Sidoti [ID^{23b}](#), F. Siegert [ID⁵⁰](#), Dj. Sijacki [ID¹⁵](#), R. Sikora [ID^{86a}](#), F. Sili [ID⁹⁰](#), J.M. Silva [ID²⁰](#), M.V. Silva Oliveira [ID²⁹](#), S.B. Silverstein [ID^{47a}](#), S. Simion [ID⁶⁶](#), R. Simoniello [ID³⁶](#), E.L. Simpson [ID⁵⁹](#), H. Simpson [ID¹⁴⁶](#), L.R. Simpson [ID¹⁰⁶](#), N.D. Simpson [ID⁹⁸](#), S. Simsek [ID⁸²](#), S. Sindhu [ID⁵⁵](#), P. Sinervo [ID¹⁵⁵](#), S. Singh [ID¹⁵⁵](#), S. Sinha [ID⁴⁸](#), S. Sinha [ID¹⁰¹](#), M. Sioli [ID^{23b,23a}](#), I. Siral [ID³⁶](#), E. Sitnikova [ID⁴⁸](#), S.Yu. Sivoklokov [ID^{37,*}](#), J. Sjölin [ID^{47a,47b}](#), A. Skaf [ID⁵⁵](#), E. Skorda [ID²⁰](#), P. Skubic [ID¹²⁰](#), M. Slawinska [ID⁸⁷](#), V. Smakhtin [ID¹⁶⁹](#), B.H. Smart [ID¹³⁴](#), J. Smiesko [ID³⁶](#), S.Yu. Smirnov [ID³⁷](#), Y. Smirnov [ID³⁷](#), L.N. Smirnova [ID^{37,a}](#), O. Smirnova [ID⁹⁸](#), A.C. Smith [ID⁴¹](#), E.A. Smith [ID³⁹](#), H.A. Smith [ID¹²⁶](#), J.L. Smith [ID⁹²](#), R. Smith [ID¹⁴³](#), M. Smizanska [ID⁹¹](#), K. Smolek [ID¹³²](#), A.A. Snesarev [ID³⁷](#), S.R. Snider [ID¹⁵⁵](#), H.L. Snoek [ID¹¹⁴](#), S. Snyder [ID²⁹](#), R. Sobie [ID^{165,x}](#), A. Soffer [ID¹⁵¹](#), C.A. Solans Sanchez [ID³⁶](#), E.Yu. Soldatov [ID³⁷](#), U. Soldevila [ID¹⁶³](#), A.A. Solodkov [ID³⁷](#), S. Solomon [ID²⁶](#), A. Soloshenko [ID³⁸](#), K. Solovieva [ID⁵⁴](#), O.V. Solovyanov [ID⁴⁰](#), V. Solovyev [ID³⁷](#), P. Sommer [ID³⁶](#), A. Sonay [ID¹³](#), W.Y. Song [ID^{156b}](#), J.M. Sonneveld [ID¹¹⁴](#), A. Sopczak [ID¹³²](#), A.L. Sopio [ID⁹⁶](#), F. Sopkova [ID^{28b}](#), V. Sothilingam [ID^{63a}](#), S. Sottocornola [ID⁶⁸](#), R. Soualah [ID^{116b}](#), Z. Soumaimi [ID^{35e}](#), D. South [ID⁴⁸](#), N. Soybelman [ID¹⁶⁹](#), S. Spagnolo [ID^{70a,70b}](#), M. Spalla [ID¹¹⁰](#), D. Sperlich [ID⁵⁴](#), G. Spigo [ID³⁶](#), S. Spinali [ID⁹¹](#), D.P. Spiteri [ID⁵⁹](#), M. Spousta [ID¹³³](#), E.J. Staats [ID³⁴](#), A. Stabile [ID^{71a,71b}](#), R. Stamen [ID^{63a}](#), A. Stampeki [ID²⁰](#), M. Standke [ID²⁴](#), E. Stanecka [ID⁸⁷](#), M.V. Stange [ID⁵⁰](#), B. Stanislaus [ID^{17a}](#), M.M. Stanitzki [ID⁴⁸](#), B. Staff [ID⁴⁸](#),

E.A. Starchenko [ID³⁷](#), G.H. Stark [ID¹³⁶](#), J. Stark [ID^{102,ab}](#), D.M. Starko [ID^{156b}](#), P. Staroba [ID¹³¹](#),
 P. Starovoitov [ID^{63a}](#), S. Stärz [ID¹⁰⁴](#), R. Staszewski [ID⁸⁷](#), G. Stavropoulos [ID⁴⁶](#), J. Steentoft [ID¹⁶¹](#),
 P. Steinberg [ID²⁹](#), B. Stelzer [ID^{142,156a}](#), H.J. Stelzer [ID¹²⁹](#), O. Stelzer-Chilton [ID^{156a}](#), H. Stenzel [ID⁵⁸](#),
 T.J. Stevenson [ID¹⁴⁶](#), G.A. Stewart [ID³⁶](#), J.R. Stewart [ID¹²¹](#), M.C. Stockton [ID³⁶](#), G. Stoicea [ID^{27b}](#),
 M. Stolarski [ID^{130a}](#), S. Stonjek [ID¹¹⁰](#), A. Straessner [ID⁵⁰](#), J. Strandberg [ID¹⁴⁴](#), S. Strandberg [ID^{47a,47b}](#),
 M. Stratmann [ID¹⁷¹](#), M. Strauss [ID¹²⁰](#), T. Strebler [ID¹⁰²](#), P. Strizenec [ID^{28b}](#), R. Ströhmer [ID¹⁶⁶](#),
 D.M. Strom [ID¹²³](#), L.R. Strom [ID⁴⁸](#), R. Stroynowski [ID⁴⁴](#), A. Strubig [ID^{47a,47b}](#), S.A. Stucci [ID²⁹](#),
 B. Stugu [ID¹⁶](#), J. Stupak [ID¹²⁰](#), N.A. Styles [ID⁴⁸](#), D. Su [ID¹⁴³](#), S. Su [ID^{62a}](#), W. Su [ID^{62d}](#), X. Su [ID^{62a,66}](#),
 K. Sugizaki [ID¹⁵³](#), V.V. Sulin [ID³⁷](#), M.J. Sullivan [ID⁹²](#), D.M.S. Sultan [ID^{78a,78b}](#), L. Sultanaliyeva [ID³⁷](#),
 S. Sultansoy [ID^{3b}](#), T. Sumida [ID⁸⁸](#), S. Sun [ID¹⁰⁶](#), S. Sun [ID¹⁷⁰](#), O. Sunneborn Gudnadottir [ID¹⁶¹](#), N. Sur [ID¹⁰²](#),
 M.R. Sutton [ID¹⁴⁶](#), H. Suzuki [ID¹⁵⁷](#), M. Svatos [ID¹³¹](#), M. Swiatlowski [ID^{156a}](#), T. Swirski [ID¹⁶⁶](#),
 I. Sykora [ID^{28a}](#), M. Sykora [ID¹³³](#), T. Sykora [ID¹³³](#), D. Ta [ID¹⁰⁰](#), K. Tackmann [ID^{48,u}](#), A. Taffard [ID¹⁶⁰](#),
 R. Tafirout [ID^{156a}](#), J.S. Tafoya Vargas [ID⁶⁶](#), E.P. Takeva [ID⁵²](#), Y. Takubo [ID⁸⁴](#), M. Talby [ID¹⁰²](#),
 A.A. Talyshev [ID³⁷](#), K.C. Tam [ID^{64b}](#), N.M. Tamir [ID¹⁵¹](#), A. Tanaka [ID¹⁵³](#), J. Tanaka [ID¹⁵³](#), R. Tanaka [ID⁶⁶](#),
 M. Tanasini [ID^{57b,57a}](#), Z. Tao [ID¹⁶⁴](#), S. Tapia Araya [ID^{137f}](#), S. Tapprogge [ID¹⁰⁰](#),
 A. Tarek Abouelfadl Mohamed [ID¹⁰⁷](#), S. Tarem [ID¹⁵⁰](#), K. Tariq [ID^{14a}](#), G. Tarna [ID^{102,27b}](#), G.F. Tartarelli [ID^{71a}](#),
 P. Tas [ID¹³³](#), M. Tasevsky [ID¹³¹](#), E. Tassi [ID^{43b,43a}](#), A.C. Tate [ID¹⁶²](#), G. Tateno [ID¹⁵³](#), Y. Tayalati [ID^{35e,w}](#),
 G.N. Taylor [ID¹⁰⁵](#), W. Taylor [ID^{156b}](#), H. Teagle [ID⁹²](#), A.S. Tee [ID¹⁷⁰](#), R. Teixeira De Lima [ID¹⁴³](#),
 P. Teixeira-Dias [ID⁹⁵](#), J.J. Teoh [ID¹⁵⁵](#), K. Terashi [ID¹⁵³](#), J. Terron [ID⁹⁹](#), S. Terzo [ID¹³](#), M. Testa [ID⁵³](#),
 R.J. Teuscher [ID^{155,x}](#), A. Thaler [ID⁷⁹](#), O. Theiner [ID⁵⁶](#), N. Themistokleous [ID⁵²](#), T. Theveneaux-Pelzer [ID¹⁰²](#),
 O. Thielmann [ID¹⁷¹](#), D.W. Thomas ⁹⁵, J.P. Thomas [ID²⁰](#), E.A. Thompson [ID^{17a}](#), P.D. Thompson [ID²⁰](#),
 E. Thomson [ID¹²⁸](#), Y. Tian [ID⁵⁵](#), V. Tikhomirov [ID^{37,a}](#), Yu.A. Tikhonov [ID³⁷](#), S. Timoshenko ³⁷,
 D. Timoshyn [ID¹³³](#), E.X.L. Ting [ID¹](#), P. Tipton [ID¹⁷²](#), S.H. Tlou [ID^{33g}](#), A. Tnourji [ID⁴⁰](#), K. Todome [ID¹⁵⁴](#),
 S. Todorova-Nova [ID¹³³](#), S. Todt ⁵⁰, M. Togawa [ID⁸⁴](#), J. Tojo [ID⁸⁹](#), S. Tokár [ID^{28a}](#), K. Tokushuku [ID⁸⁴](#),
 O. Toldaiev [ID⁶⁸](#), R. Tombs [ID³²](#), M. Tomoto [ID^{84,111}](#), L. Tompkins [ID^{143,o}](#), K.W. Topolnicki [ID^{86b}](#),
 E. Torrence [ID¹²³](#), H. Torres [ID^{102,ab}](#), E. Torró Pastor [ID¹⁶³](#), M. Toscani [ID³⁰](#), C. Tosciri [ID³⁹](#), M. Tost [ID¹¹](#),
 D.R. Tovey [ID¹³⁹](#), A. Traeet ¹⁶, I.S. Trandafir [ID^{27b}](#), T. Trefzger [ID¹⁶⁶](#), A. Tricoli [ID²⁹](#), I.M. Trigger [ID^{156a}](#),
 S. Trincaz-Duvoid [ID¹²⁷](#), D.A. Trischuk [ID²⁶](#), B. Trocmé [ID⁶⁰](#), C. Troncon [ID^{71a}](#), L. Truong [ID^{33c}](#),
 M. Trzebinski [ID⁸⁷](#), A. Trzupek [ID⁸⁷](#), F. Tsai [ID¹⁴⁵](#), M. Tsai [ID¹⁰⁶](#), A. Tsiamis [ID^{152,e}](#), P.V. Tsiareshka ³⁷,
 S. Tsigaridas [ID^{156a}](#), A. Tsirigotis [ID^{152,s}](#), V. Tsiskaridze [ID¹⁵⁵](#), E.G. Tskhadadze [ID^{149a}](#),
 M. Tsopoulou [ID^{152,e}](#), Y. Tsujikawa [ID⁸⁸](#), I.I. Tsukerman [ID³⁷](#), V. Tsulaia [ID^{17a}](#), S. Tsuno [ID⁸⁴](#), O. Tsur ¹⁵⁰,
 K. Tsuri [ID¹¹⁸](#), D. Tsybychev [ID¹⁴⁵](#), Y. Tu [ID^{64b}](#), A. Tudorache [ID^{27b}](#), V. Tudorache [ID^{27b}](#), A.N. Tuna [ID³⁶](#),
 S. Turchikhin [ID^{57b,57a}](#), I. Turk Cakir [ID^{3a}](#), R. Turra [ID^{71a}](#), T. Turtuvshin [ID^{38,y}](#), P.M. Tuts [ID⁴¹](#),
 S. Tzamarias [ID^{152,e}](#), P. Tzanis [ID¹⁰](#), E. Tzovara [ID¹⁰⁰](#), F. Ukegawa [ID¹⁵⁷](#), P.A. Ulloa Poblete [ID^{137c,137b}](#),
 E.N. Umaka [ID²⁹](#), G. Unal [ID³⁶](#), M. Unal [ID¹¹](#), A. Undrus [ID²⁹](#), G. Unel [ID¹⁶⁰](#), J. Urban [ID^{28b}](#),
 P. Urquijo [ID¹⁰⁵](#), G. Usai [ID⁸](#), R. Ushioda [ID¹⁵⁴](#), M. Usman [ID¹⁰⁸](#), Z. Uysal [ID^{21b}](#), L. Vacabant [ID¹⁰²](#),
 V. Vacek [ID¹³²](#), B. Vachon [ID¹⁰⁴](#), K.O.H. Vadla [ID¹²⁵](#), T. Vafeiadis [ID³⁶](#), A. Vaitkus [ID⁹⁶](#), C. Valderanis [ID¹⁰⁹](#),
 E. Valdes Santurio [ID^{47a,47b}](#), M. Valente [ID^{156a}](#), S. Valentinetti [ID^{23b,23a}](#), A. Valero [ID¹⁶³](#),
 E. Valiente Moreno [ID¹⁶³](#), A. Vallier [ID^{102,ab}](#), J.A. Valls Ferrer [ID¹⁶³](#), D.R. Van Arneman [ID¹¹⁴](#),
 T.R. Van Daalen [ID¹³⁸](#), A. Van Der Graaf [ID⁴⁹](#), P. Van Gemmeren [ID⁶](#), M. Van Rijnbach [ID^{125,36}](#),
 S. Van Stroud [ID⁹⁶](#), I. Van Vulpen [ID¹¹⁴](#), M. Vanadia [ID^{76a,76b}](#), W. Vandelli [ID³⁶](#), M. Vandebroucke [ID¹³⁵](#),
 E.R. Vandewall [ID¹²¹](#), D. Vannicola [ID¹⁵¹](#), L. Vannoli [ID^{57b,57a}](#), R. Vari [ID^{75a}](#), E.W. Varnes [ID⁷](#),
 C. Varni [ID^{17b}](#), T. Varol [ID¹⁴⁸](#), D. Varouchas [ID⁶⁶](#), L. Varriale [ID¹⁶³](#), K.E. Varvell [ID¹⁴⁷](#), M.E. Vasile [ID^{27b}](#),
 L. Vaslin ⁴⁰, G.A. Vasquez [ID¹⁶⁵](#), A. Vasyukov [ID³⁸](#), F. Vazeille [ID⁴⁰](#), T. Vazquez Schroeder [ID³⁶](#),
 J. Veatch [ID³¹](#), V. Vecchio [ID¹⁰¹](#), M.J. Veen [ID¹⁰³](#), I. Veliscek [ID¹²⁶](#), L.M. Veloce [ID¹⁵⁵](#), F. Veloso [ID^{130a,130c}](#),
 S. Veneziano [ID^{75a}](#), A. Ventura [ID^{70a,70b}](#), S. Ventura Gonzalez [ID¹³⁵](#), A. Verbytskyi [ID¹¹⁰](#),
 M. Verducci [ID^{74a,74b}](#), C. Vergis [ID²⁴](#), M. Verissimo De Araujo [ID^{83b}](#), W. Verkerke [ID¹¹⁴](#),

J.C. Vermeulen [ID¹¹⁴](#), C. Vernieri [ID¹⁴³](#), M. Vessella [ID¹⁰³](#), M.C. Vetterli [ID^{142,ah}](#), A. Vgenopoulos [ID^{152,e}](#), N. Viaux Maira [ID^{137f}](#), T. Vickey [ID¹³⁹](#), O.E. Vickey Boeriu [ID¹³⁹](#), G.H.A. Viehhauser [ID¹²⁶](#), L. Vigani [ID^{63b}](#), M. Villa [ID^{23b,23a}](#), M. Villaplana Perez [ID¹⁶³](#), E.M. Villhauer [ID⁵²](#), E. Vilucchi [ID⁵³](#), M.G. Vincter [ID³⁴](#), G.S. Virdee [ID²⁰](#), A. Vishwakarma [ID⁵²](#), A. Visibile [ID¹¹⁴](#), C. Vittori [ID³⁶](#), I. Vivarelli [ID¹⁴⁶](#), V. Vladimirov [ID¹⁶⁷](#), E. Voevodina [ID¹¹⁰](#), F. Vogel [ID¹⁰⁹](#), P. Vokac [ID¹³²](#), Yu. Volkotrub [ID^{86a}](#), J. Von Ahnen [ID⁴⁸](#), E. Von Toerne [ID²⁴](#), B. Vormwald [ID³⁶](#), V. Vorobel [ID¹³³](#), K. Vorobev [ID³⁷](#), M. Vos [ID¹⁶³](#), K. Voss [ID¹⁴¹](#), J.H. Vossebeld [ID⁹²](#), M. Vozak [ID¹¹⁴](#), L. Vozdecky [ID⁹⁴](#), N. Vranjes [ID¹⁵](#), M. Vranjes Milosavljevic [ID¹⁵](#), M. Vreeswijk [ID¹¹⁴](#), R. Vuillermet [ID³⁶](#), O. Vujinovic [ID¹⁰⁰](#), I. Vukotic [ID³⁹](#), S. Wada [ID¹⁵⁷](#), C. Wagner [ID¹⁰³](#), J.M. Wagner [ID^{17a}](#), W. Wagner [ID¹⁷¹](#), S. Wahdan [ID¹⁷¹](#), H. Wahlberg [ID⁹⁰](#), M. Wakida [ID¹¹¹](#), J. Walder [ID¹³⁴](#), R. Walker [ID¹⁰⁹](#), W. Walkowiak [ID¹⁴¹](#), A. Wall [ID¹²⁸](#), T. Wamorkar [ID⁶](#), A.Z. Wang [ID¹⁷⁰](#), C. Wang [ID¹⁰⁰](#), C. Wang [ID^{62c}](#), H. Wang [ID^{17a}](#), J. Wang [ID^{64a}](#), R.-J. Wang [ID¹⁰⁰](#), R. Wang [ID⁶¹](#), R. Wang [ID⁶](#), S.M. Wang [ID¹⁴⁸](#), S. Wang [ID^{62b}](#), T. Wang [ID^{62a}](#), W.T. Wang [ID⁸⁰](#), W. Wang [ID^{14a}](#), X. Wang [ID^{14c}](#), X. Wang [ID¹⁶²](#), X. Wang [ID^{62c}](#), Y. Wang [ID^{62d}](#), Y. Wang [ID^{14c}](#), Z. Wang [ID¹⁰⁶](#), Z. Wang [ID^{62d,51,62c}](#), Z. Wang [ID¹⁰⁶](#), A. Warburton [ID¹⁰⁴](#), R.J. Ward [ID²⁰](#), N. Warrack [ID⁵⁹](#), A.T. Watson [ID²⁰](#), H. Watson [ID⁵⁹](#), M.F. Watson [ID²⁰](#), E. Watton [ID^{59,134}](#), G. Watts [ID¹³⁸](#), B.M. Waugh [ID⁹⁶](#), C. Weber [ID²⁹](#), H.A. Weber [ID¹⁸](#), M.S. Weber [ID¹⁹](#), S.M. Weber [ID^{63a}](#), C. Wei [ID^{62a}](#), Y. Wei [ID¹²⁶](#), A.R. Weidberg [ID¹²⁶](#), E.J. Weik [ID¹¹⁷](#), J. Weingarten [ID⁴⁹](#), M. Weirich [ID¹⁰⁰](#), C. Weiser [ID⁵⁴](#), C.J. Wells [ID⁴⁸](#), T. Wenaus [ID²⁹](#), B. Wendland [ID⁴⁹](#), T. Wengler [ID³⁶](#), N.S. Wenke [ID¹¹⁰](#), N. Wermes [ID²⁴](#), M. Wessels [ID^{63a}](#), A.M. Wharton [ID⁹¹](#), A.S. White [ID⁶¹](#), A. White [ID⁸](#), M.J. White [ID¹](#), D. Whiteson [ID¹⁶⁰](#), L. Wickremasinghe [ID¹²⁴](#), W. Wiedenmann [ID¹⁷⁰](#), C. Wiel [ID⁵⁰](#), M. Wielaers [ID¹³⁴](#), C. Wiglesworth [ID⁴²](#), D.J. Wilbern [ID¹²⁰](#), H.G. Wilkens [ID³⁶](#), D.M. Williams [ID⁴¹](#), H.H. Williams [ID¹²⁸](#), S. Williams [ID³²](#), S. Willocq [ID¹⁰³](#), B.J. Wilson [ID¹⁰¹](#), P.J. Windischhofer [ID³⁹](#), F.I. Winkel [ID³⁰](#), F. Winklmeier [ID¹²³](#), B.T. Winter [ID⁵⁴](#), J.K. Winter [ID¹⁰¹](#), M. Wittgen [ID¹⁴³](#), M. Wobisch [ID⁹⁷](#), Z. Wolffs [ID¹¹⁴](#), J. Wollrath [ID¹⁶⁰](#), M.W. Wolter [ID⁸⁷](#), H. Wolters [ID^{130a,130c}](#), A.F. Wongel [ID⁴⁸](#), S.D. Worm [ID⁴⁸](#), B.K. Wosiek [ID⁸⁷](#), K.W. Woźniak [ID⁸⁷](#), S. Wozniewski [ID⁵⁵](#), K. Wraight [ID⁵⁹](#), C. Wu [ID²⁰](#), J. Wu [ID^{14a,14e}](#), M. Wu [ID^{64a}](#), M. Wu [ID¹¹³](#), S.L. Wu [ID¹⁷⁰](#), X. Wu [ID⁵⁶](#), Y. Wu [ID^{62a}](#), Z. Wu [ID¹³⁵](#), J. Wuerzinger [ID^{110,af}](#), T.R. Wyatt [ID¹⁰¹](#), B.M. Wynne [ID⁵²](#), S. Xella [ID⁴²](#), L. Xia [ID^{14c}](#), M. Xia [ID^{14b}](#), J. Xiang [ID^{64c}](#), M. Xie [ID^{62a}](#), X. Xie [ID^{62a}](#), S. Xin [ID^{14a,14e}](#), J. Xiong [ID^{17a}](#), D. Xu [ID^{14a}](#), H. Xu [ID^{62a}](#), L. Xu [ID^{62a}](#), R. Xu [ID¹²⁸](#), T. Xu [ID¹⁰⁶](#), Y. Xu [ID^{14b}](#), Z. Xu [ID⁵²](#), Z. Xu [ID^{14a}](#), B. Yabsley [ID¹⁴⁷](#), S. Yacoob [ID^{33a}](#), Y. Yamaguchi [ID¹⁵⁴](#), E. Yamashita [ID¹⁵³](#), H. Yamauchi [ID¹⁵⁷](#), T. Yamazaki [ID^{17a}](#), Y. Yamazaki [ID⁸⁵](#), J. Yan [ID^{62c}](#), S. Yan [ID¹²⁶](#), Z. Yan [ID²⁵](#), H.J. Yang [ID^{62c,62d}](#), H.T. Yang [ID^{62a}](#), S. Yang [ID^{62a}](#), T. Yang [ID^{64c}](#), X. Yang [ID^{62a}](#), X. Yang [ID^{14a}](#), Y. Yang [ID⁴⁴](#), Y. Yang [ID^{62a}](#), Z. Yang [ID^{62a}](#), W-M. Yao [ID^{17a}](#), Y.C. Yap [ID⁴⁸](#), H. Ye [ID^{14c}](#), H. Ye [ID⁵⁵](#), J. Ye [ID^{14a}](#), S. Ye [ID²⁹](#), X. Ye [ID^{62a}](#), Y. Yeh [ID⁹⁶](#), I. Yeletskikh [ID³⁸](#), B.K. Yeo [ID^{17b}](#), M.R. Yexley [ID⁹⁶](#), P. Yin [ID⁴¹](#), K. Yorita [ID¹⁶⁸](#), S. Younas [ID^{27b}](#), C.J.S. Young [ID³⁶](#), C. Young [ID¹⁴³](#), C. Yu [ID^{14a,14e}](#), Y. Yu [ID^{62a}](#), M. Yuan [ID¹⁰⁶](#), R. Yuan [ID^{62b,k}](#), L. Yue [ID⁹⁶](#), M. Zaazoua [ID^{62a}](#), B. Zabinski [ID⁸⁷](#), E. Zaid [ID⁵²](#), T. Zakareishvili [ID^{149b}](#), N. Zakharchuk [ID³⁴](#), S. Zambito [ID⁵⁶](#), J.A. Zamora Saa [ID^{137d,137b}](#), J. Zang [ID¹⁵³](#), D. Zanzi [ID⁵⁴](#), O. Zaplatilek [ID¹³²](#), C. Zeitnitz [ID¹⁷¹](#), H. Zeng [ID^{14a}](#), J.C. Zeng [ID¹⁶²](#), D.T. Zenger Jr [ID²⁶](#), O. Zenin [ID³⁷](#), T. Ženiš [ID^{28a}](#), S. Zenz [ID⁹⁴](#), S. Zerradi [ID^{35a}](#), D. Zerwas [ID⁶⁶](#), M. Zhai [ID^{14a,14e}](#), B. Zhang [ID^{14c}](#), D.F. Zhang [ID¹³⁹](#), J. Zhang [ID^{62b}](#), J. Zhang [ID⁶](#), K. Zhang [ID^{14a,14e}](#), L. Zhang [ID^{14c}](#), P. Zhang [ID^{14a,14e}](#), R. Zhang [ID¹⁷⁰](#), S. Zhang [ID¹⁰⁶](#), T. Zhang [ID¹⁵³](#), X. Zhang [ID^{62c}](#), X. Zhang [ID^{62b}](#), Y. Zhang [ID^{62c,5}](#), Y. Zhang [ID⁹⁶](#), Z. Zhang [ID^{17a}](#), Z. Zhang [ID⁶⁶](#), H. Zhao [ID¹³⁸](#), P. Zhao [ID⁵¹](#), T. Zhao [ID^{62b}](#), Y. Zhao [ID¹³⁶](#), Z. Zhao [ID^{62a}](#), A. Zhemchugov [ID³⁸](#), J. Zheng [ID^{14c}](#), K. Zheng [ID¹⁶²](#), X. Zheng [ID^{62a}](#), Z. Zheng [ID¹⁴³](#), D. Zhong [ID¹⁶²](#), B. Zhou [ID¹⁰⁶](#), H. Zhou [ID⁷](#), N. Zhou [ID^{62c}](#), Y. Zhou [ID⁷](#), C.G. Zhu [ID^{62b}](#), J. Zhu [ID¹⁰⁶](#), Y. Zhu [ID^{62c}](#), Y. Zhu [ID^{62a}](#), X. Zhuang [ID^{14a}](#), K. Zhukov [ID³⁷](#), V. Zhulanov [ID³⁷](#), N.I. Zimine [ID³⁸](#), J. Zinsser [ID^{63b}](#), M. Ziolkowski [ID¹⁴¹](#), L. Živković [ID¹⁵](#), A. Zoccoli [ID^{23b,23a}](#), K. Zoch [ID⁵⁶](#), T.G. Zorbas [ID¹³⁹](#), O. Zormpa [ID⁴⁶](#), W. Zou [ID⁴¹](#), L. Zwalinski [ID³⁶](#).

- ¹Department of Physics, University of Adelaide, Adelaide; Australia.
- ²Department of Physics, University of Alberta, Edmonton AB; Canada.
- ^{3(a)}Department of Physics, Ankara University, Ankara; ^(b)Division of Physics, TOBB University of Economics and Technology, Ankara; Türkiye.
- ⁴LAPP, Université Savoie Mont Blanc, CNRS/IN2P3, Annecy; France.
- ⁵APC, Université Paris Cité, CNRS/IN2P3, Paris; France.
- ⁶High Energy Physics Division, Argonne National Laboratory, Argonne IL; United States of America.
- ⁷Department of Physics, University of Arizona, Tucson AZ; United States of America.
- ⁸Department of Physics, University of Texas at Arlington, Arlington TX; United States of America.
- ⁹Physics Department, National and Kapodistrian University of Athens, Athens; Greece.
- ¹⁰Physics Department, National Technical University of Athens, Zografou; Greece.
- ¹¹Department of Physics, University of Texas at Austin, Austin TX; United States of America.
- ¹²Institute of Physics, Azerbaijan Academy of Sciences, Baku; Azerbaijan.
- ¹³Institut de Física d'Altes Energies (IFAE), Barcelona Institute of Science and Technology, Barcelona; Spain.
- ^{14(a)}Institute of High Energy Physics, Chinese Academy of Sciences, Beijing; ^(b)Physics Department, Tsinghua University, Beijing; ^(c)Department of Physics, Nanjing University, Nanjing; ^(d)School of Science, Shenzhen Campus of Sun Yat-sen University; ^(e)University of Chinese Academy of Science (UCAS), Beijing; China.
- ¹⁵Institute of Physics, University of Belgrade, Belgrade; Serbia.
- ¹⁶Department for Physics and Technology, University of Bergen, Bergen; Norway.
- ^{17(a)}Physics Division, Lawrence Berkeley National Laboratory, Berkeley CA; ^(b)University of California, Berkeley CA; United States of America.
- ¹⁸Institut für Physik, Humboldt Universität zu Berlin, Berlin; Germany.
- ¹⁹Albert Einstein Center for Fundamental Physics and Laboratory for High Energy Physics, University of Bern, Bern; Switzerland.
- ²⁰School of Physics and Astronomy, University of Birmingham, Birmingham; United Kingdom.
- ^{21(a)}Department of Physics, Bogazici University, Istanbul; ^(b)Department of Physics Engineering, Gaziantep University, Gaziantep; ^(c)Department of Physics, Istanbul University, Istanbul; Türkiye.
- ^{22(a)}Facultad de Ciencias y Centro de Investigaciones, Universidad Antonio Nariño, Bogotá; ^(b)Departamento de Física, Universidad Nacional de Colombia, Bogotá; Colombia.
- ^{23(a)}Dipartimento di Fisica e Astronomia A. Righi, Università di Bologna, Bologna; ^(b)INFN Sezione di Bologna; Italy.
- ²⁴Physikalisches Institut, Universität Bonn, Bonn; Germany.
- ²⁵Department of Physics, Boston University, Boston MA; United States of America.
- ²⁶Department of Physics, Brandeis University, Waltham MA; United States of America.
- ^{27(a)}Transilvania University of Brasov, Brasov; ^(b)Horia Hulubei National Institute of Physics and Nuclear Engineering, Bucharest; ^(c)Department of Physics, Alexandru Ioan Cuza University of Iasi, Iasi; ^(d)National Institute for Research and Development of Isotopic and Molecular Technologies, Physics Department, Cluj-Napoca; ^(e)University Politehnica Bucharest, Bucharest; ^(f)West University in Timisoara, Timisoara; ^(g)Faculty of Physics, University of Bucharest, Bucharest; Romania.
- ^{28(a)}Faculty of Mathematics, Physics and Informatics, Comenius University, Bratislava; ^(b)Department of Subnuclear Physics, Institute of Experimental Physics of the Slovak Academy of Sciences, Kosice; Slovak Republic.
- ²⁹Physics Department, Brookhaven National Laboratory, Upton NY; United States of America.
- ³⁰Universidad de Buenos Aires, Facultad de Ciencias Exactas y Naturales, Departamento de Física, y CONICET, Instituto de Física de Buenos Aires (IFIBA), Buenos Aires; Argentina.

- ³¹California State University, CA; United States of America.
- ³²Cavendish Laboratory, University of Cambridge, Cambridge; United Kingdom.
- ³³(^a) Department of Physics, University of Cape Town, Cape Town; (^b) iThemba Labs, Western Cape; (^c) Department of Mechanical Engineering Science, University of Johannesburg, Johannesburg; (^d) National Institute of Physics, University of the Philippines Diliman (Philippines); (^e) University of South Africa, Department of Physics, Pretoria; (^f) University of Zululand, KwaDlangezwa; (^g) School of Physics, University of the Witwatersrand, Johannesburg; South Africa.
- ³⁴Department of Physics, Carleton University, Ottawa ON; Canada.
- ³⁵(^a) Faculté des Sciences Ain Chock, Réseau Universitaire de Physique des Hautes Energies - Université Hassan II, Casablanca; (^b) Faculté des Sciences, Université Ibn-Tofail, Kénitra; (^c) Faculté des Sciences Semlalia, Université Cadi Ayyad, LPHEA-Marrakech; (^d) LPMR, Faculté des Sciences, Université Mohamed Premier, Oujda; (^e) Faculté des sciences, Université Mohammed V, Rabat; (^f) Institute of Applied Physics, Mohammed VI Polytechnic University, Ben Guerir; Morocco.
- ³⁶CERN, Geneva; Switzerland.
- ³⁷Affiliated with an institute covered by a cooperation agreement with CERN.
- ³⁸Affiliated with an international laboratory covered by a cooperation agreement with CERN.
- ³⁹Enrico Fermi Institute, University of Chicago, Chicago IL; United States of America.
- ⁴⁰LPC, Université Clermont Auvergne, CNRS/IN2P3, Clermont-Ferrand; France.
- ⁴¹Nevis Laboratory, Columbia University, Irvington NY; United States of America.
- ⁴²Niels Bohr Institute, University of Copenhagen, Copenhagen; Denmark.
- ⁴³(^a) Dipartimento di Fisica, Università della Calabria, Rende; (^b) INFN Gruppo Collegato di Cosenza, Laboratori Nazionali di Frascati; Italy.
- ⁴⁴Physics Department, Southern Methodist University, Dallas TX; United States of America.
- ⁴⁵Physics Department, University of Texas at Dallas, Richardson TX; United States of America.
- ⁴⁶National Centre for Scientific Research "Demokritos", Agia Paraskevi; Greece.
- ⁴⁷(^a) Department of Physics, Stockholm University; (^b) Oskar Klein Centre, Stockholm; Sweden.
- ⁴⁸Deutsches Elektronen-Synchrotron DESY, Hamburg and Zeuthen; Germany.
- ⁴⁹Fakultät Physik, Technische Universität Dortmund, Dortmund; Germany.
- ⁵⁰Institut für Kern- und Teilchenphysik, Technische Universität Dresden, Dresden; Germany.
- ⁵¹Department of Physics, Duke University, Durham NC; United States of America.
- ⁵²SUPA - School of Physics and Astronomy, University of Edinburgh, Edinburgh; United Kingdom.
- ⁵³INFN e Laboratori Nazionali di Frascati, Frascati; Italy.
- ⁵⁴Physikalisches Institut, Albert-Ludwigs-Universität Freiburg, Freiburg; Germany.
- ⁵⁵II. Physikalisches Institut, Georg-August-Universität Göttingen, Göttingen; Germany.
- ⁵⁶Département de Physique Nucléaire et Corpusculaire, Université de Genève, Genève; Switzerland.
- ⁵⁷(^a) Dipartimento di Fisica, Università di Genova, Genova; (^b) INFN Sezione di Genova; Italy.
- ⁵⁸II. Physikalisches Institut, Justus-Liebig-Universität Giessen, Giessen; Germany.
- ⁵⁹SUPA - School of Physics and Astronomy, University of Glasgow, Glasgow; United Kingdom.
- ⁶⁰LPSC, Université Grenoble Alpes, CNRS/IN2P3, Grenoble INP, Grenoble; France.
- ⁶¹Laboratory for Particle Physics and Cosmology, Harvard University, Cambridge MA; United States of America.
- ⁶²(^a) Department of Modern Physics and State Key Laboratory of Particle Detection and Electronics, University of Science and Technology of China, Hefei; (^b) Institute of Frontier and Interdisciplinary Science and Key Laboratory of Particle Physics and Particle Irradiation (MOE), Shandong University, Qingdao; (^c) School of Physics and Astronomy, Shanghai Jiao Tong University, Key Laboratory for Particle Astrophysics and Cosmology (MOE), SKLPPC, Shanghai; (^d) Tsung-Dao Lee Institute, Shanghai; China.
- ⁶³(^a) Kirchhoff-Institut für Physik, Ruprecht-Karls-Universität Heidelberg, Heidelberg; (^b) Physikalisches

Institut, Ruprecht-Karls-Universität Heidelberg, Heidelberg; Germany.

^{64(a)}Department of Physics, Chinese University of Hong Kong, Shatin, N.T., Hong Kong;^(b)Department of Physics, University of Hong Kong, Hong Kong;^(c)Department of Physics and Institute for Advanced Study, Hong Kong University of Science and Technology, Clear Water Bay, Kowloon, Hong Kong; China.

⁶⁵Department of Physics, National Tsing Hua University, Hsinchu; Taiwan.

⁶⁶IJCLab, Université Paris-Saclay, CNRS/IN2P3, 91405, Orsay; France.

⁶⁷Centro Nacional de Microelectrónica (IMB-CNM-CSIC), Barcelona; Spain.

⁶⁸Department of Physics, Indiana University, Bloomington IN; United States of America.

^{69(a)}INFN Gruppo Collegato di Udine, Sezione di Trieste, Udine;^(b)ICTP, Trieste;^(c)Dipartimento Politecnico di Ingegneria e Architettura, Università di Udine, Udine; Italy.

^{70(a)}INFN Sezione di Lecce;^(b)Dipartimento di Matematica e Fisica, Università del Salento, Lecce; Italy.

^{71(a)}INFN Sezione di Milano;^(b)Dipartimento di Fisica, Università di Milano, Milano; Italy.

^{72(a)}INFN Sezione di Napoli;^(b)Dipartimento di Fisica, Università di Napoli, Napoli; Italy.

^{73(a)}INFN Sezione di Pavia;^(b)Dipartimento di Fisica, Università di Pavia, Pavia; Italy.

^{74(a)}INFN Sezione di Pisa;^(b)Dipartimento di Fisica E. Fermi, Università di Pisa, Pisa; Italy.

^{75(a)}INFN Sezione di Roma;^(b)Dipartimento di Fisica, Sapienza Università di Roma, Roma; Italy.

^{76(a)}INFN Sezione di Roma Tor Vergata;^(b)Dipartimento di Fisica, Università di Roma Tor Vergata, Roma; Italy.

^{77(a)}INFN Sezione di Roma Tre;^(b)Dipartimento di Matematica e Fisica, Università Roma Tre, Roma; Italy.

^{78(a)}INFN-TIFPA;^(b)Università degli Studi di Trento, Trento; Italy.

⁷⁹Universität Innsbruck, Department of Astro and Particle Physics, Innsbruck; Austria.

⁸⁰University of Iowa, Iowa City IA; United States of America.

⁸¹Department of Physics and Astronomy, Iowa State University, Ames IA; United States of America.

⁸²Istinye University, Sarıyer, İstanbul; Türkiye.

^{83(a)}Departamento de Engenharia Elétrica, Universidade Federal de Juiz de Fora (UFJF), Juiz de Fora;^(b)Universidade Federal do Rio De Janeiro COPPE/EE/IF, Rio de Janeiro;^(c)Instituto de Física, Universidade de São Paulo, São Paulo;^(d)Rio de Janeiro State University, Rio de Janeiro; Brazil.

⁸⁴KEK, High Energy Accelerator Research Organization, Tsukuba; Japan.

⁸⁵Graduate School of Science, Kobe University, Kobe; Japan.

^{86(a)}AGH University of Krakow, Faculty of Physics and Applied Computer Science, Krakow;^(b)Marian Smoluchowski Institute of Physics, Jagiellonian University, Krakow; Poland.

⁸⁷Institute of Nuclear Physics Polish Academy of Sciences, Krakow; Poland.

⁸⁸Faculty of Science, Kyoto University, Kyoto; Japan.

⁸⁹Research Center for Advanced Particle Physics and Department of Physics, Kyushu University, Fukuoka ; Japan.

⁹⁰Instituto de Física La Plata, Universidad Nacional de La Plata and CONICET, La Plata; Argentina.

⁹¹Physics Department, Lancaster University, Lancaster; United Kingdom.

⁹²Oliver Lodge Laboratory, University of Liverpool, Liverpool; United Kingdom.

⁹³Department of Experimental Particle Physics, Jožef Stefan Institute and Department of Physics, University of Ljubljana, Ljubljana; Slovenia.

⁹⁴School of Physics and Astronomy, Queen Mary University of London, London; United Kingdom.

⁹⁵Department of Physics, Royal Holloway University of London, Egham; United Kingdom.

⁹⁶Department of Physics and Astronomy, University College London, London; United Kingdom.

⁹⁷Louisiana Tech University, Ruston LA; United States of America.

⁹⁸Fysiska institutionen, Lunds universitet, Lund; Sweden.

⁹⁹Departamento de Física Teórica C-15 and CIAFF, Universidad Autónoma de Madrid, Madrid; Spain.

- ¹⁰⁰Institut für Physik, Universität Mainz, Mainz; Germany.
- ¹⁰¹School of Physics and Astronomy, University of Manchester, Manchester; United Kingdom.
- ¹⁰²CPPM, Aix-Marseille Université, CNRS/IN2P3, Marseille; France.
- ¹⁰³Department of Physics, University of Massachusetts, Amherst MA; United States of America.
- ¹⁰⁴Department of Physics, McGill University, Montreal QC; Canada.
- ¹⁰⁵School of Physics, University of Melbourne, Victoria; Australia.
- ¹⁰⁶Department of Physics, University of Michigan, Ann Arbor MI; United States of America.
- ¹⁰⁷Department of Physics and Astronomy, Michigan State University, East Lansing MI; United States of America.
- ¹⁰⁸Group of Particle Physics, University of Montreal, Montreal QC; Canada.
- ¹⁰⁹Fakultät für Physik, Ludwig-Maximilians-Universität München, München; Germany.
- ¹¹⁰Max-Planck-Institut für Physik (Werner-Heisenberg-Institut), München; Germany.
- ¹¹¹Graduate School of Science and Kobayashi-Maskawa Institute, Nagoya University, Nagoya; Japan.
- ¹¹²Department of Physics and Astronomy, University of New Mexico, Albuquerque NM; United States of America.
- ¹¹³Institute for Mathematics, Astrophysics and Particle Physics, Radboud University/Nikhef, Nijmegen; Netherlands.
- ¹¹⁴Nikhef National Institute for Subatomic Physics and University of Amsterdam, Amsterdam; Netherlands.
- ¹¹⁵Department of Physics, Northern Illinois University, DeKalb IL; United States of America.
- ^{116(a)}New York University Abu Dhabi, Abu Dhabi;^(b)University of Sharjah, Sharjah; United Arab Emirates.
- ¹¹⁷Department of Physics, New York University, New York NY; United States of America.
- ¹¹⁸Ochanomizu University, Otsuka, Bunkyo-ku, Tokyo; Japan.
- ¹¹⁹Ohio State University, Columbus OH; United States of America.
- ¹²⁰Homer L. Dodge Department of Physics and Astronomy, University of Oklahoma, Norman OK; United States of America.
- ¹²¹Department of Physics, Oklahoma State University, Stillwater OK; United States of America.
- ¹²²Palacký University, Joint Laboratory of Optics, Olomouc; Czech Republic.
- ¹²³Institute for Fundamental Science, University of Oregon, Eugene, OR; United States of America.
- ¹²⁴Graduate School of Science, Osaka University, Osaka; Japan.
- ¹²⁵Department of Physics, University of Oslo, Oslo; Norway.
- ¹²⁶Department of Physics, Oxford University, Oxford; United Kingdom.
- ¹²⁷LPNHE, Sorbonne Université, Université Paris Cité, CNRS/IN2P3, Paris; France.
- ¹²⁸Department of Physics, University of Pennsylvania, Philadelphia PA; United States of America.
- ¹²⁹Department of Physics and Astronomy, University of Pittsburgh, Pittsburgh PA; United States of America.
- ^{130(a)}Laboratório de Instrumentação e Física Experimental de Partículas - LIP, Lisboa;^(b)Departamento de Física, Faculdade de Ciências, Universidade de Lisboa, Lisboa;^(c)Departamento de Física, Universidade de Coimbra, Coimbra;^(d)Centro de Física Nuclear da Universidade de Lisboa, Lisboa;^(e)Departamento de Física, Universidade do Minho, Braga;^(f)Departamento de Física Teórica y del Cosmos, Universidad de Granada, Granada (Spain);^(g)Departamento de Física, Instituto Superior Técnico, Universidade de Lisboa, Lisboa; Portugal.
- ¹³¹Institute of Physics of the Czech Academy of Sciences, Prague; Czech Republic.
- ¹³²Czech Technical University in Prague, Prague; Czech Republic.
- ¹³³Charles University, Faculty of Mathematics and Physics, Prague; Czech Republic.
- ¹³⁴Particle Physics Department, Rutherford Appleton Laboratory, Didcot; United Kingdom.

- ¹³⁵IRFU, CEA, Université Paris-Saclay, Gif-sur-Yvette; France.
- ¹³⁶Santa Cruz Institute for Particle Physics, University of California Santa Cruz, Santa Cruz CA; United States of America.
- ^{137(a)}Departamento de Física, Pontificia Universidad Católica de Chile, Santiago; ^(b)Millennium Institute for Subatomic physics at high energy frontier (SAPHIR), Santiago; ^(c)Instituto de Investigación Multidisciplinario en Ciencia y Tecnología, y Departamento de Física, Universidad de La Serena; ^(d)Universidad Andres Bello, Department of Physics, Santiago; ^(e)Instituto de Alta Investigación, Universidad de Tarapacá, Arica; ^(f)Departamento de Física, Universidad Técnica Federico Santa María, Valparaíso; Chile.
- ¹³⁸Department of Physics, University of Washington, Seattle WA; United States of America.
- ¹³⁹Department of Physics and Astronomy, University of Sheffield, Sheffield; United Kingdom.
- ¹⁴⁰Department of Physics, Shinshu University, Nagano; Japan.
- ¹⁴¹Department Physik, Universität Siegen, Siegen; Germany.
- ¹⁴²Department of Physics, Simon Fraser University, Burnaby BC; Canada.
- ¹⁴³SLAC National Accelerator Laboratory, Stanford CA; United States of America.
- ¹⁴⁴Department of Physics, Royal Institute of Technology, Stockholm; Sweden.
- ¹⁴⁵Departments of Physics and Astronomy, Stony Brook University, Stony Brook NY; United States of America.
- ¹⁴⁶Department of Physics and Astronomy, University of Sussex, Brighton; United Kingdom.
- ¹⁴⁷School of Physics, University of Sydney, Sydney; Australia.
- ¹⁴⁸Institute of Physics, Academia Sinica, Taipei; Taiwan.
- ^{149(a)}E. Andronikashvili Institute of Physics, Iv. Javakhishvili Tbilisi State University, Tbilisi; ^(b)High Energy Physics Institute, Tbilisi State University, Tbilisi; ^(c)University of Georgia, Tbilisi; Georgia.
- ¹⁵⁰Department of Physics, Technion, Israel Institute of Technology, Haifa; Israel.
- ¹⁵¹Raymond and Beverly Sackler School of Physics and Astronomy, Tel Aviv University, Tel Aviv; Israel.
- ¹⁵²Department of Physics, Aristotle University of Thessaloniki, Thessaloniki; Greece.
- ¹⁵³International Center for Elementary Particle Physics and Department of Physics, University of Tokyo, Tokyo; Japan.
- ¹⁵⁴Department of Physics, Tokyo Institute of Technology, Tokyo; Japan.
- ¹⁵⁵Department of Physics, University of Toronto, Toronto ON; Canada.
- ^{156(a)}TRIUMF, Vancouver BC; ^(b)Department of Physics and Astronomy, York University, Toronto ON; Canada.
- ¹⁵⁷Division of Physics and Tomonaga Center for the History of the Universe, Faculty of Pure and Applied Sciences, University of Tsukuba, Tsukuba; Japan.
- ¹⁵⁸Department of Physics and Astronomy, Tufts University, Medford MA; United States of America.
- ¹⁵⁹United Arab Emirates University, Al Ain; United Arab Emirates.
- ¹⁶⁰Department of Physics and Astronomy, University of California Irvine, Irvine CA; United States of America.
- ¹⁶¹Department of Physics and Astronomy, University of Uppsala, Uppsala; Sweden.
- ¹⁶²Department of Physics, University of Illinois, Urbana IL; United States of America.
- ¹⁶³Instituto de Física Corpuscular (IFIC), Centro Mixto Universidad de Valencia - CSIC, Valencia; Spain.
- ¹⁶⁴Department of Physics, University of British Columbia, Vancouver BC; Canada.
- ¹⁶⁵Department of Physics and Astronomy, University of Victoria, Victoria BC; Canada.
- ¹⁶⁶Fakultät für Physik und Astronomie, Julius-Maximilians-Universität Würzburg, Würzburg; Germany.
- ¹⁶⁷Department of Physics, University of Warwick, Coventry; United Kingdom.
- ¹⁶⁸Waseda University, Tokyo; Japan.
- ¹⁶⁹Department of Particle Physics and Astrophysics, Weizmann Institute of Science, Rehovot; Israel.

- ¹⁷⁰Department of Physics, University of Wisconsin, Madison WI; United States of America.
- ¹⁷¹Fakultät für Mathematik und Naturwissenschaften, Fachgruppe Physik, Bergische Universität Wuppertal, Wuppertal; Germany.
- ¹⁷²Department of Physics, Yale University, New Haven CT; United States of America.
- ^a Also Affiliated with an institute covered by a cooperation agreement with CERN.
- ^b Also at An-Najah National University, Nablus; Palestine.
- ^c Also at Borough of Manhattan Community College, City University of New York, New York NY; United States of America.
- ^d Also at Center for High Energy Physics, Peking University; China.
- ^e Also at Center for Interdisciplinary Research and Innovation (CIRI-AUTH), Thessaloniki; Greece.
- ^f Also at Centro Studi e Ricerche Enrico Fermi; Italy.
- ^g Also at CERN, Geneva; Switzerland.
- ^h Also at Département de Physique Nucléaire et Corpusculaire, Université de Genève, Genève; Switzerland.
- ⁱ Also at Departament de Fisica de la Universitat Autonoma de Barcelona, Barcelona; Spain.
- ^j Also at Department of Financial and Management Engineering, University of the Aegean, Chios; Greece.
- ^k Also at Department of Physics and Astronomy, Michigan State University, East Lansing MI; United States of America.
- ^l Also at Department of Physics, Ben Gurion University of the Negev, Beer Sheva; Israel.
- ^m Also at Department of Physics, California State University, Sacramento; United States of America.
- ⁿ Also at Department of Physics, King's College London, London; United Kingdom.
- ^o Also at Department of Physics, Stanford University, Stanford CA; United States of America.
- ^p Also at Department of Physics, University of Fribourg, Fribourg; Switzerland.
- ^q Also at Department of Physics, University of Thessaly; Greece.
- ^r Also at Department of Physics, Westmont College, Santa Barbara; United States of America.
- ^s Also at Hellenic Open University, Patras; Greece.
- ^t Also at Institutio Catalana de Recerca i Estudis Avancats, ICREA, Barcelona; Spain.
- ^u Also at Institut für Experimentalphysik, Universität Hamburg, Hamburg; Germany.
- ^v Also at Institute for Nuclear Research and Nuclear Energy (INRNE) of the Bulgarian Academy of Sciences, Sofia; Bulgaria.
- ^w Also at Institute of Applied Physics, Mohammed VI Polytechnic University, Ben Guerir; Morocco.
- ^x Also at Institute of Particle Physics (IPP); Canada.
- ^y Also at Institute of Physics and Technology, Ulaanbaatar; Mongolia.
- ^z Also at Institute of Physics, Azerbaijan Academy of Sciences, Baku; Azerbaijan.
- ^{aa} Also at Institute of Theoretical Physics, Ilia State University, Tbilisi; Georgia.
- ^{ab} Also at L2IT, Université de Toulouse, CNRS/IN2P3, UPS, Toulouse; France.
- ^{ac} Also at Lawrence Livermore National Laboratory, Livermore; United States of America.
- ^{ad} Also at National Institute of Physics, University of the Philippines Diliman (Philippines); Philippines.
- ^{ae} Also at Ochanomizu University, Otsuka, Bunkyo-ku, Tokyo; Japan.
- ^{af} Also at Technical University of Munich, Munich; Germany.
- ^{ag} Also at The Collaborative Innovation Center of Quantum Matter (CICQM), Beijing; China.
- ^{ah} Also at TRIUMF, Vancouver BC; Canada.
- ^{ai} Also at Università di Napoli Parthenope, Napoli; Italy.
- ^{aj} Also at University of Colorado Boulder, Department of Physics, Colorado; United States of America.
- ^{ak} Also at Washington College, Chestertown, MD; United States of America.
- ^{al} Also at Yeditepe University, Physics Department, Istanbul; Türkiye.
- * Deceased